ANTENNA MEASUREMENT REPORT

8000-6220126-230206-01

Characterisation of two

WLan Antennas

Ordered by

Robert Bosch Car Multi Media GmbH

Robert-Bosch-Str. 200
D-31132 Hildesheim
Germany

perfomed at

IMST GmbH

Test Centre Antennas

Carl-Friedrich-Gauss-Str. 2-4
D-47475Kamp-Lintfort
GERMANY

1 Table of Contents

2 FIGURES

3 TABLES

4 General Information

Customer :	Robert Bosch Car Multi Media GmbH Mr. Ralf Eimertenbrink Robert-Bosch-Str. 200 D-31132 Hildesheim Germany

Devices under test (DUT): Metal case equipped with two WLan antennas

Subject:	Determination of the Gain, the 3D antenna pattern, the efficiency and the matching.
Date of measurement:	02. – 06.02.2023
Performed:	Stefan Weitz
Quotation-No.:	5220070-B
Order-No.:	4503413016
Project-No.:	8000_6220126
Department:	Antennas & EM Modelling
Responsible:	Aline Friedrich +49-2842-981-337

Performed:..................................... Reviewed: i.V. ....

Stefan Weitz	Aline Friedrich
Test engineer	Head of laboratory

5 PREFACE

In this measurement campaign two dual band WLan antennas in a metal case have been measured as described in the following.

The patterns of the DUTs (Devices Under Test) have been measured three-dimensional at WLan frequencies. The measurements have been done with two orthogonal polarisations of the measurement antenna. After the measurement the efficiencies of the DUT has been determined.

The results are documented as tables and diagrams in chapter 9.

6 DESCRIPTION AND MOUNTING OF THE DUTS

6.1 DUT Type

The DUT consisted of a metal case with two dual band WLan antennas and an inseparably mounted RF-cable with a SMA male connector. The antennas operates in the 2.4 GHz and 5 GHz WLan frequency range. See Figure 6-1.

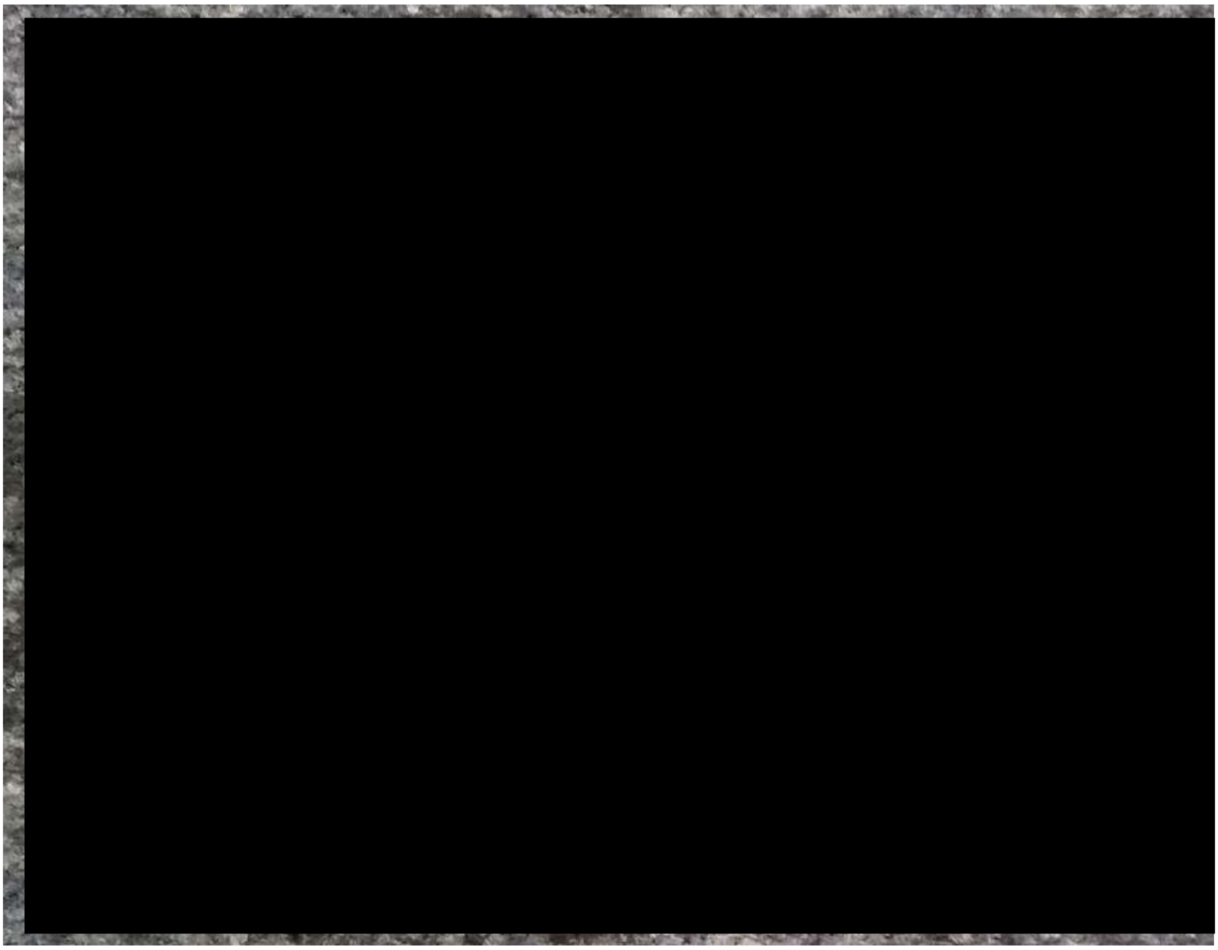

Figure 6-1: DUT with connector

Because of the inseparably mounted RF-cable antenna and cable has been treated as one unit.

6.2 Measurement environment

The measurements have been performed in the air conditioned and completely shielded anechoic chamber (Range II) B83117-A1431-T161 of IMST GmbH. This minimizes measurement errors caused by variations in temperature, disturbing signals and reflections.

Movement of the DUT has been done by a „Roll over Azimuth"-positioner. The Mast that carries the roll axis is made from Kevlar™. The accuracy of the azimuth positioner is 0.03°. During measurement the azimuth positioner is covered with absorbers.

The following figure shows the mounting of the DUT for the measurement.

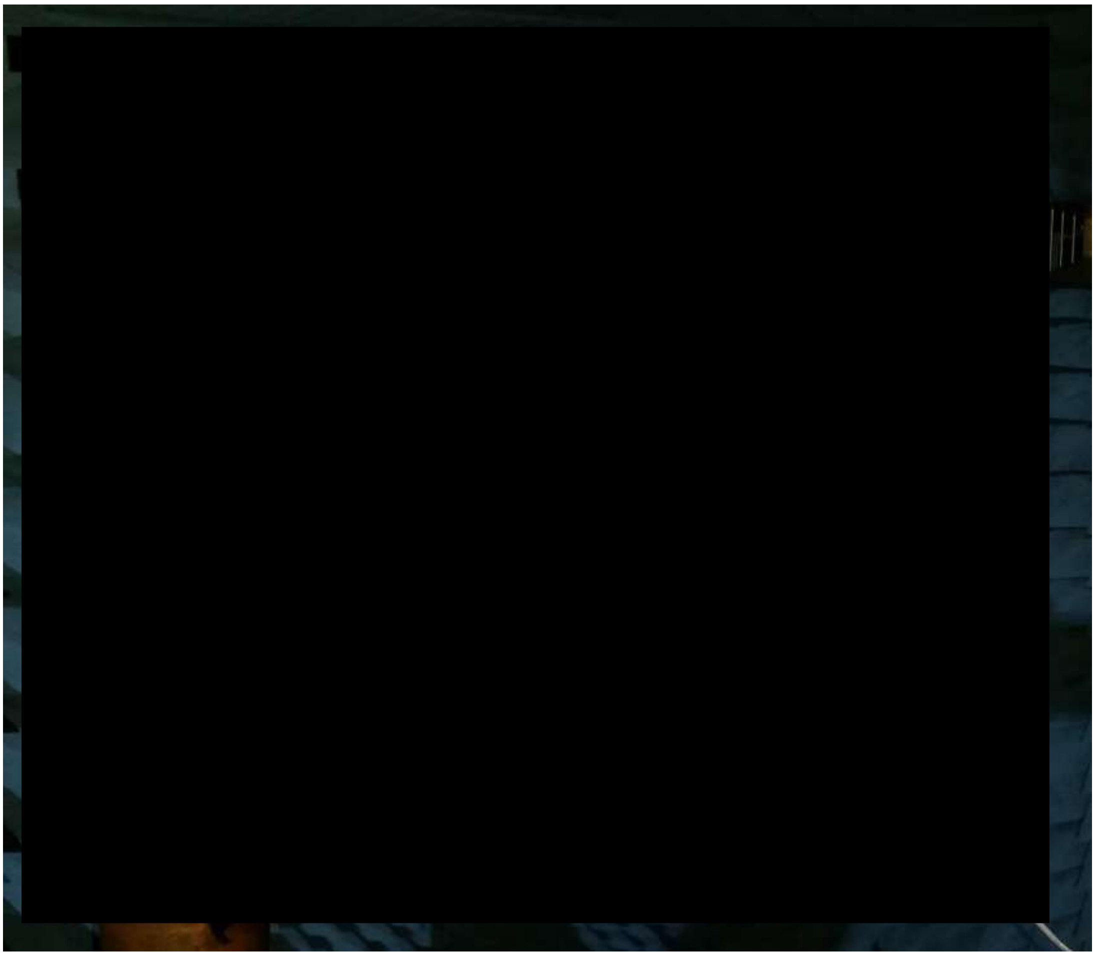

Figure 6-2: Mounting of the DUT.

During measurement the DUT was mounted on a ROHACELL® bracket. ROHACELL® is a rigid foam material which has nearly the same ε_R as air.

The distance between the measurement antenna and the rotation centre of the DUT was ca. 2.23 m during measurement (Far field conditions).

6.3 Connection description

To minimize errors caused by mismatching the feeding cable was equipped with an attenuator with a very low VSWR. The SMA connector of the attenuator was the reference plane for the pattern measurement.

During measurement no actions were taken to suppress surface waves.

7 3D-Radiation Pattern and Matching Measurement

7.1 Subject

The three-dimensional antenna pattern measurements with two orthogonal polarisations of the measurement antenna enable the determination of the gain and the efficiency.

The matching measurement shows the S_{11} of the DUT over measured frequency range.

7.2 Used measurement devices

All calibrations and measurements have been done with the devices that are stated in the following table. The date of the last calibration is shown in the column "Cal. Date".

Type	Device	Ser. No.	Cal. Date
ZVL Rohde & Schwarz	Network/Spectrum analyser 9 kHz – 13.6 GHz	10114	07.2019
SH800 Satimo	Dual ridged Horn (Ref. Ant.) 0.8 -12.0GHz	157	08.2019
SH800 Satimo	Dual ridged Horn (Meas. Ant.) 0.8 -12.0GHz	78	08.2019
SH800 Satimo	Dual ridged Horn (Meas. Ant.) 0.8 -12.0GHz	77	08.2019
B83117-A1431-T161 Siemens Matsushita	Anechoic Chamber	Project No. 007-A34-089/99A	N/A
AL-DBDR-3G/AL-560 Orbit/FR	Roll-over-azimuth positioner	434	N/A
AL-4164-MC Orbit/FR	Controller	25	N/A
DARIC 2.0 IMST	Control and measurement software		N/A
Rohacell bracket	Free space mounting		N/A
S8150 Copper Mountain	2 Port Vector Network analyzer 100 kHz - 18 GHz	21280020	08.2021
02CK10A-150 Rosenberger	Calibration Kit DC – 40 GHz	U3901	07.2019

Table 7-1: Devices used for calibration and measurement

7.3 Pattern Measurement Setup

Figure 7-1 shows the principle setup for the pattern measurement.

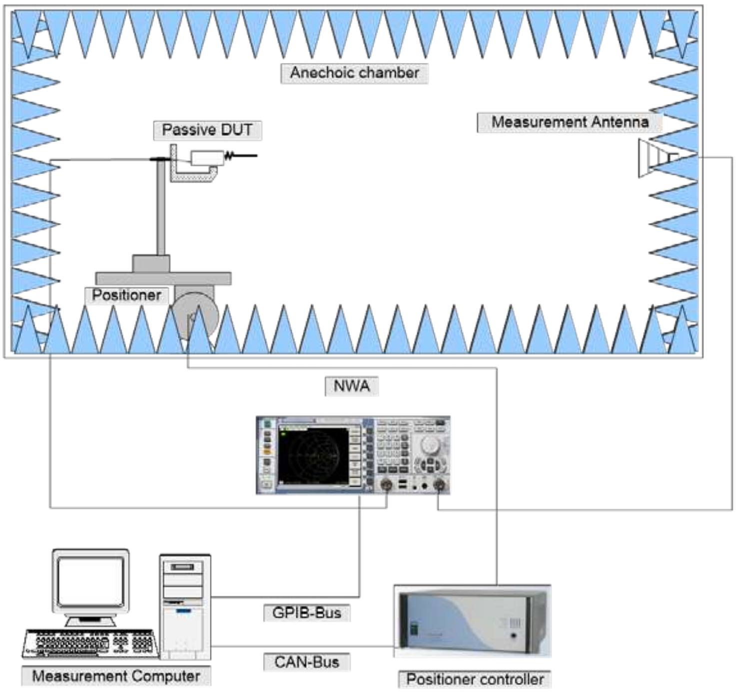

Figure 7-1: Standard setup for pattern measurement.

Figure 7-2 shows the mechanical pattern measurement setup. It is a standard setup for small antenna measurement. Additional setup information could be found in chapter 6.2.

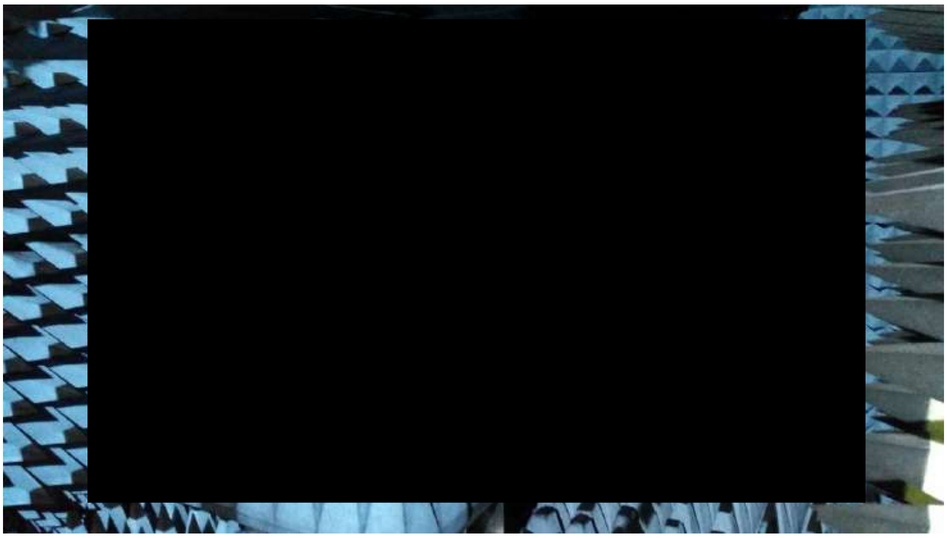

Figure 7-2: Pattern measurement setup.

For calibration and pattern measurement broad band horns type SH800 from Satimo (Microwave Vision Company, MVC) has been used.

Before the calibration was done the position of the measurement and the calibration antenna was checked by a positioning laser. The same procedure was used for the positioning of the DUT.

7.4 Coordinate System During Measurement

For the measurements the theta/phi coordinate system has been used as shown in Figure 7-3. Also the movement of the measurement antenna (MA) with its polarisations are shown.

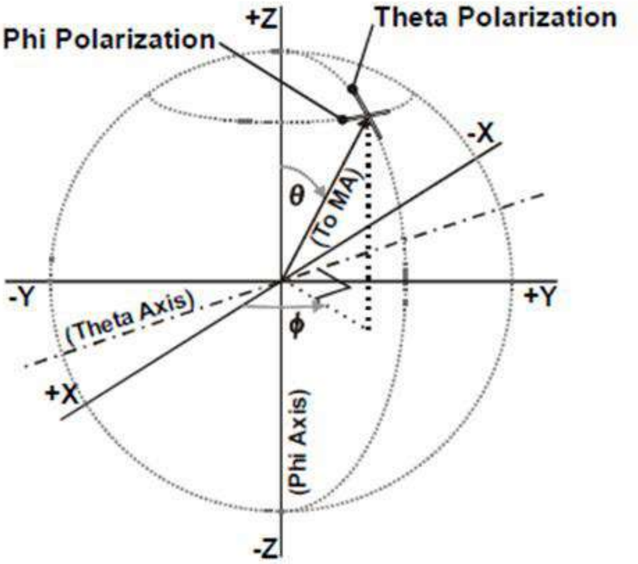

Figure 7-3: Theta/Phi coordinate system.

In Figure 7-4 the position of the DUT in the theta/phi coordinate system is shown which has been used for measurement and evaluation.

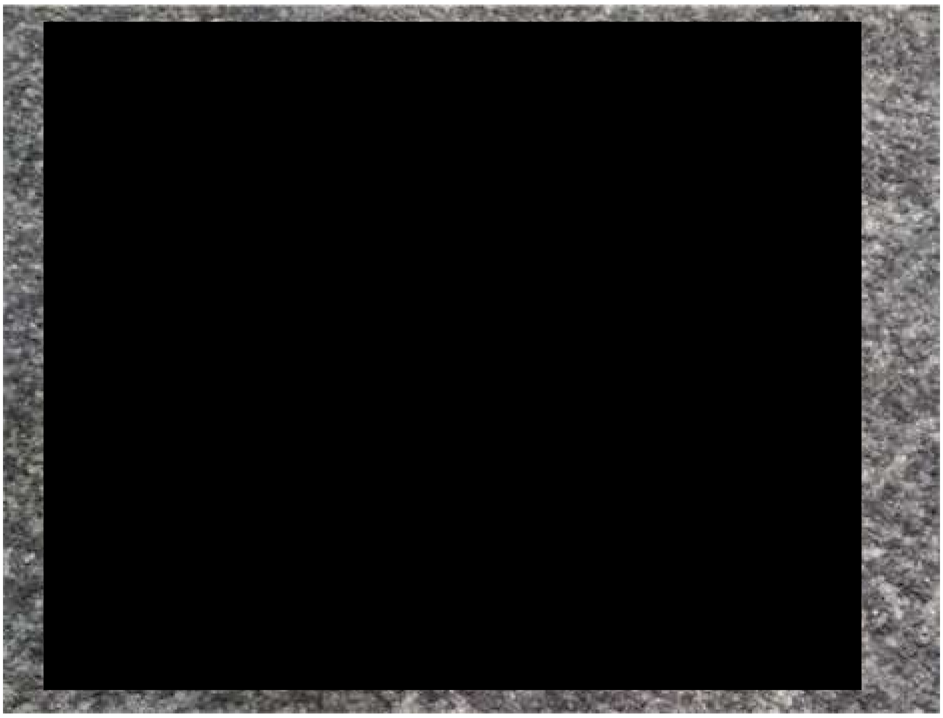

Figure 7-4: Position of the DUT in the theta/phi coordinate system

7.5 Matching measurement

The following picture shows the setup of the matching (S_{11}/S_{22}) measurement.

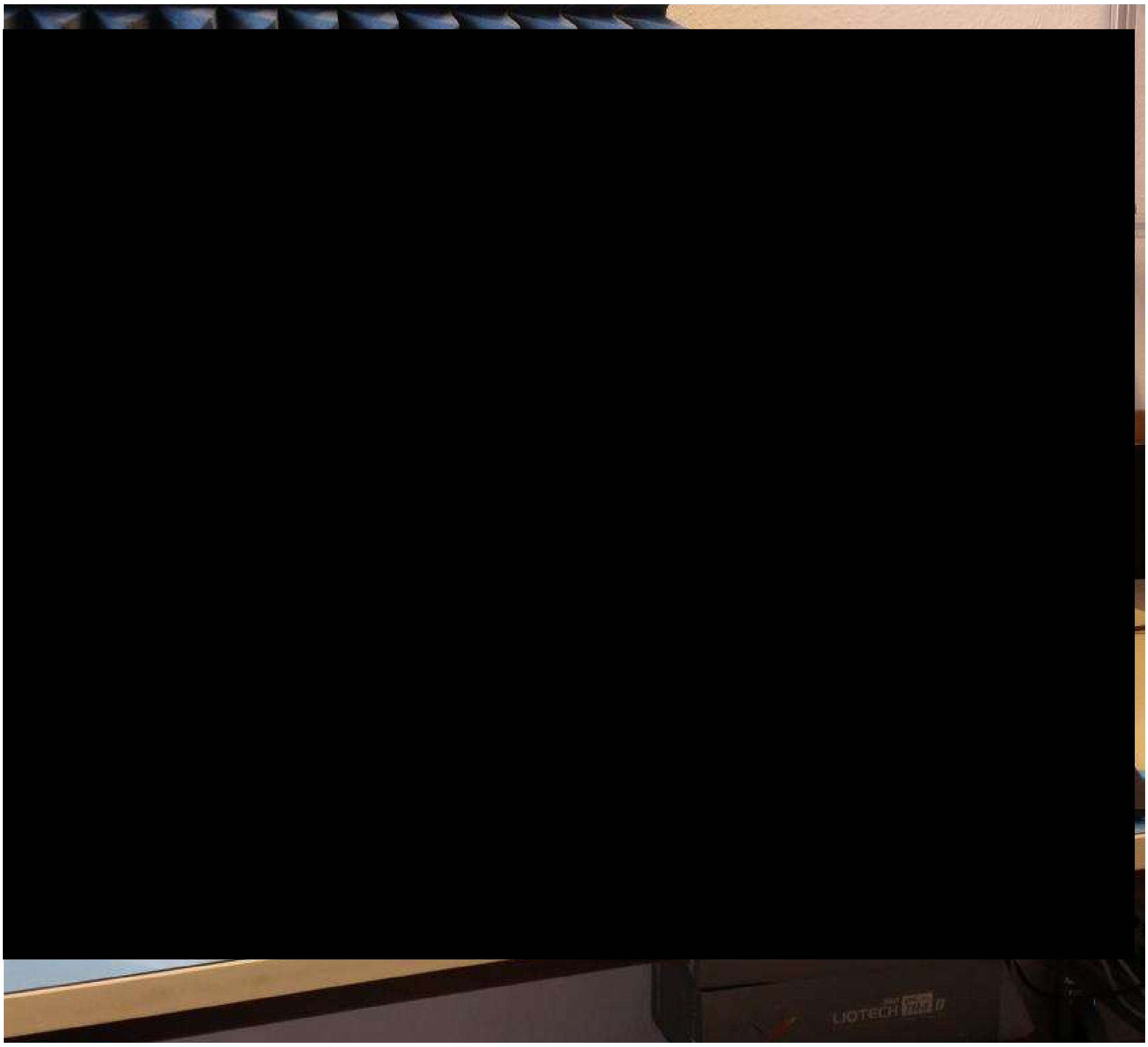

Figure 7-5: Matching measurement setup.

During matching measurement the DUT was located on a Styrofoam block. This minimizes external influence of the measurement results. The matching measurement was performed over a frequency range from 1000 MHz up to 7000 MHz with a resolution of 24001 points. The 2-port NWA S5810 from Copper Mountain was calibrated with a full-two-port calibration. The calibration was performed with the 02CK10-ARPC-2.92 calibration kit from Rosenberger.

7.6 Far field measurement report, results and accuracy

The “Far field measurement report” in chapter 8 gives an overview about the performed measurements.

The results of the 3d antenna pattern measurement, the efficiency evaluation and the matching measurement are shown in chapter 9.

The accuracy of the measurement results has been specified with ±1 dB.

8 Far Field Measurement Report

FF-Measurement-Report

Operator: SW
Date from: 03.- 06.02.2023
Project: 8000_6220126
Object: Two dual band WLan antennas
Temp: 23°C +/-1°

Setup-Files	Frequencies / MHz	
S1: n/a	f1: 1000 - 7000	24001 points
S2: Bosch_CMM.dam	f2: 2412 - 2484	3 points
	f3: 5180 - 5825	3 points

No.	File	Frequency /MHz	Meas.-Axis Roll/°	Step-Axis Azimuthl/°	Step-Axis Polarisation	Remarks	Setupfile
1	Bosch_Matching.s2p	f1	n/a	n/a	n/a		
2	20230202_114824_Dualband_WLan_W701.cal.dmdf	f2, f3	0/+355 (5)	0/+180 (5)	Theta/Phi		S2
3	20230202_133426_Dualband_WLan_W702.cal.dmdf	"	"	"	"		"

Table 8-1: Far field measurement report

Meas.-Report_Bosch_Car_Multi_Media_8000_6220126_2300206_01.docx\24.02.2023\V1.0\SW

9 Results

9.1 Max. gain and efficiency

The following table shows the matching and efficiency values of the DUT. Also measurement angles with maximum gain values are shown.

	f	S11	η	Max. Gain at Polarisation Θ			Max. Gain at Polarisation Φ			Max. Gain absolut		
	MHz	dB	%	dBi	Θ [°]	Φ [°]	dBi	Θ [°]	Φ [°]	dBi	Θ [°]	Φ [°]
W701 Wlan 2.4 GHz	2412	-9.08	25.8	-2.0	5	270	-1.2	25	360	-1.0	25	345
	2448	-15.70	31.8	-1.4	5	275	-0.4	35	355	-0.3	35	355
	2484	-8.89	26.0	-2.5	5	275	-1.6	30	355	-1.4	60	60

Table 9-1: S11, efficiency and maximum gain of the W701 at WLan 2.4 GHz.

	f	S11	η	Max. Gain at Polarisation Θ			Max. Gain at Polarisation Φ			Max. Gain absolut		
	MHz	dB	%	dBi	Θ [°]	Φ [°]	dBi	Θ [°]	Φ [°]	dBi	Θ [°]	Φ [°]
W701 Wlan 5GHz	5180	-20.57	45.5	1.7	35	70	-0.6	95	70	3.1	35	70
	5502.5	-8.77	32.9	2.0	60	35	-1.0	60	35	3.1	40	60
	5825	-8.63	18.1	-0.5	40	65	-3.3	65	30	0.5	50	50

Table 9-2: S11, efficiency and maximum gain of the W701 at WLan 5GHz.

	f	S11	η	Max. Gain at Polarisation Θ			Max. Gain at Polarisation Φ			Max. Gain absolut		
	MHz	dB	%	dBi	Θ [°]	Φ [°]	dBi	Θ [°]	Φ [°]	dBi	Θ [°]	Φ [°]
W702 Wlan 2.4 GHz	2412	-9.90	41.2	-0.1	0	275	1.2	35	360	1.2	35	5
	2448	-12.00	47.0	0.4	0	270	1.6	25	360	1.6	25	360
	2484	-5.09	35.0	-1.1	0	265	0.0	40	360	0.0	60	295

Table 9-3: S11, efficiency and maximum gain of the W702 at WLan 2.4 GHz.

	f	S11	η	Max. Gain at Polarisation Θ			Max. Gain at Polarisation Φ			Max. Gain absolut		
	MHz	dB	%	dBi	Θ [°]	Φ [°]	dBi	Θ [°]	Φ [°]	dBi	Θ [°]	Φ [°]
W702 Wlan 5GHz	5180	-10.97	69.7	3.0	50	105	0.5	45	360	3.9	55	75
	5502.5	-15.67	72.6	4.3	45	90	1.3	55	25	5.4	50	65
	5825	-6.20	44.7	2.4	50	75	0.0	60	25	3.4	50	55

Table 9-4: S11, efficiency and maximum gain of the W702 at WLan 5 GHz.

9.2 Matching diagrams of the W701 antenna

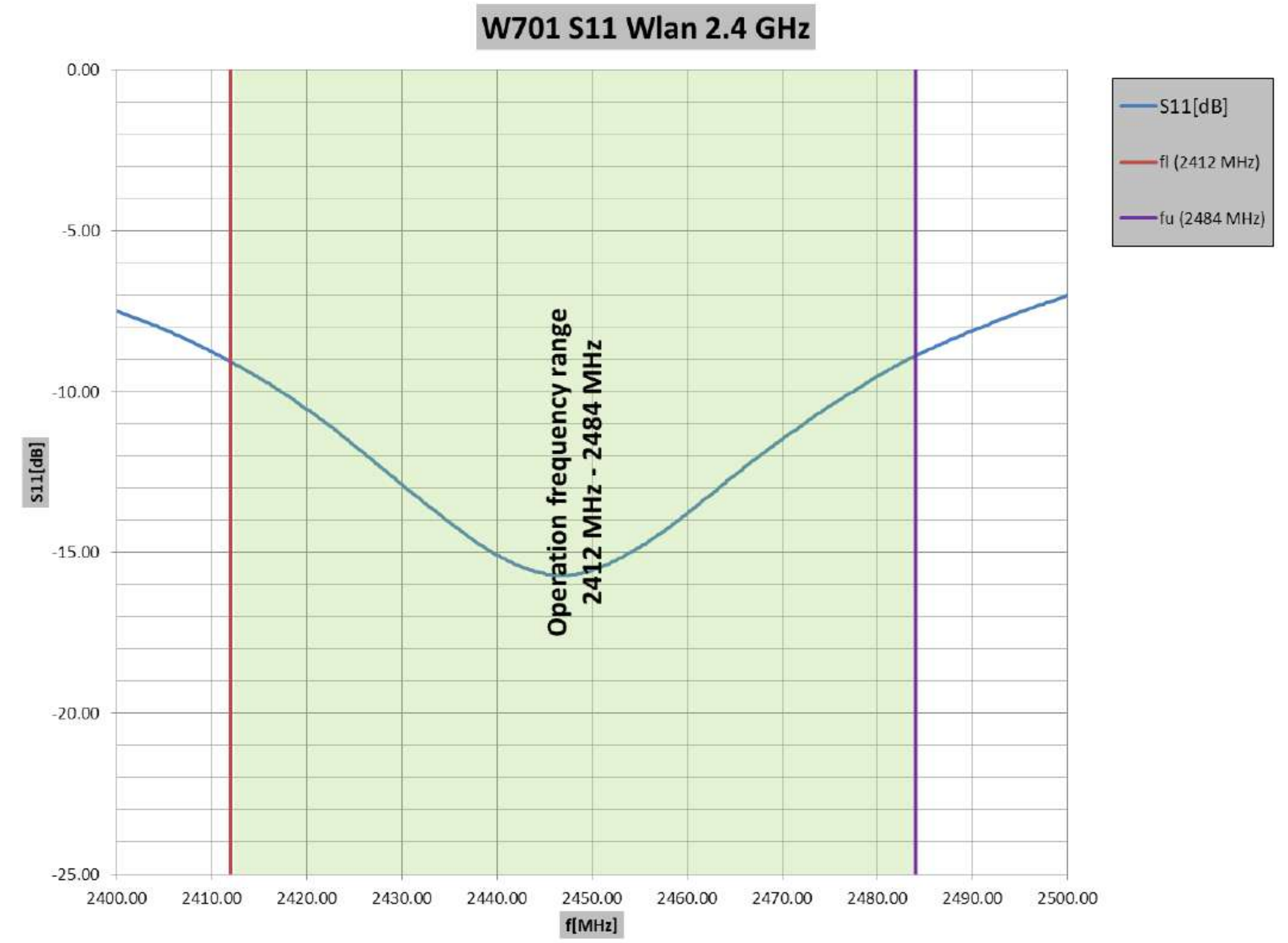

Figure 9-1: Matching Diagram, W701 @ 2.4 GHz

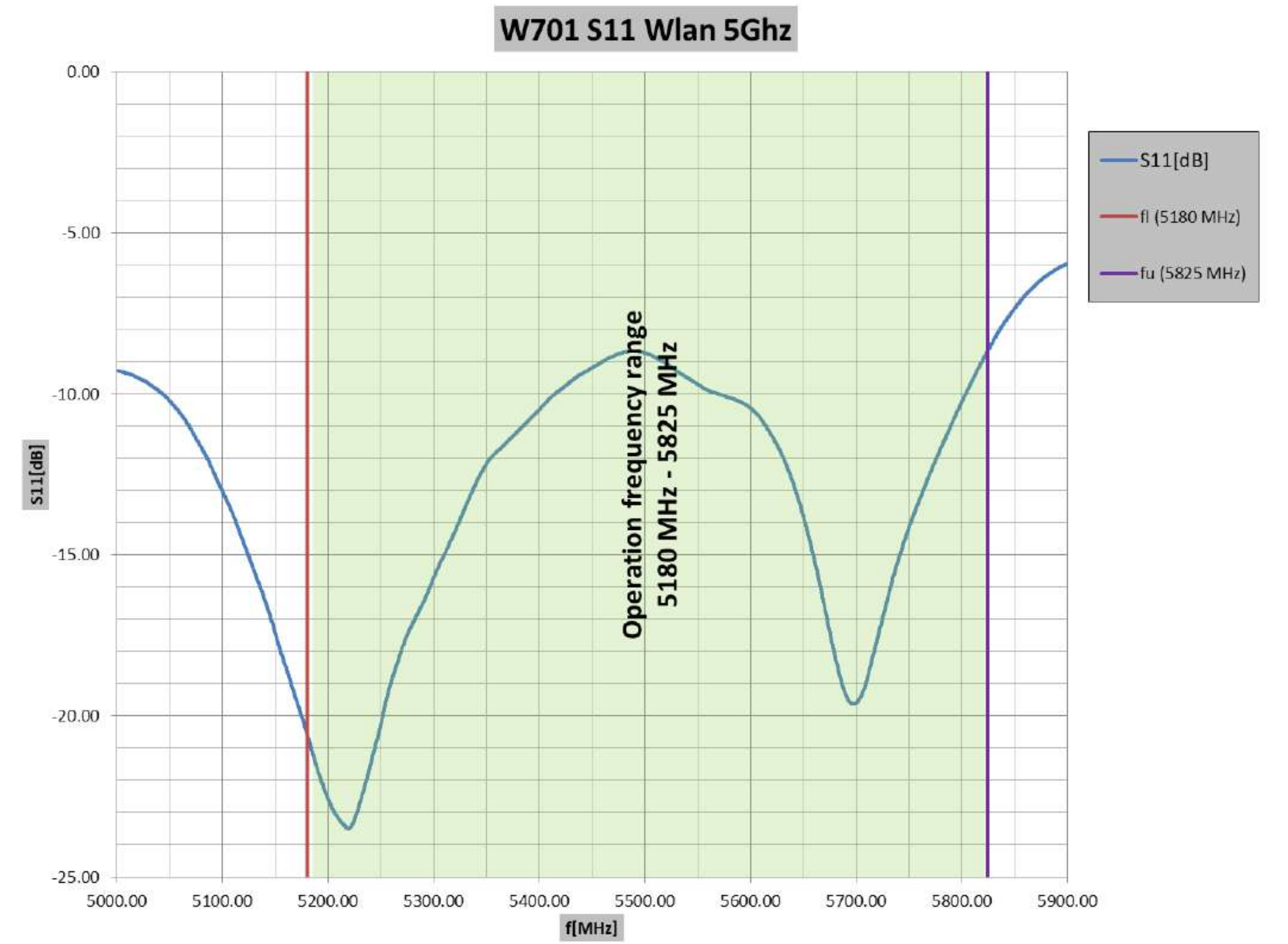

Figure 9-2: Matching Diagram, W701 @ 5 GHz

9.3 Matching diagram of the W702 antenna

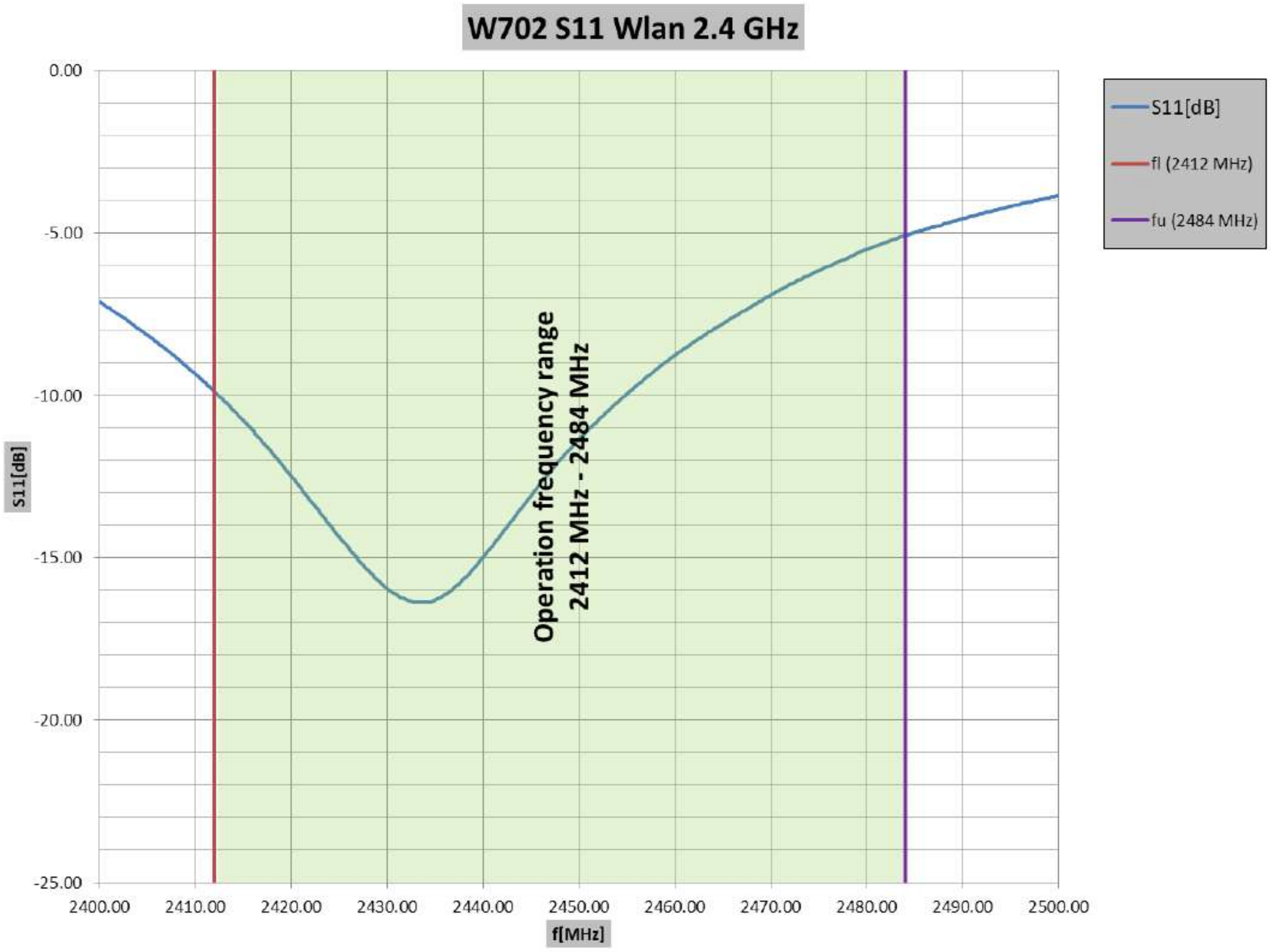

Figure 9-3: Matching Diagram, W702 @ 2.4 GHz

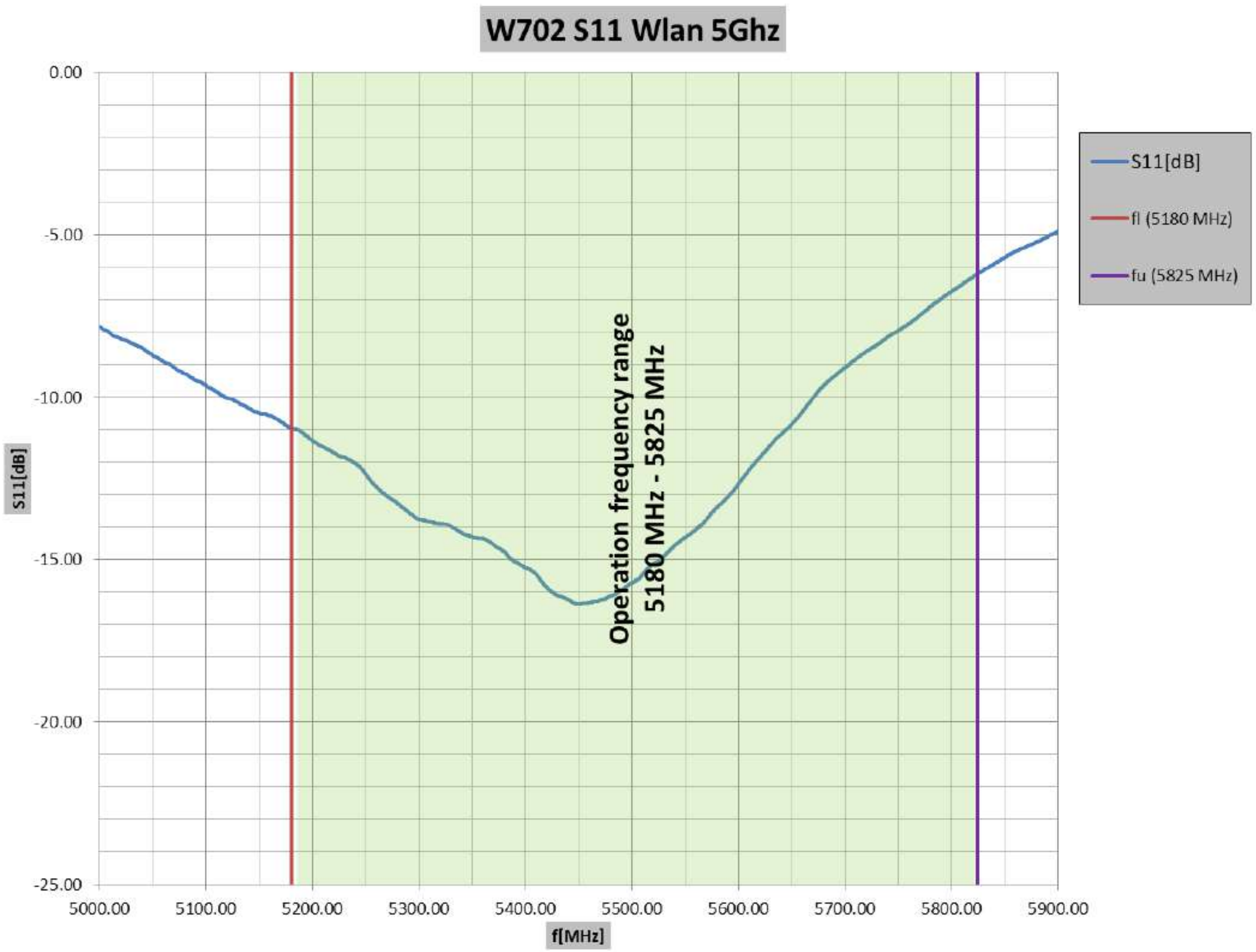

Figure 9-4: Matching Diagram, W702 @ 5 GHz

9.4 Pattern diagrams of the W701 antenna

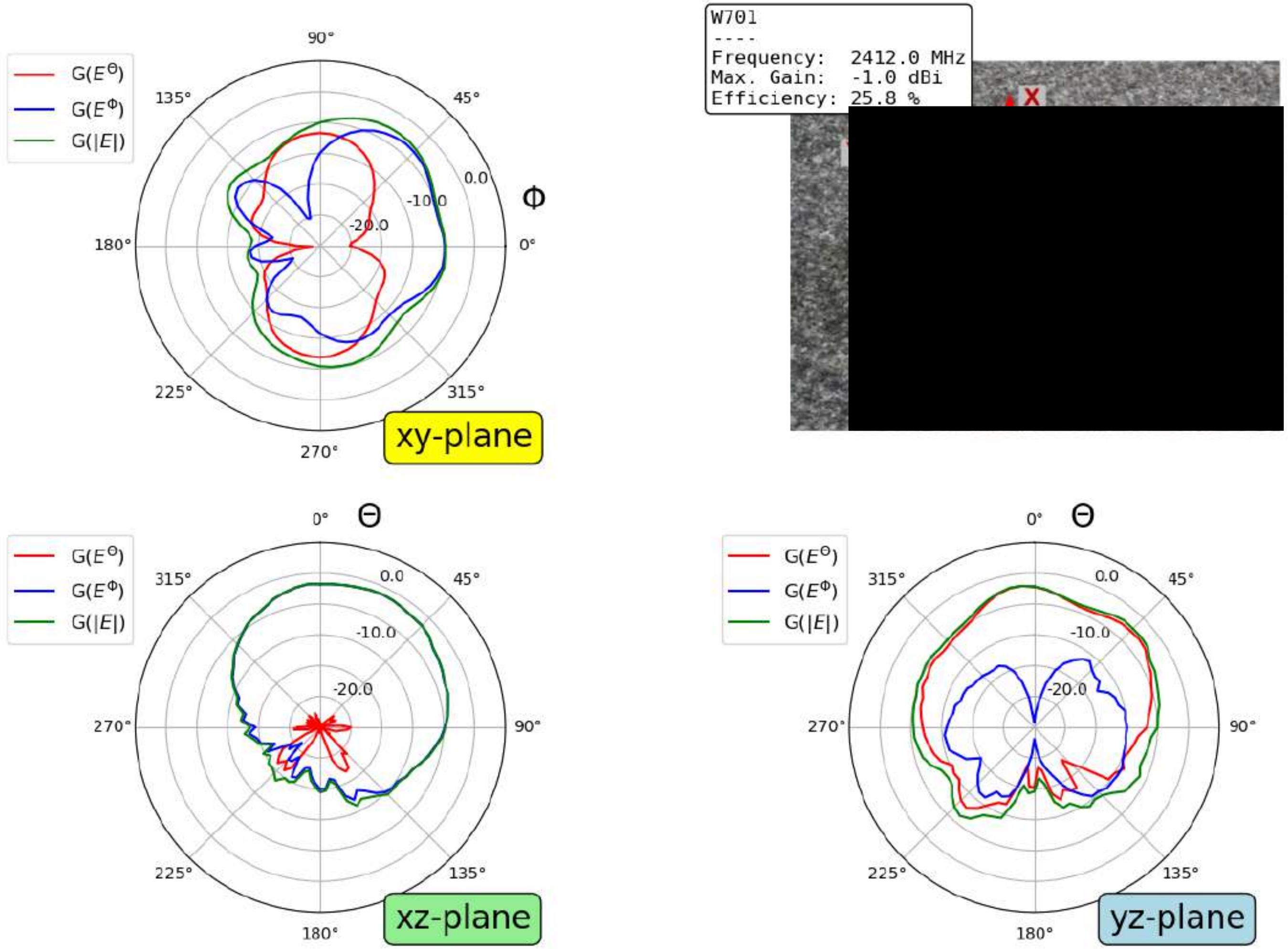

Figure 9-5: E-Theta/E-Phi/Sum Polar Diagram, W701 @ 2412 MHz

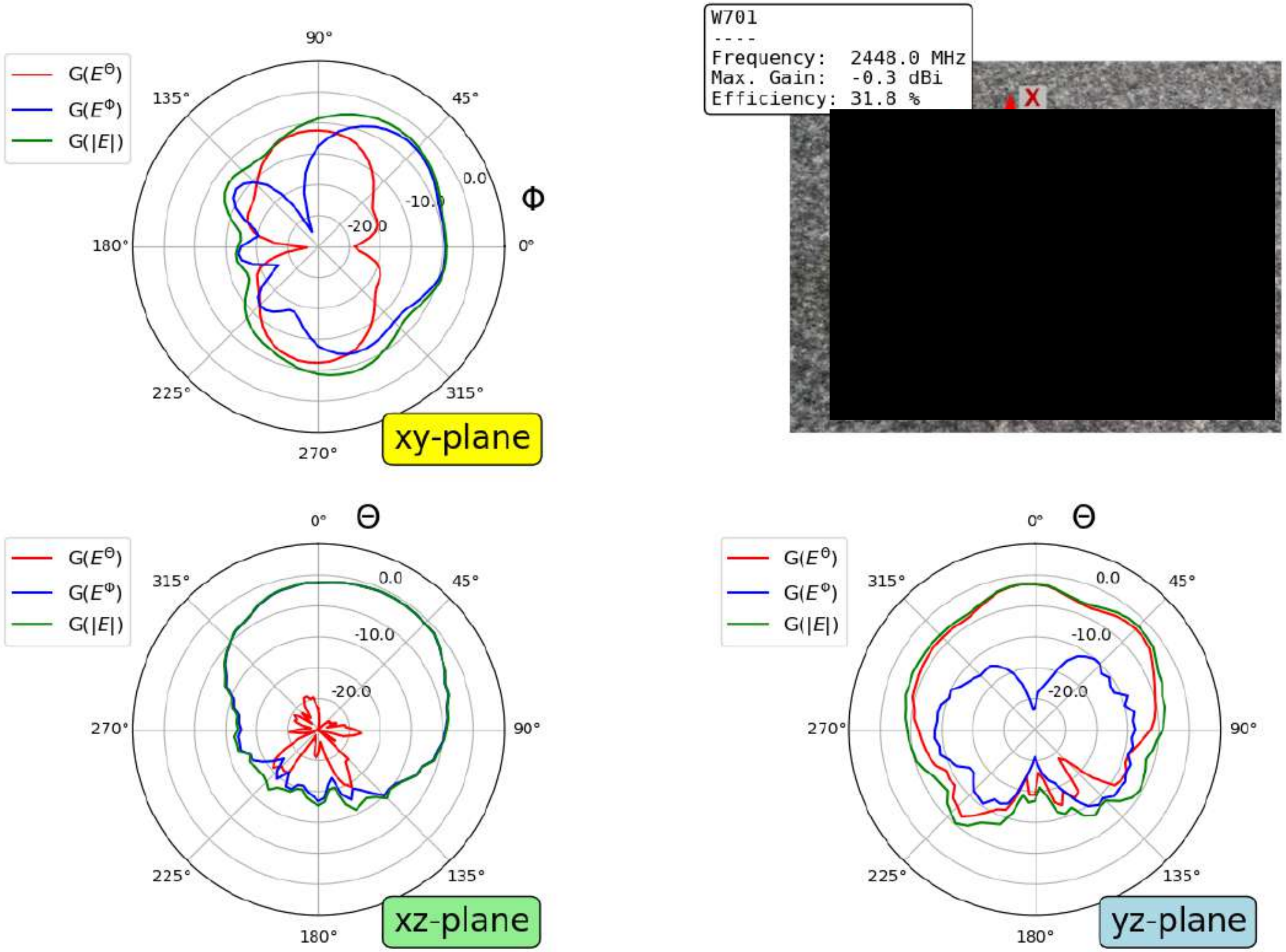

Figure 9-6: E-Theta/E-Phi/Sum Polar Diagram, W701 @ 2448 MHz

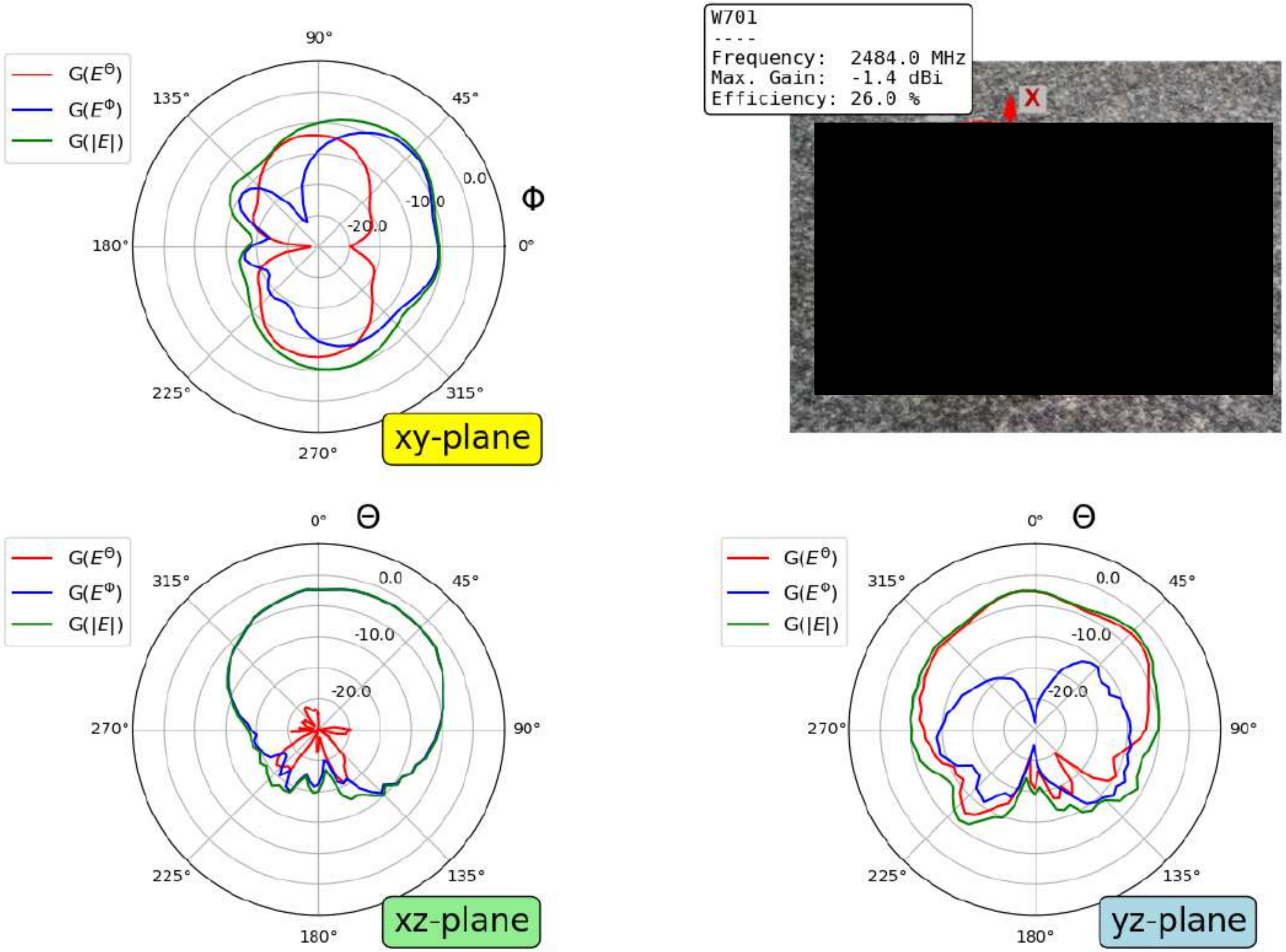

Figure 9-7: E-Theta/E-Phi/Sum Polar Diagram, W701 @ 2484 MHz

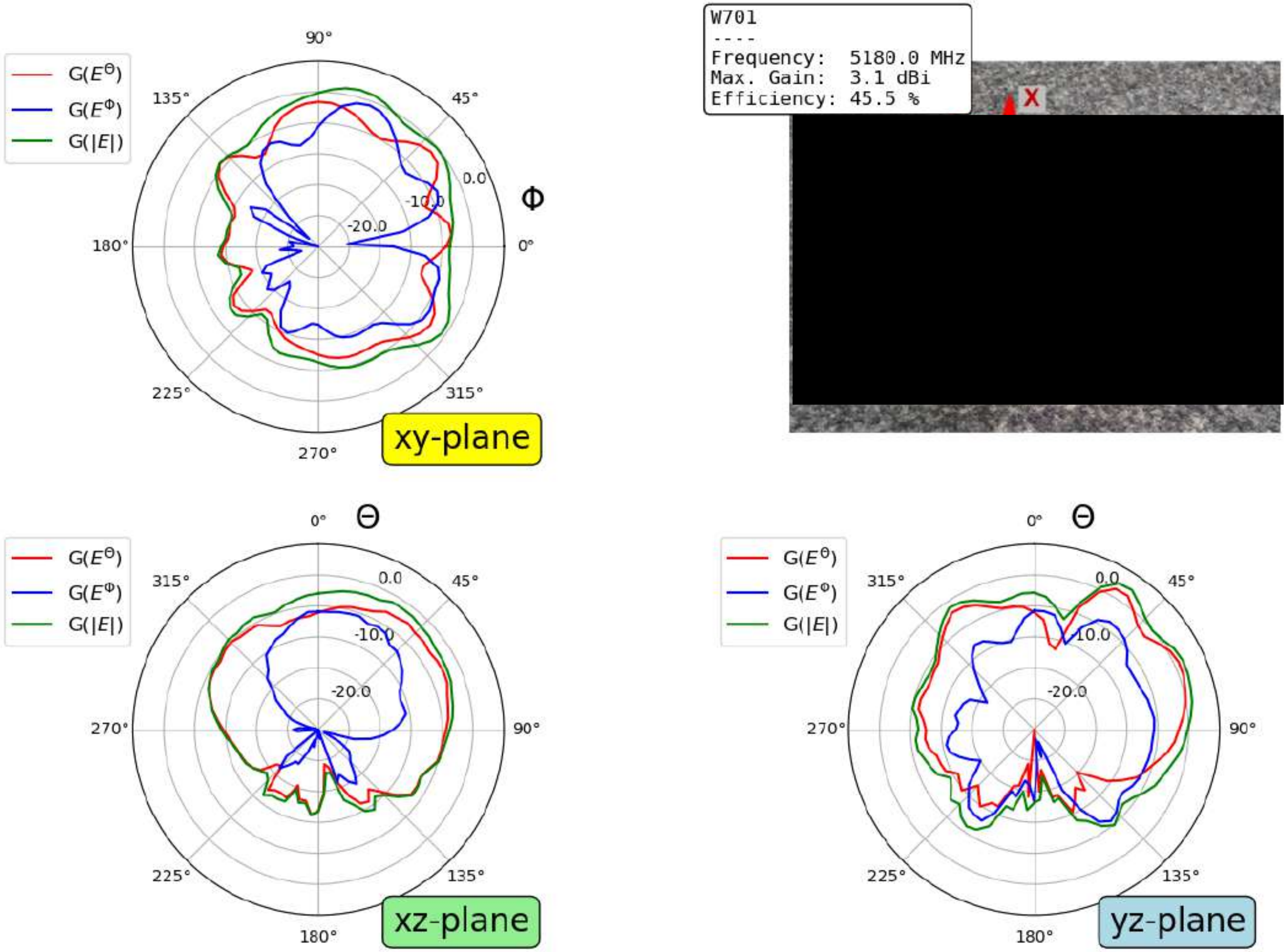

Figure 9-8: E-Theta/E-Phi/Sum Polar Diagram, W701 @ 5180 MHz

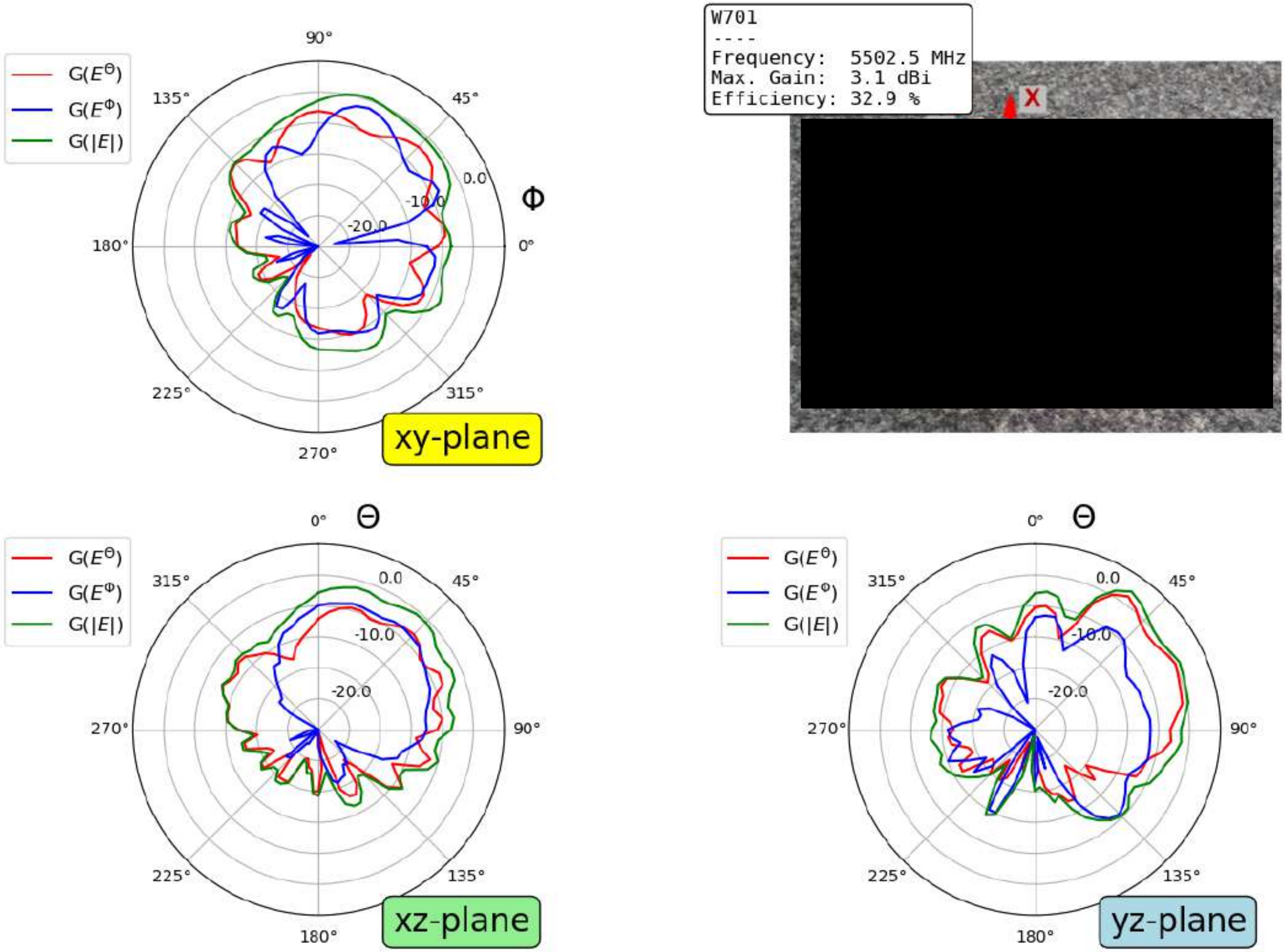

Figure 9-9: E-Theta/E-Phi/Sum Polar Diagram, W701 @ 5502.5 MHz

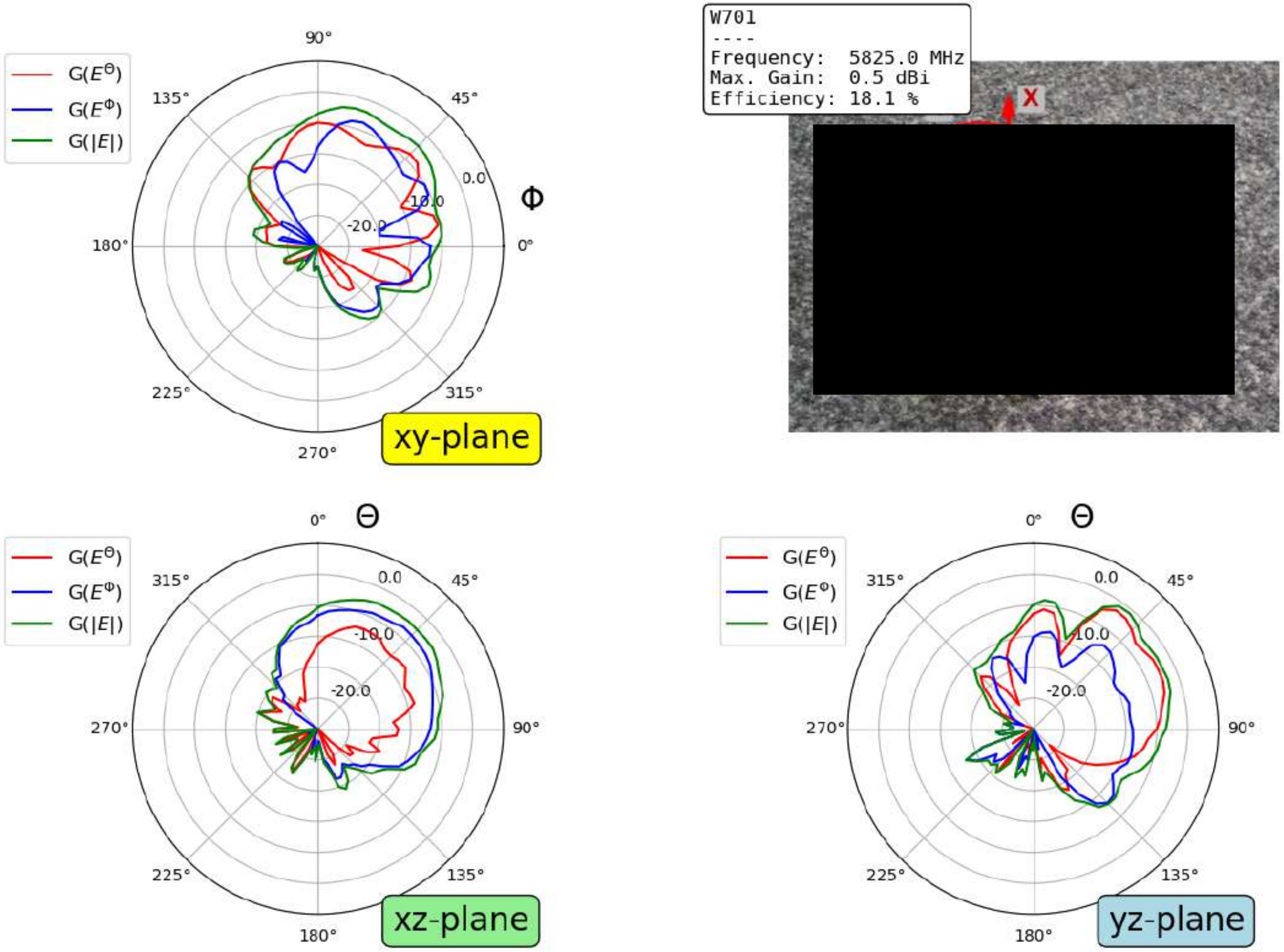

Figure 9-10: E-Theta/E-Phi/Sum Polar Diagram, W701 @ 5825 MHz

9.5 Pattern diagrams W702 antenna

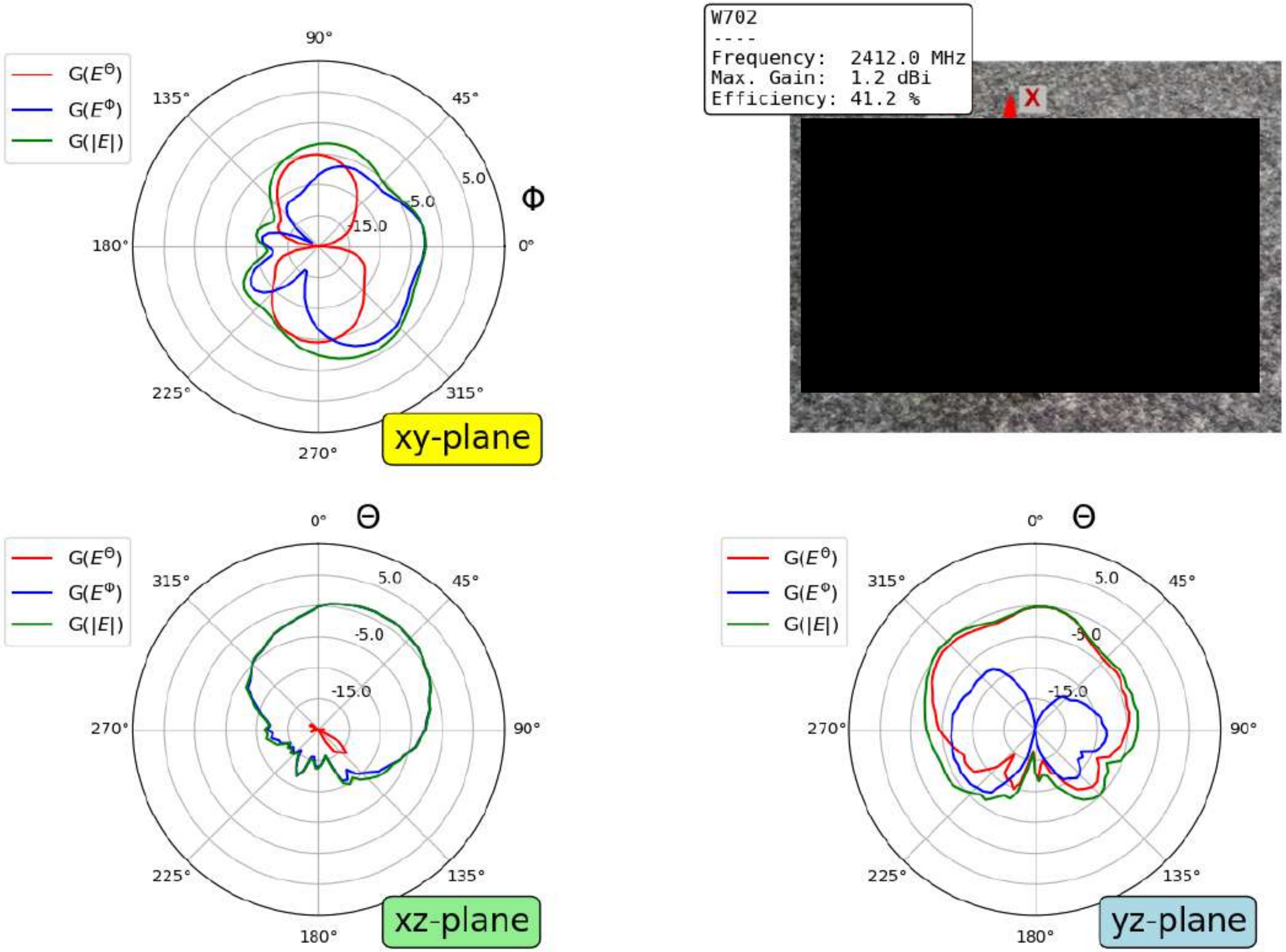

Figure 9-11: E-Theta/E-Phi/Sum Polar Diagram, W702 @ 2412 MHz

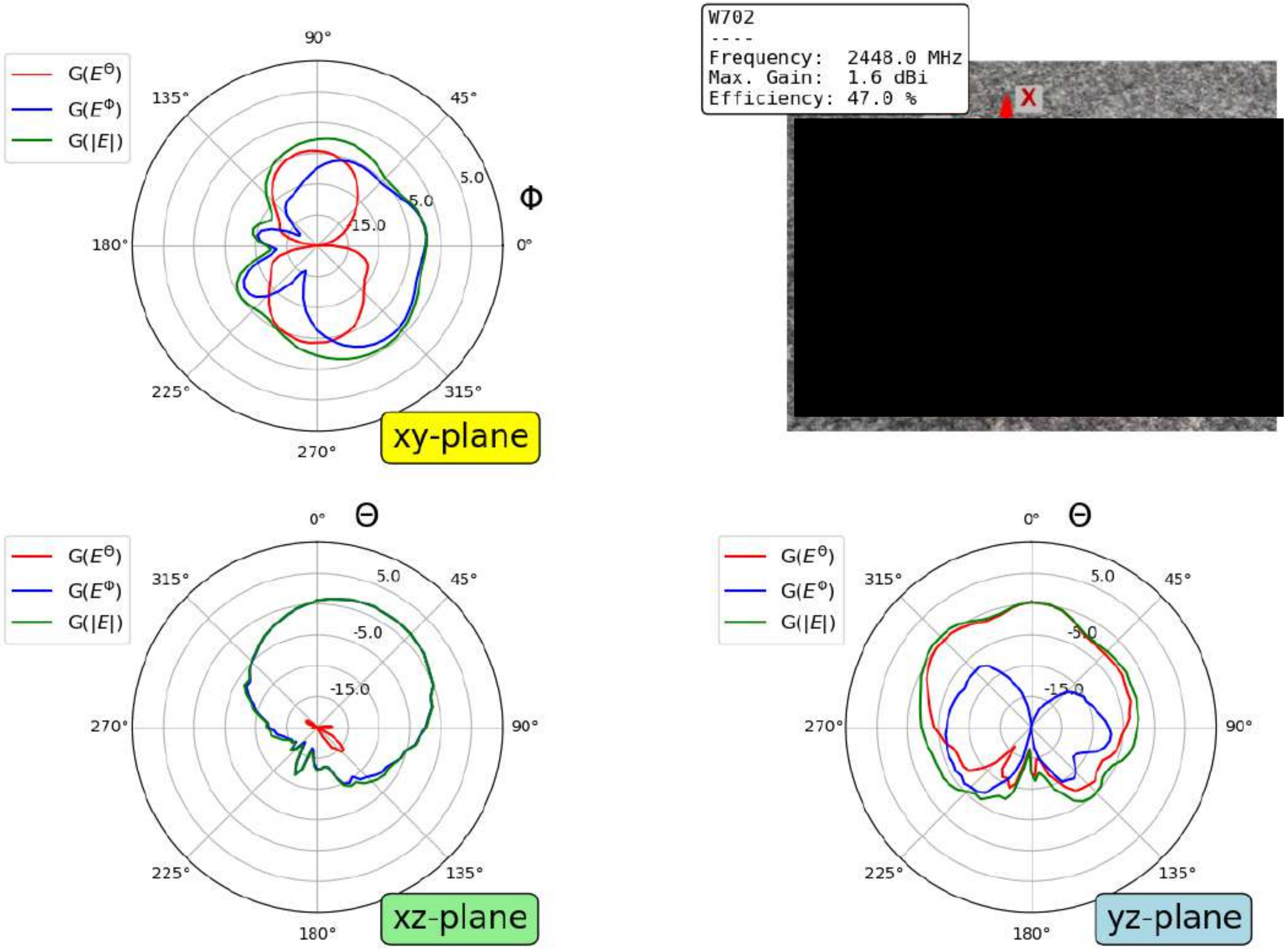

Figure 9-12: E-Theta/E-Phi/Sum Polar Diagram, W702 @ 2448 MHz

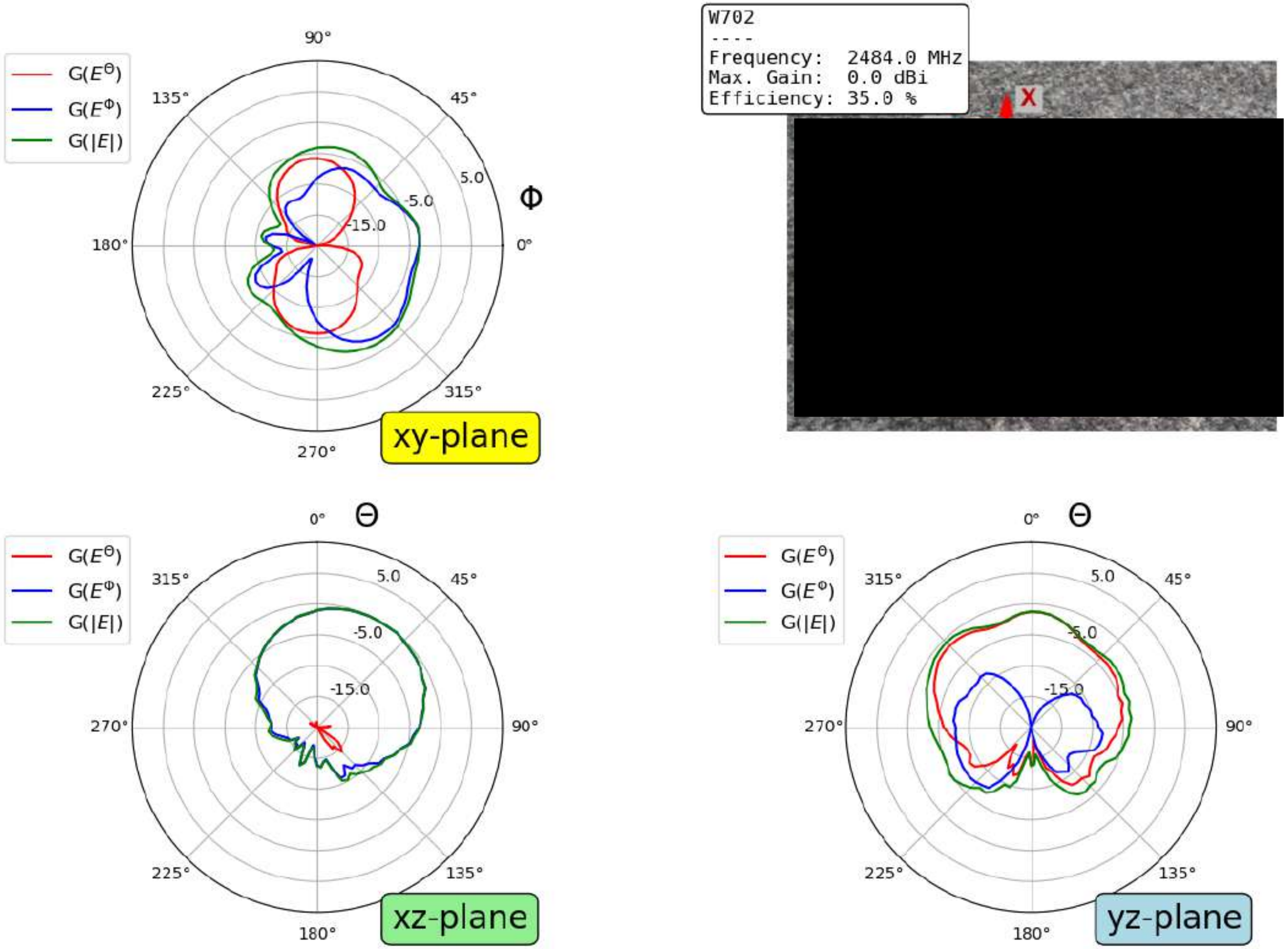

Figure 9-13: E-Theta/E-Phi/Sum Polar Diagram, W702 @ 2484 MHz

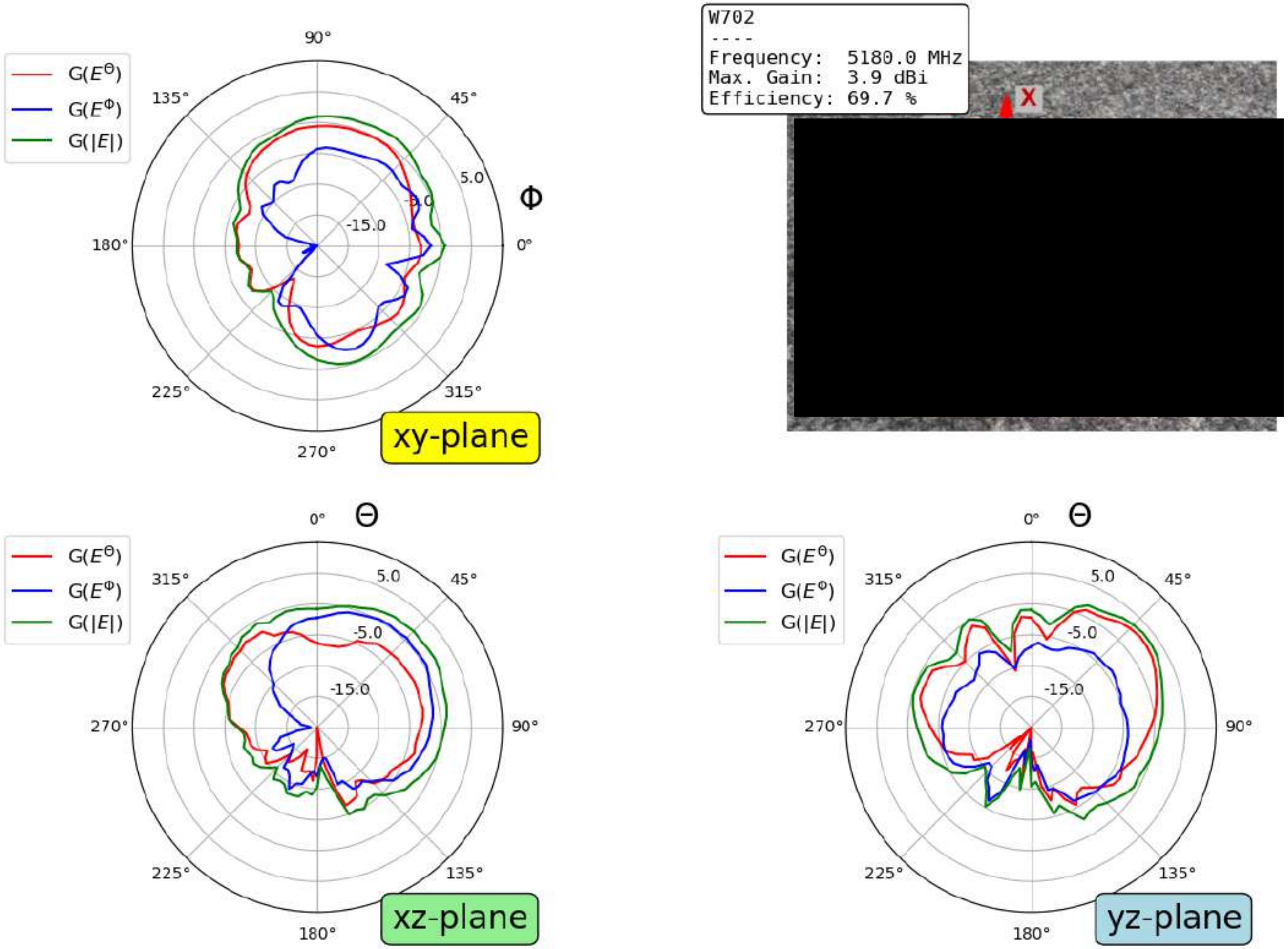

Figure 9-14: E-Theta/E-Phi/Sum Polar Diagram, W702 @ 5180 MHz

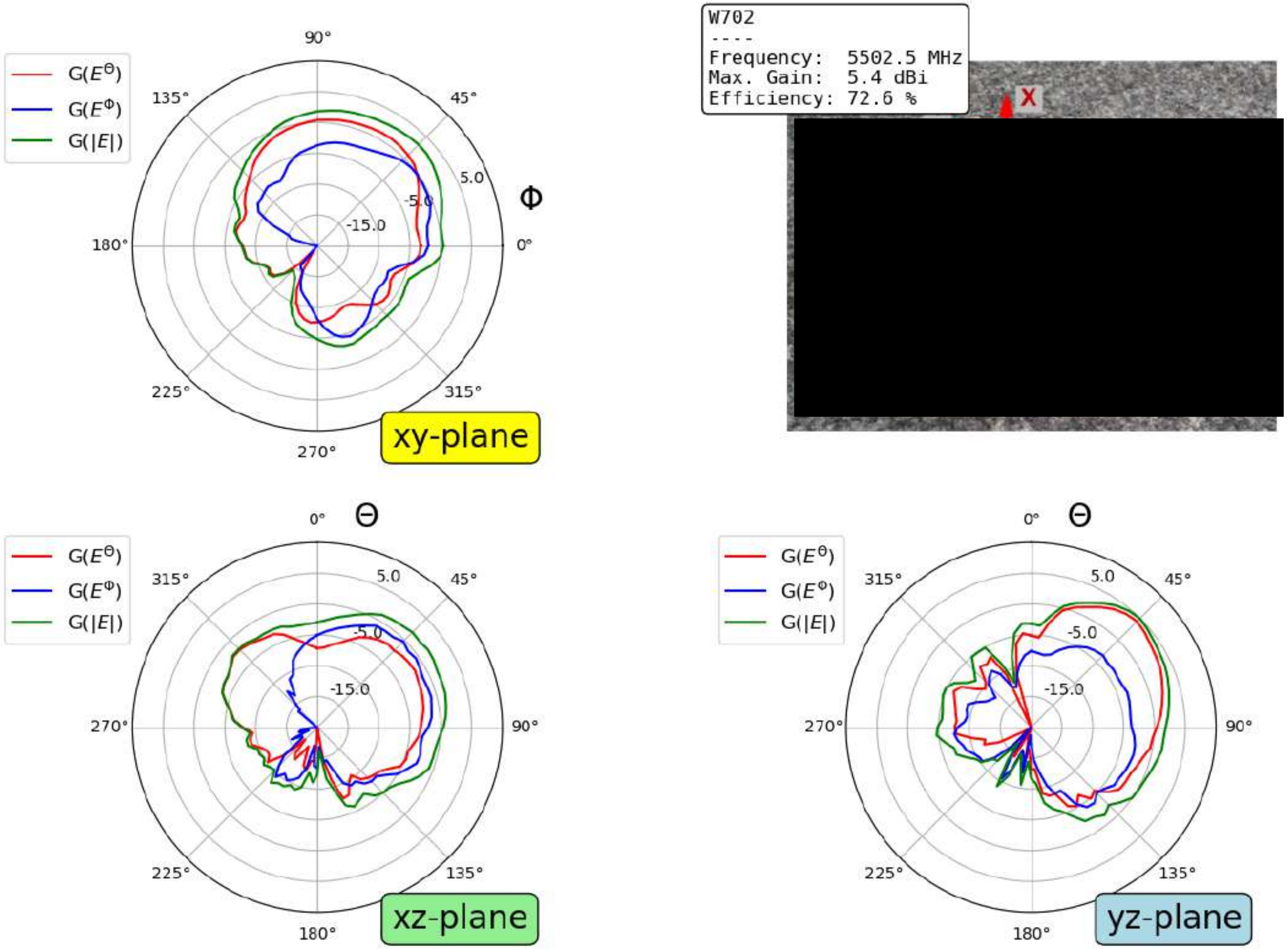

Figure 9-15: E-Theta/E-Phi/Sum Polar Diagram, W702 @ 5502.5 MHz

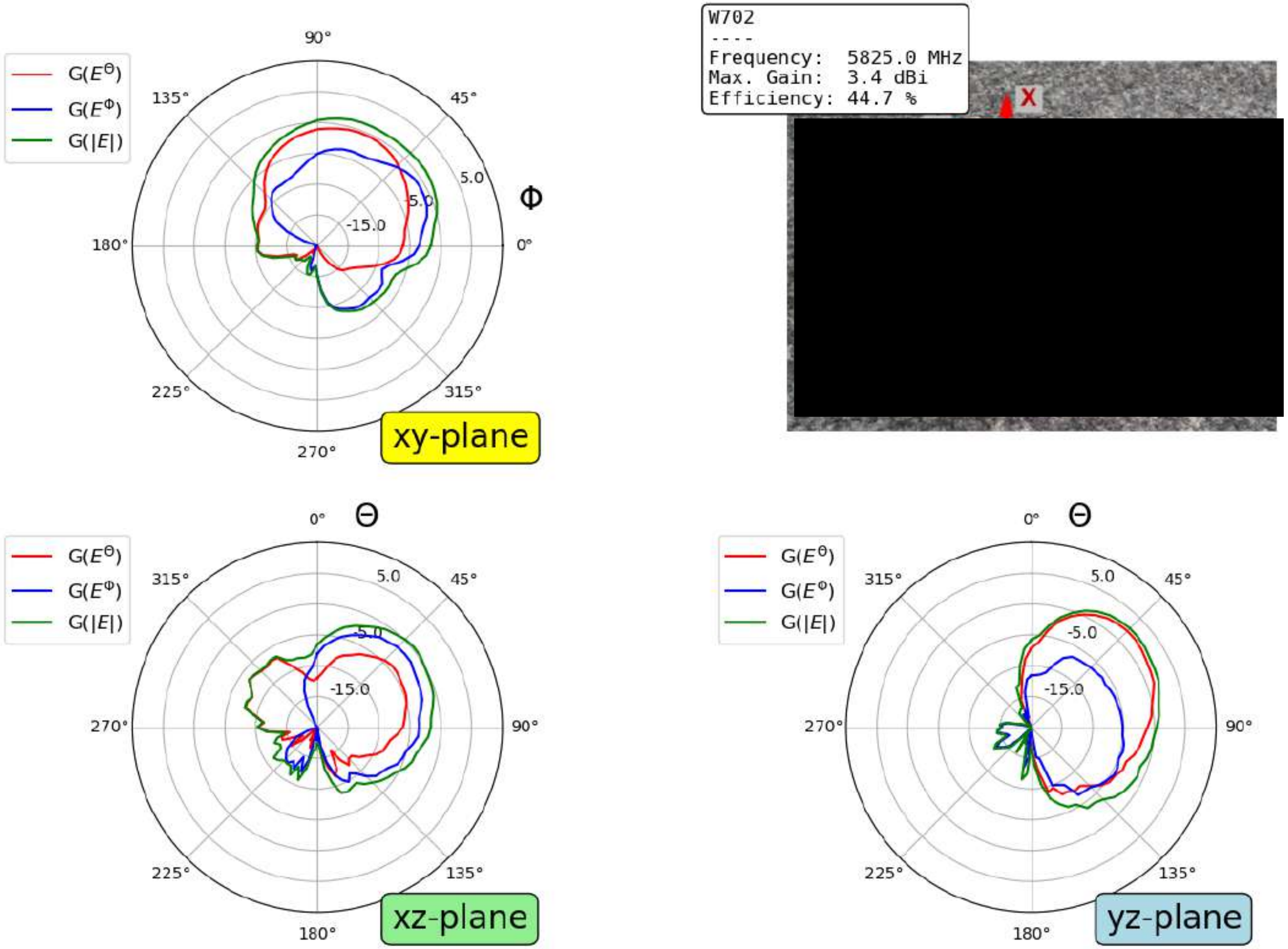

Figure 9-16: E-Theta/E-Phi/Sum Polar Diagram, W702 @ 5825 MHz

9.6 Intensity diagrams of the W701 antenna

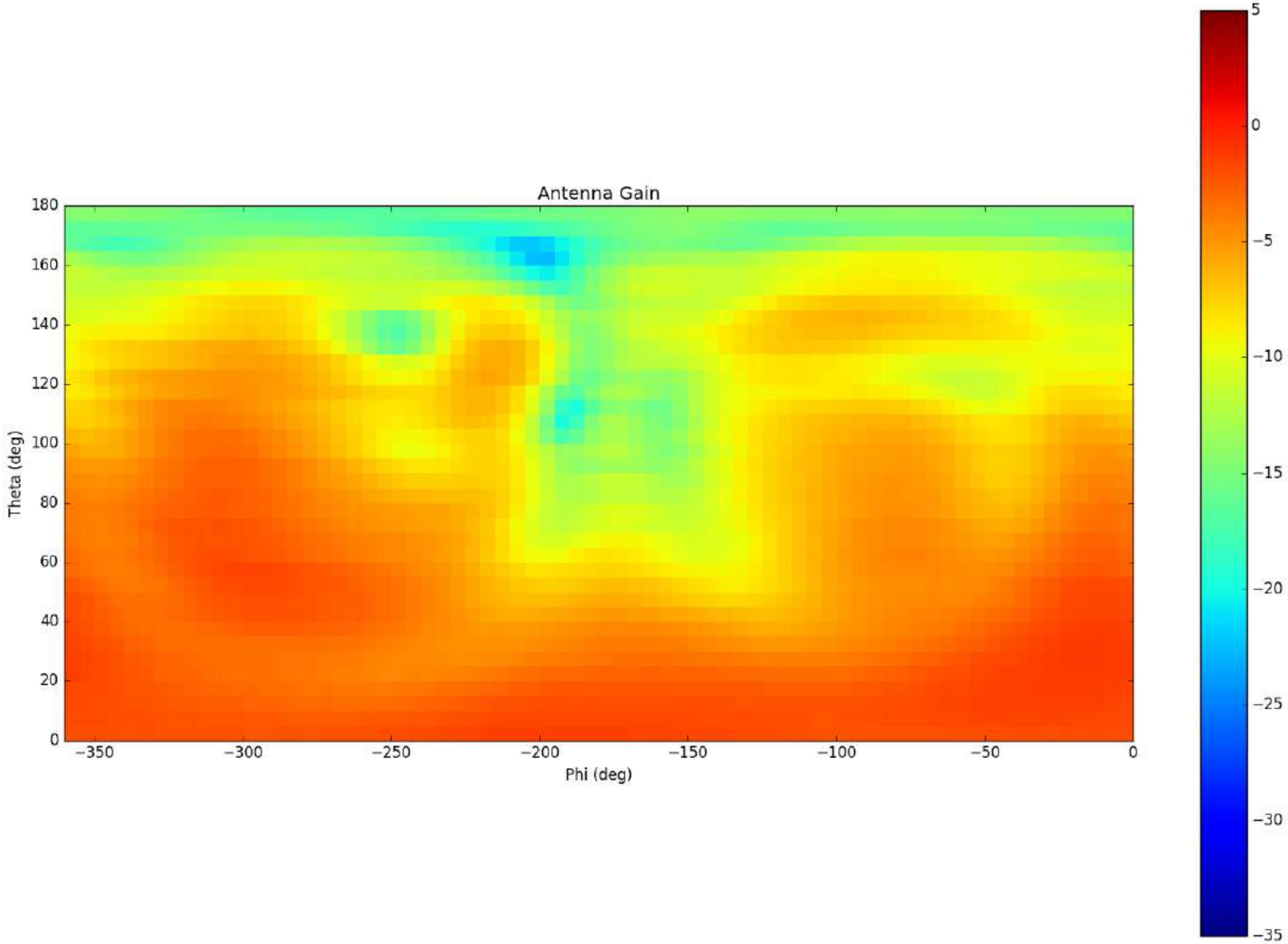

Figure 9-17: E-Theta Intensity Diagram, W701 @ 2412 MHz

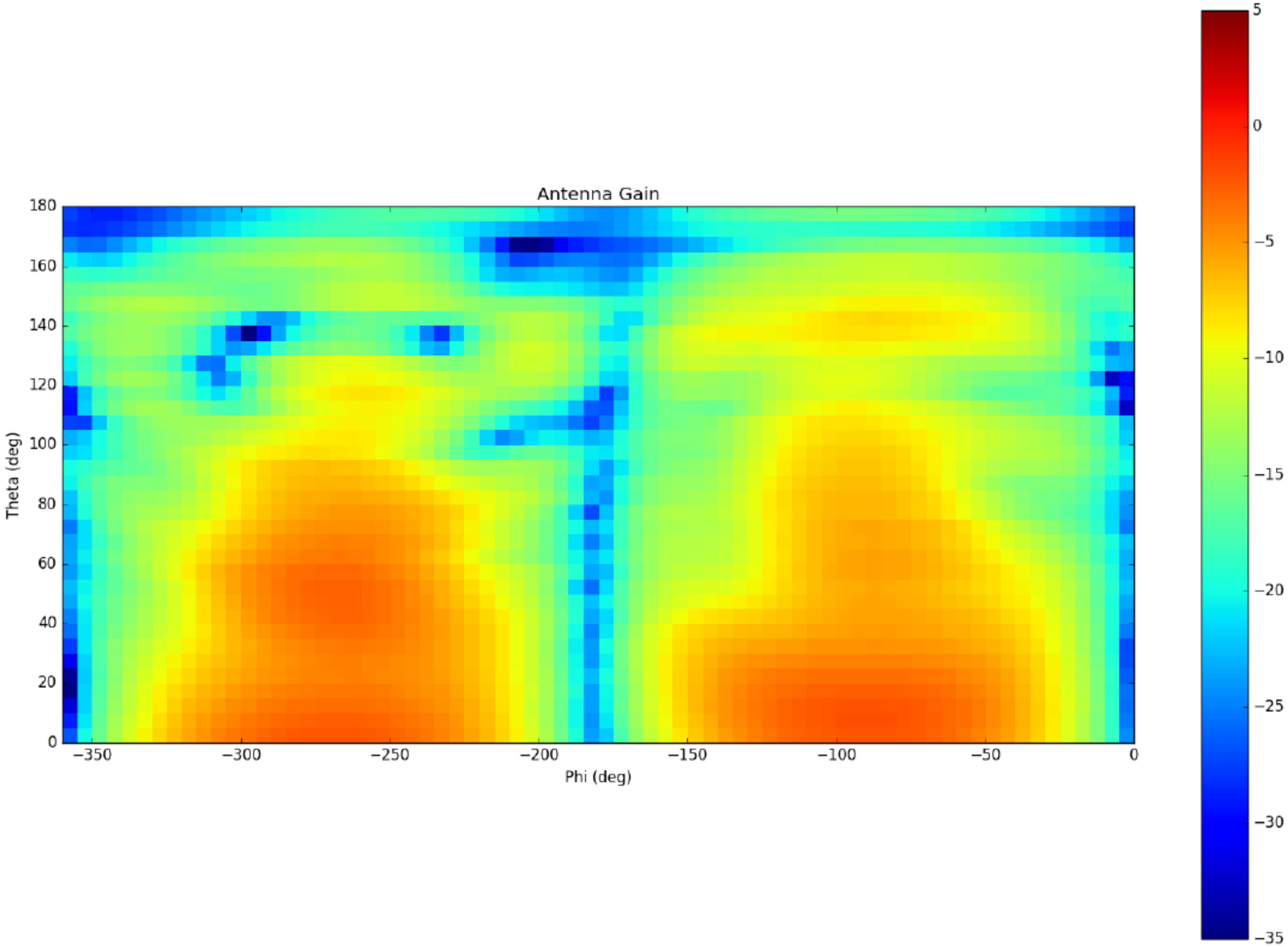

Figure 9-18: E-Phi Intensity Diagram, W701 @ 2412 MHz

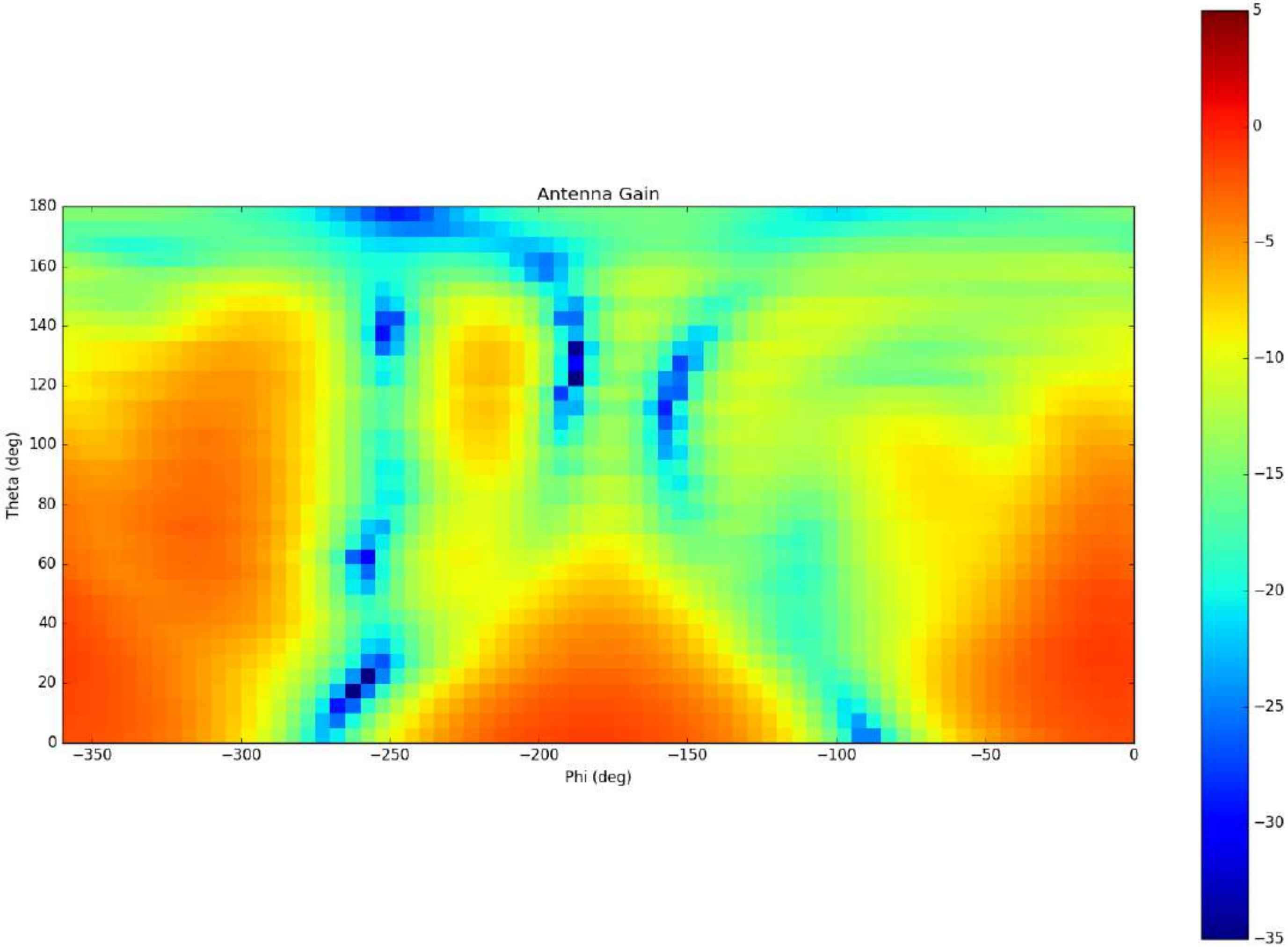

Figure 9-19: Sum Intensity Diagram, W701 @ 2412 MHz

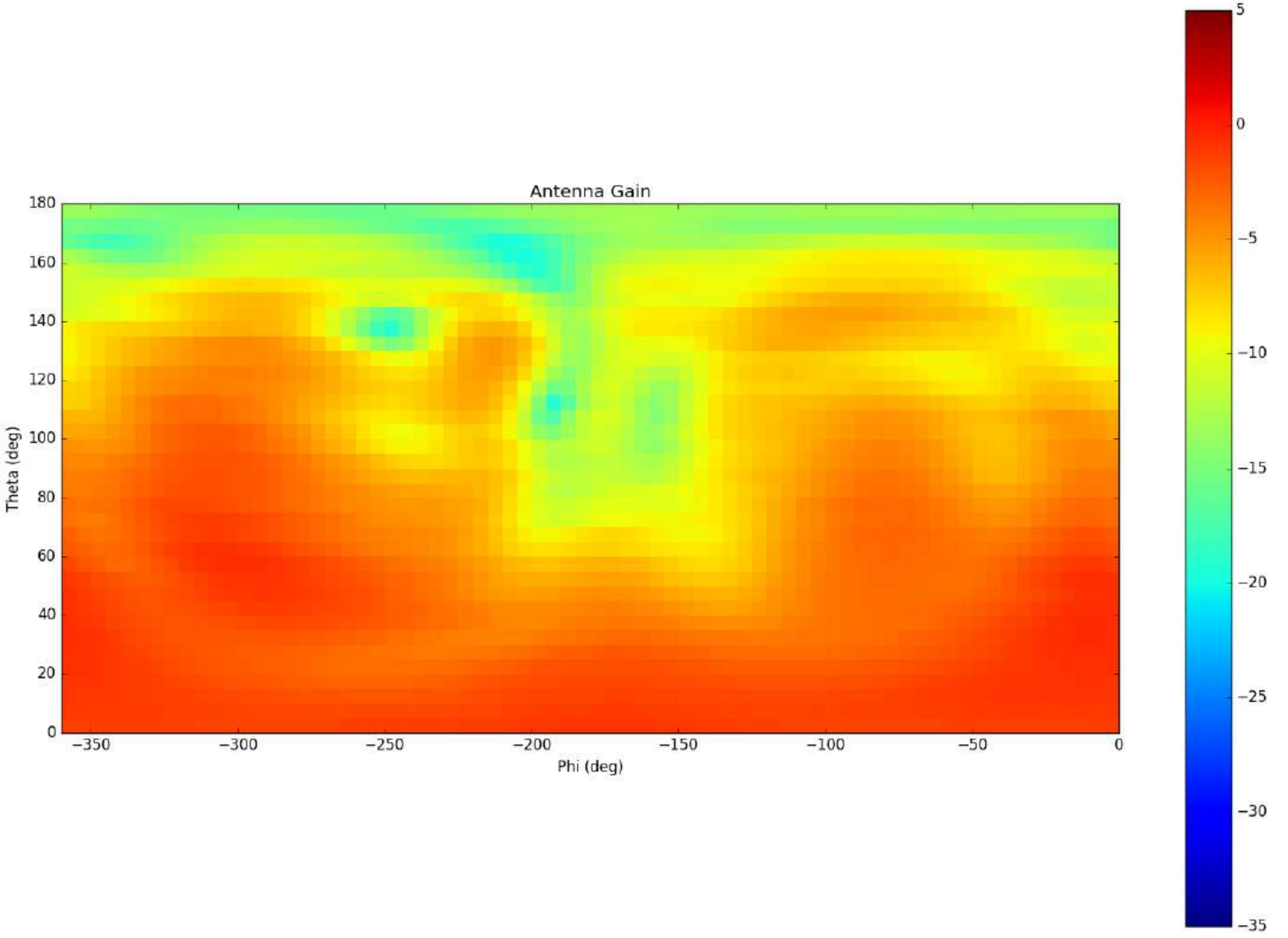

Figure 9-20: E-Theta Intensity Diagram, W701 @ 2448 MHz

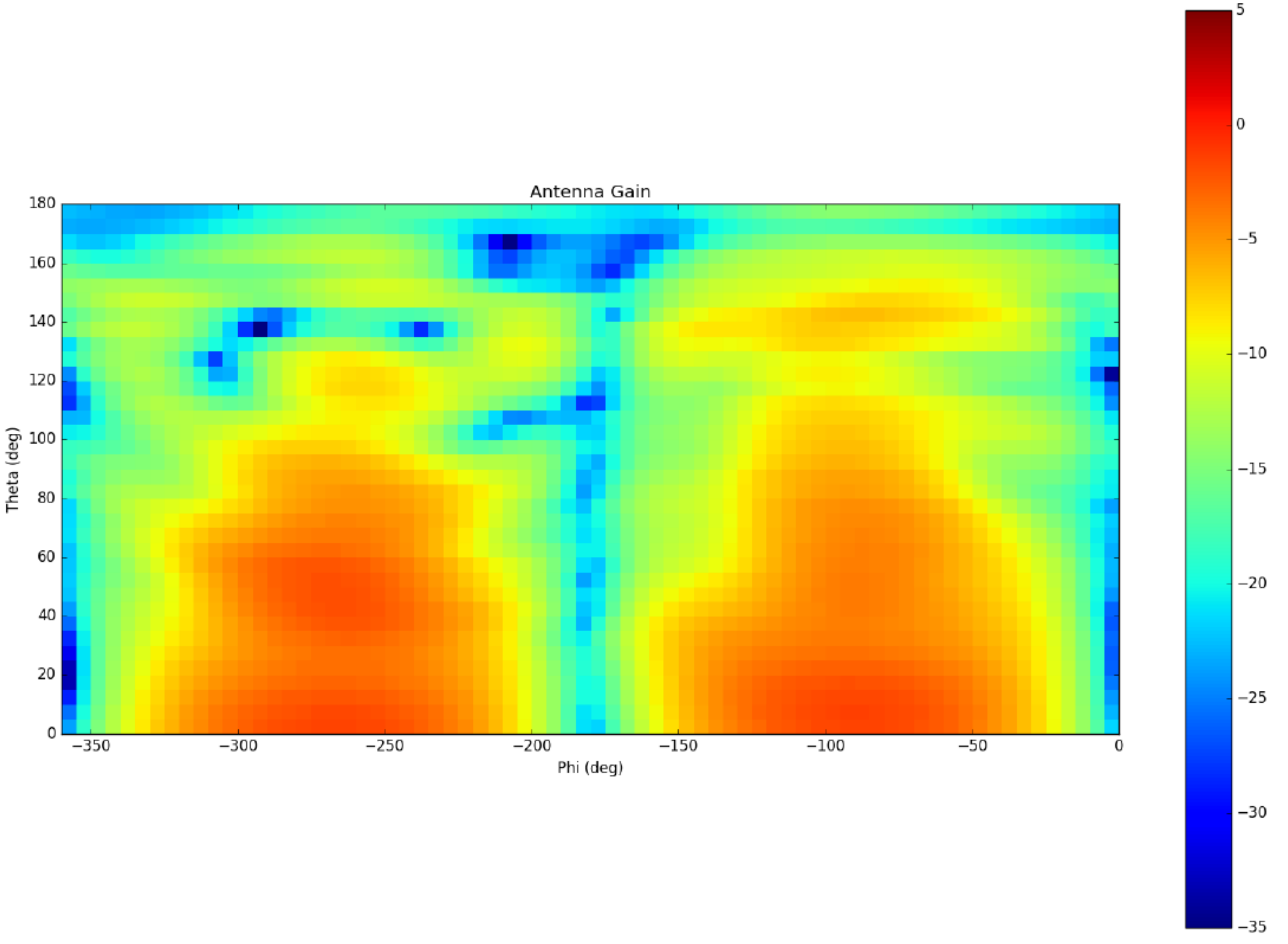

Figure 9-21: E-Phi Intensity Diagram, W701 @ 2448 MHz

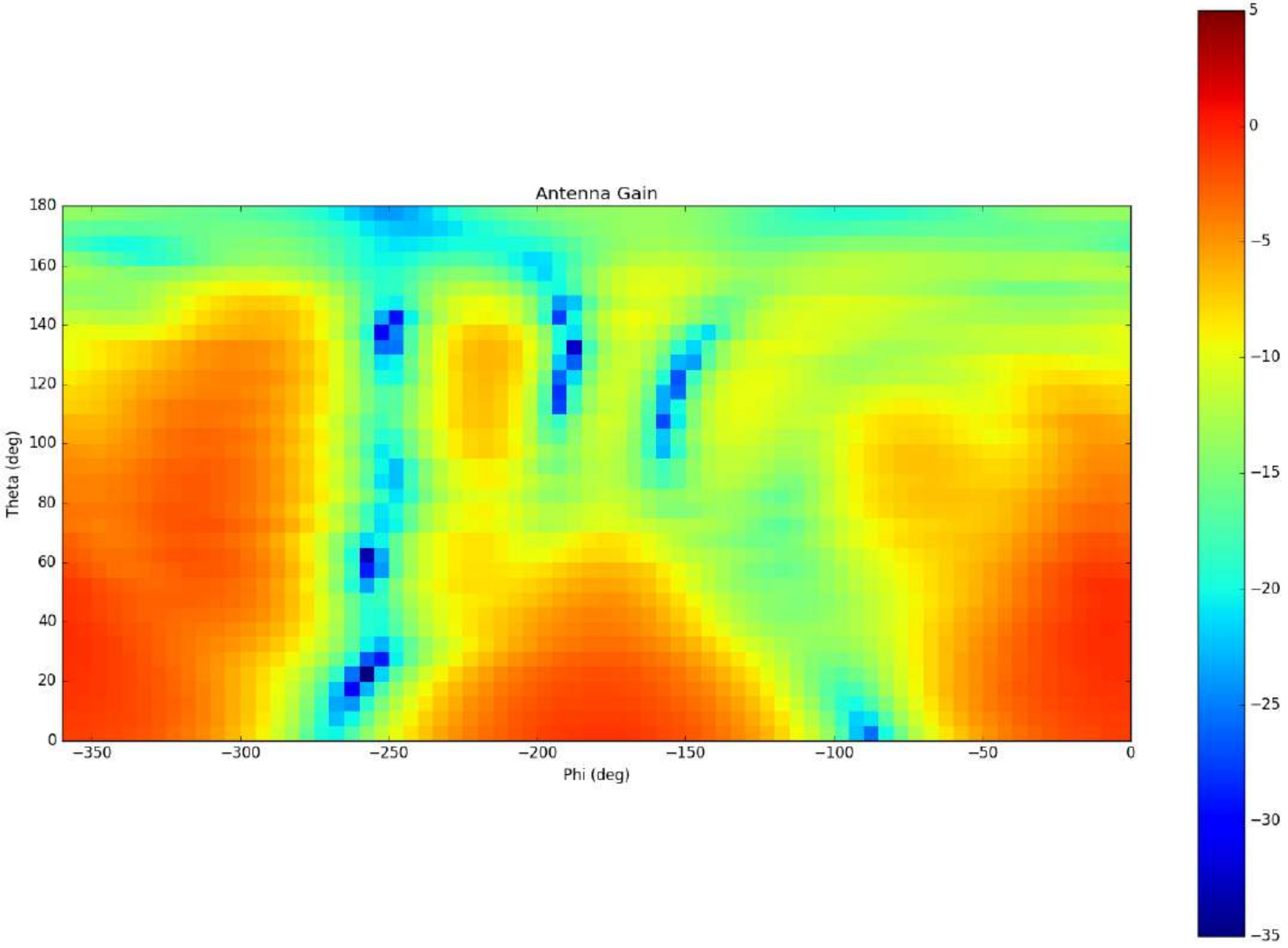

Figure 9-22: Sum Intensity Diagram, W701 @ 2448 MHz

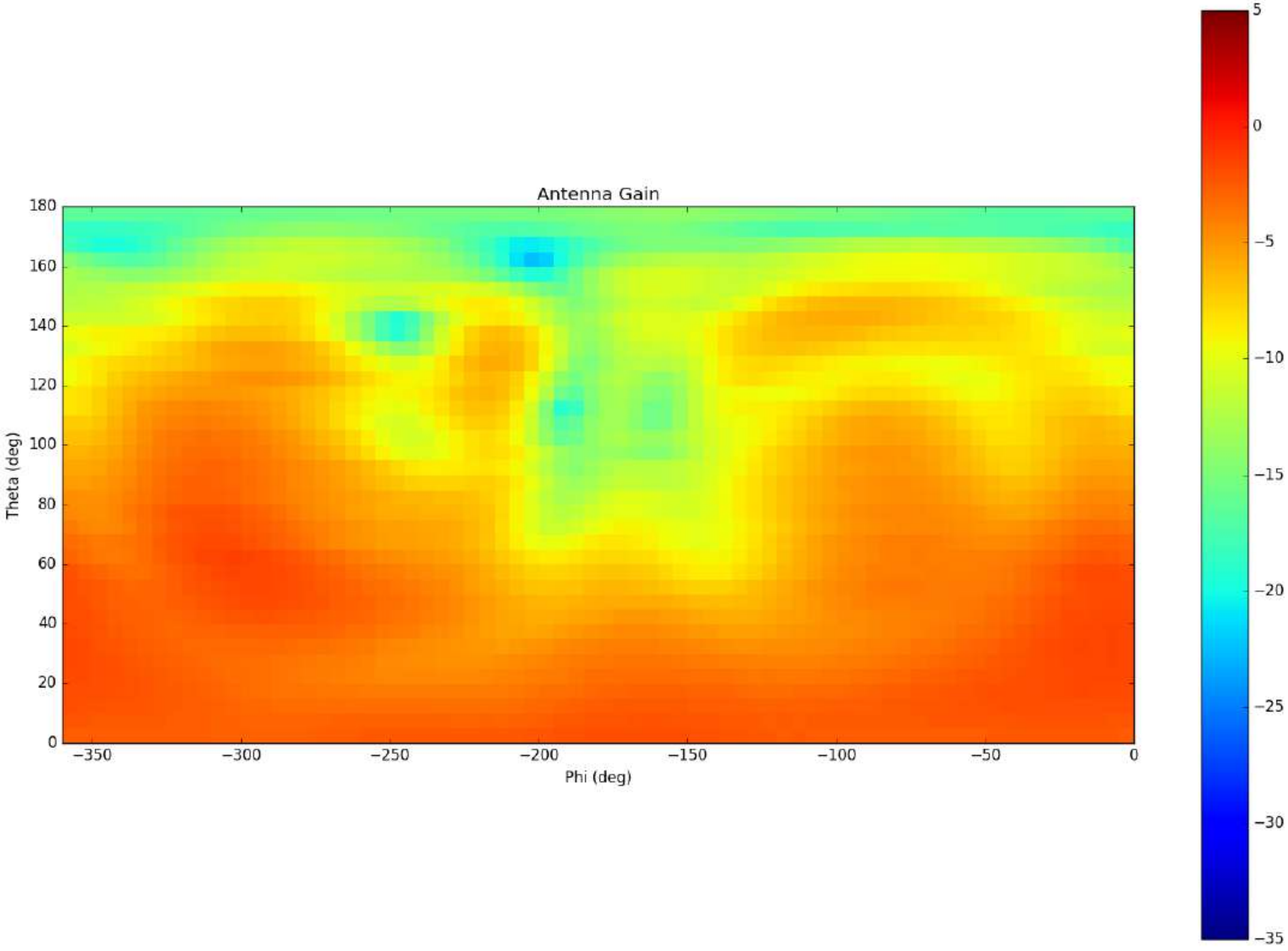

Figure 9-23: E-Theta Intensity Diagram, W701 @ 2484 MHz

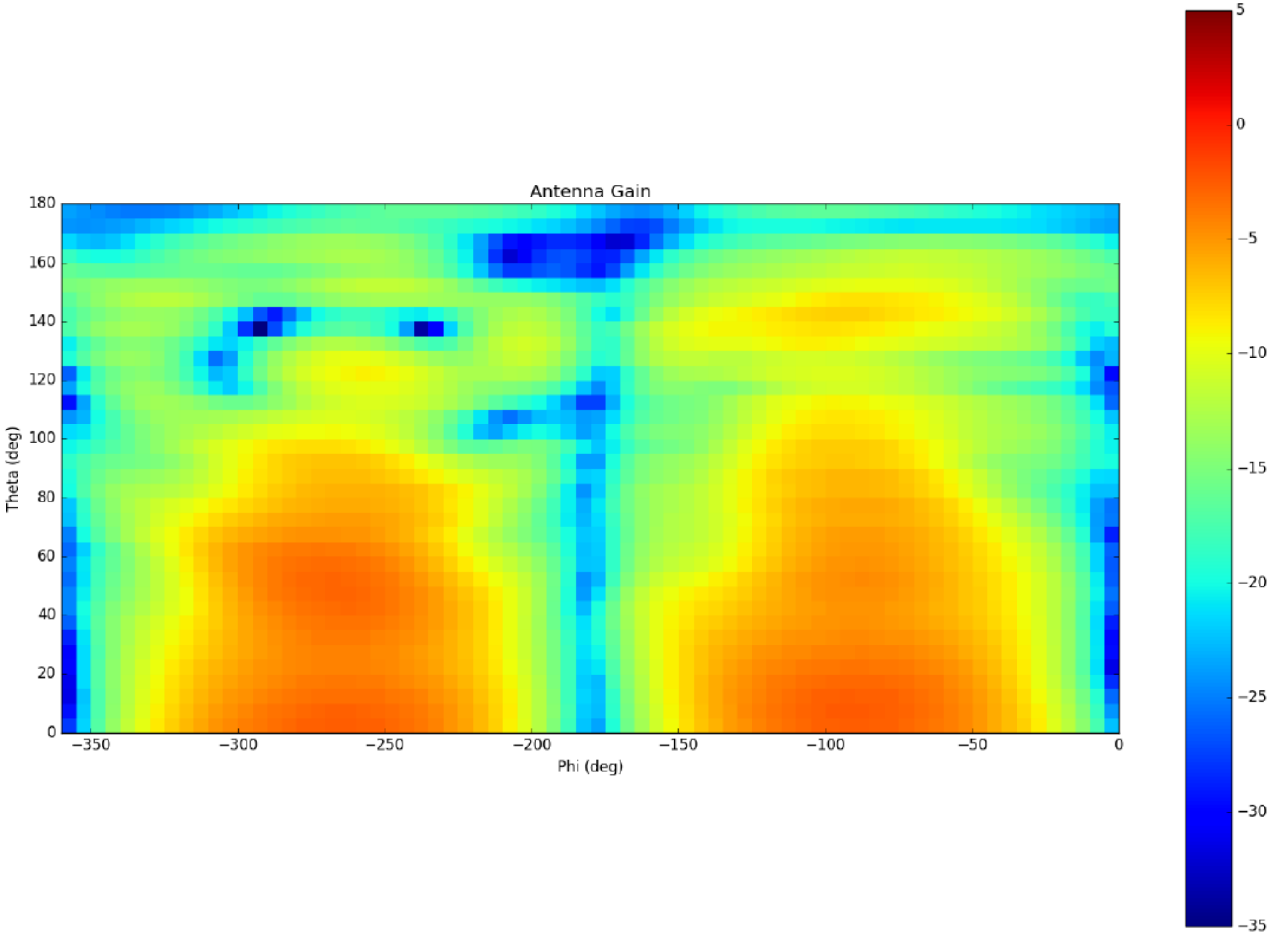

Figure 9-24: E-Phi Intensity Diagram, W701 @ 2484 MHz

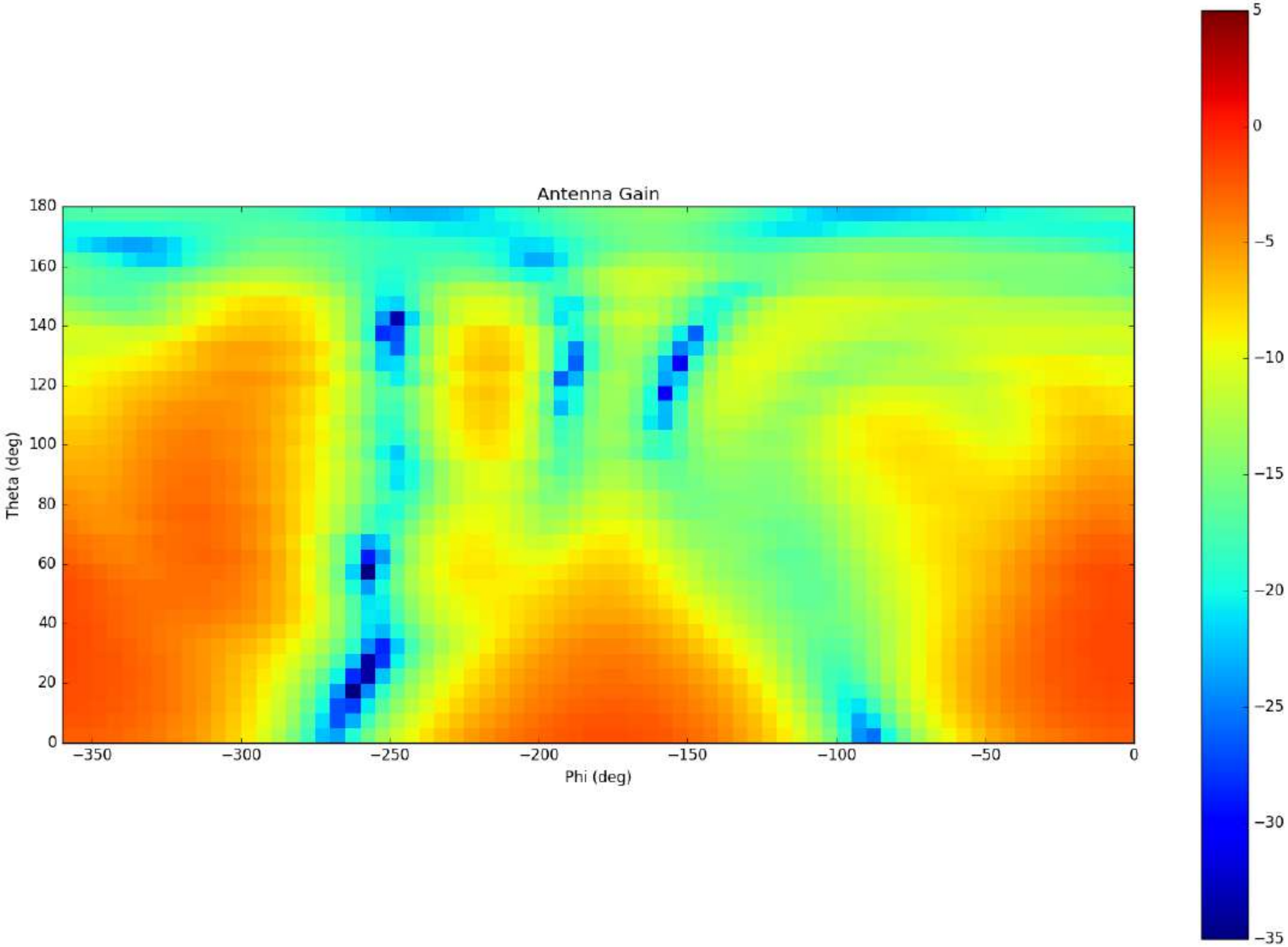

Figure 9-25: Sum Intensity Diagram, W701 @ 2484 MHz

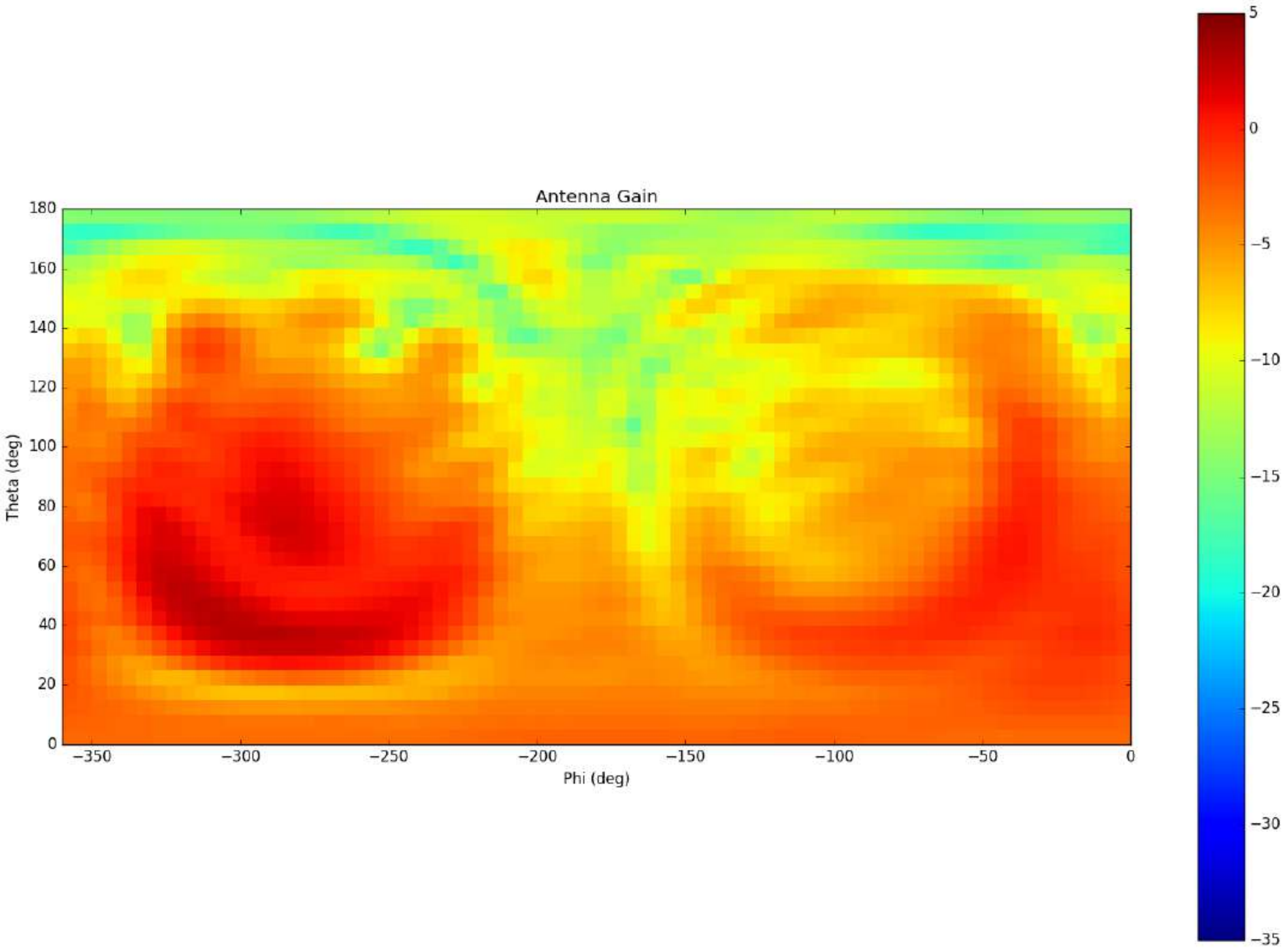

Figure 9-26: E-Theta Intensity Diagram, W701 @ 5180 MHz

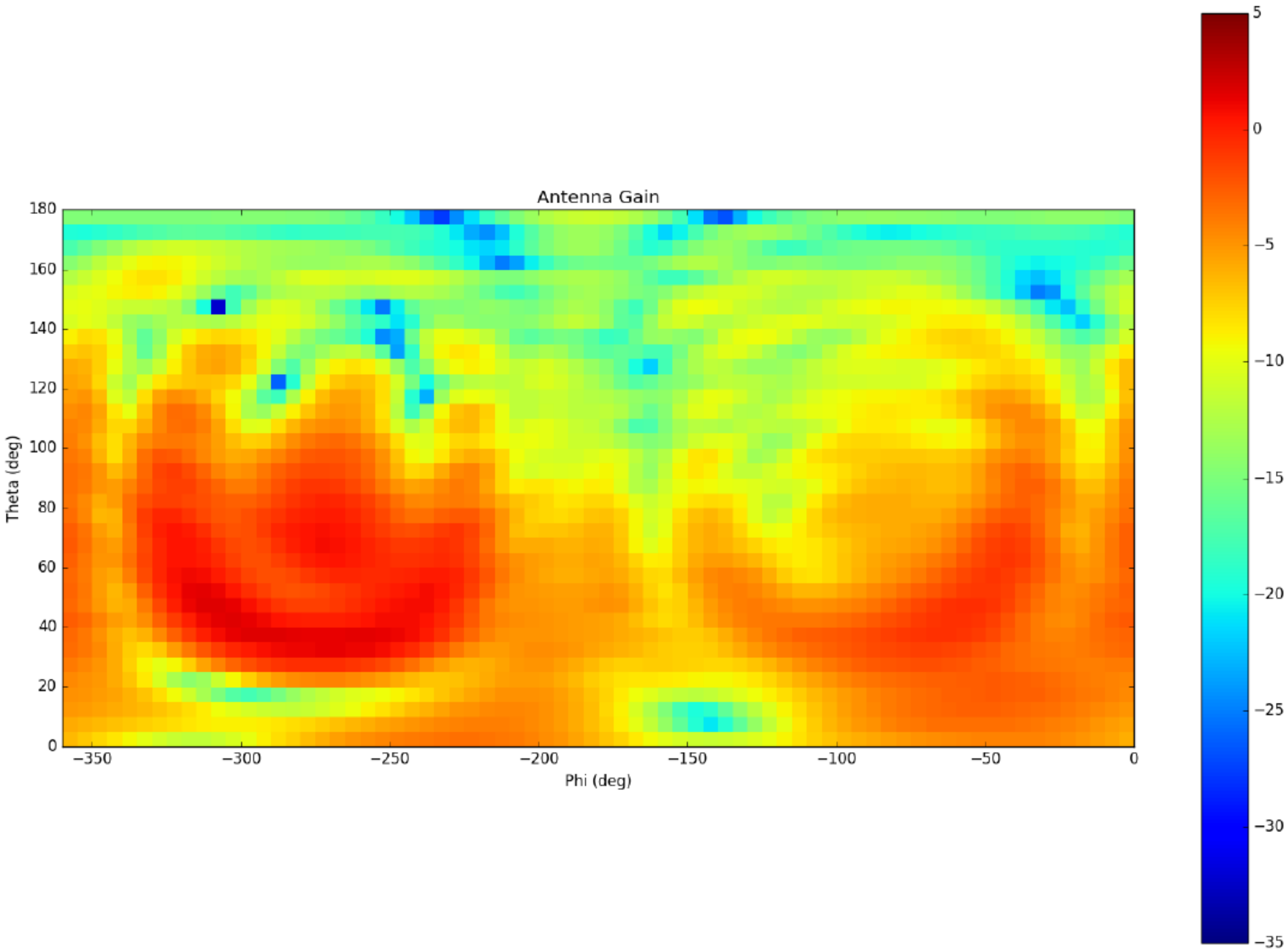

Figure 9-27: E-Phi Intensity Diagram, W701 @ 5180 MHz

Meas.-Report_Bosch_Car_Multi_Media_8000_6220126_2300206_01.docx\24.02.2023\V1.0\SW

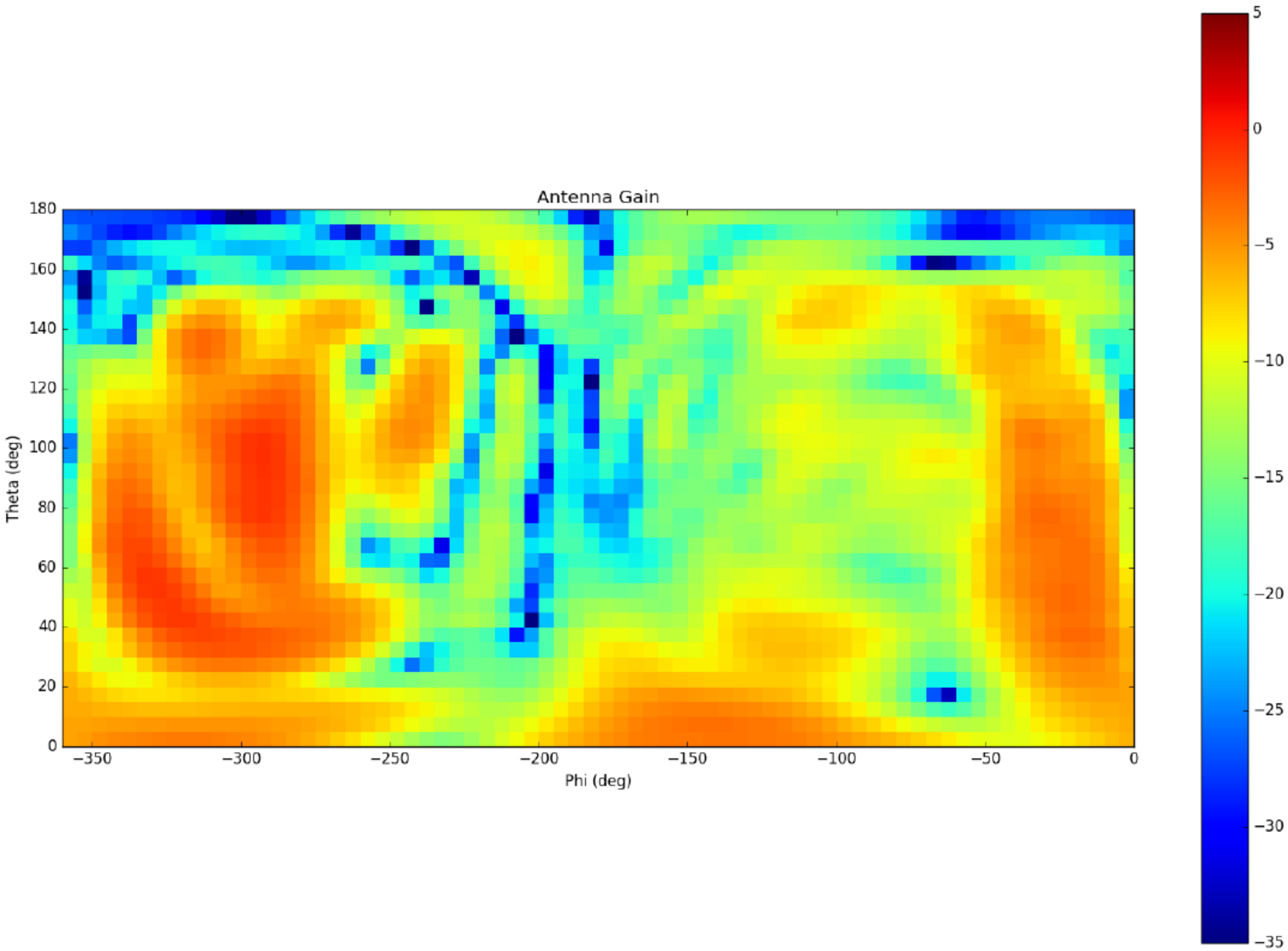

Figure 9-28: Sum Intensity Diagram, W701 @ 5180 MHz

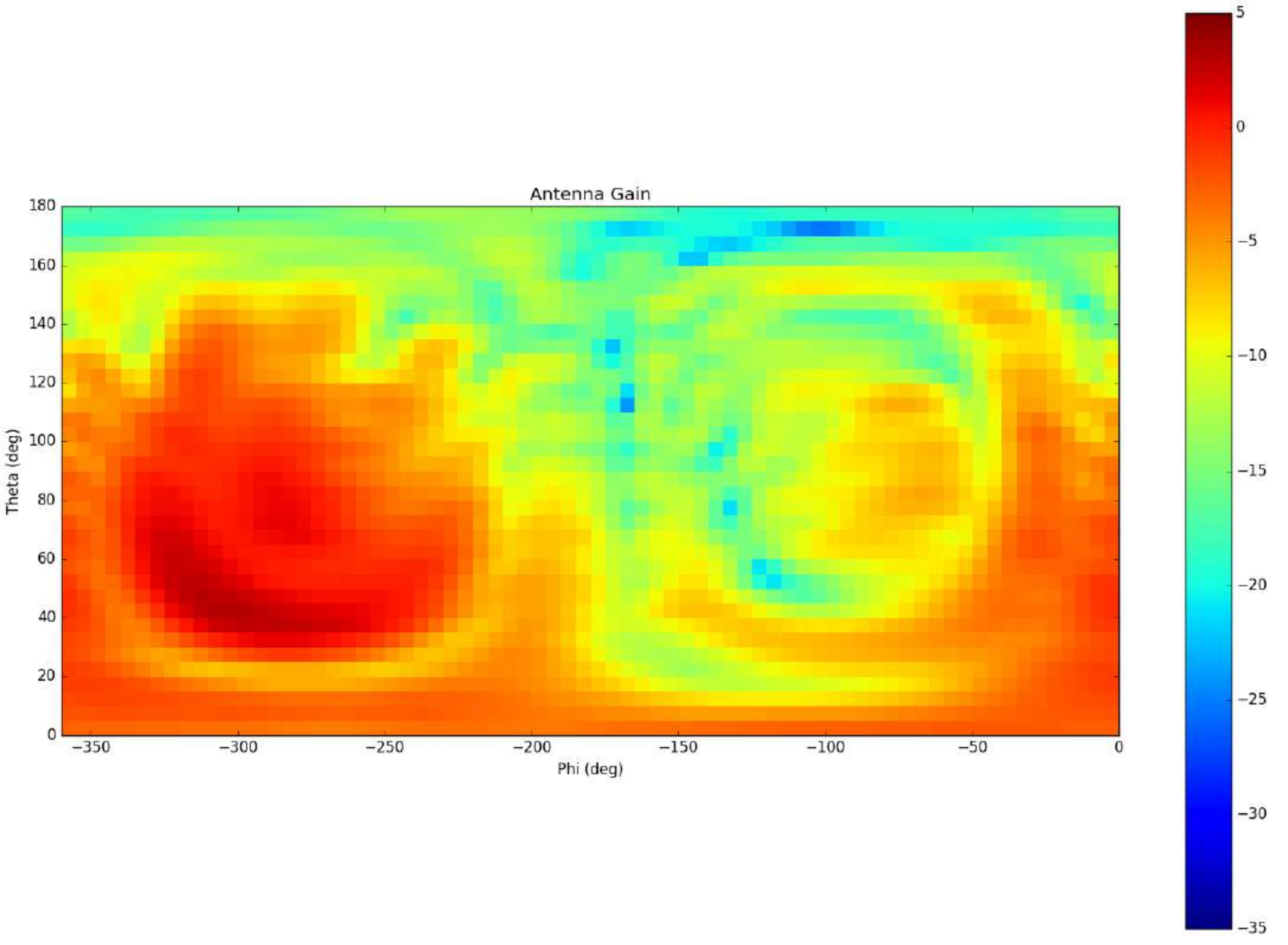

Figure 9-29: E-Theta Intensity Diagram, W701 @ 5502.5 MHz

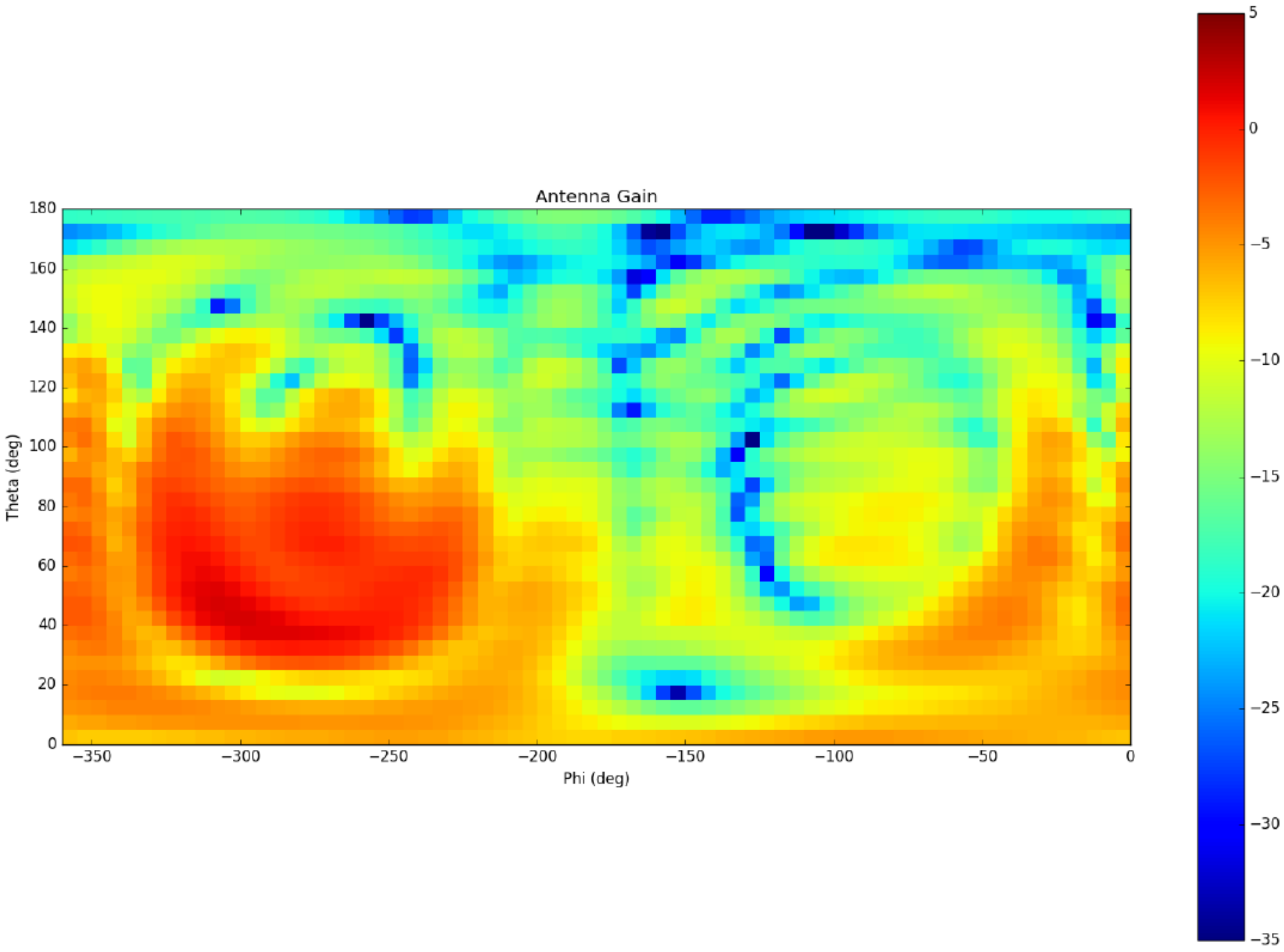

Figure 9-30: E-Phi Intensity Diagram, W701 @ 5502.5 MHz

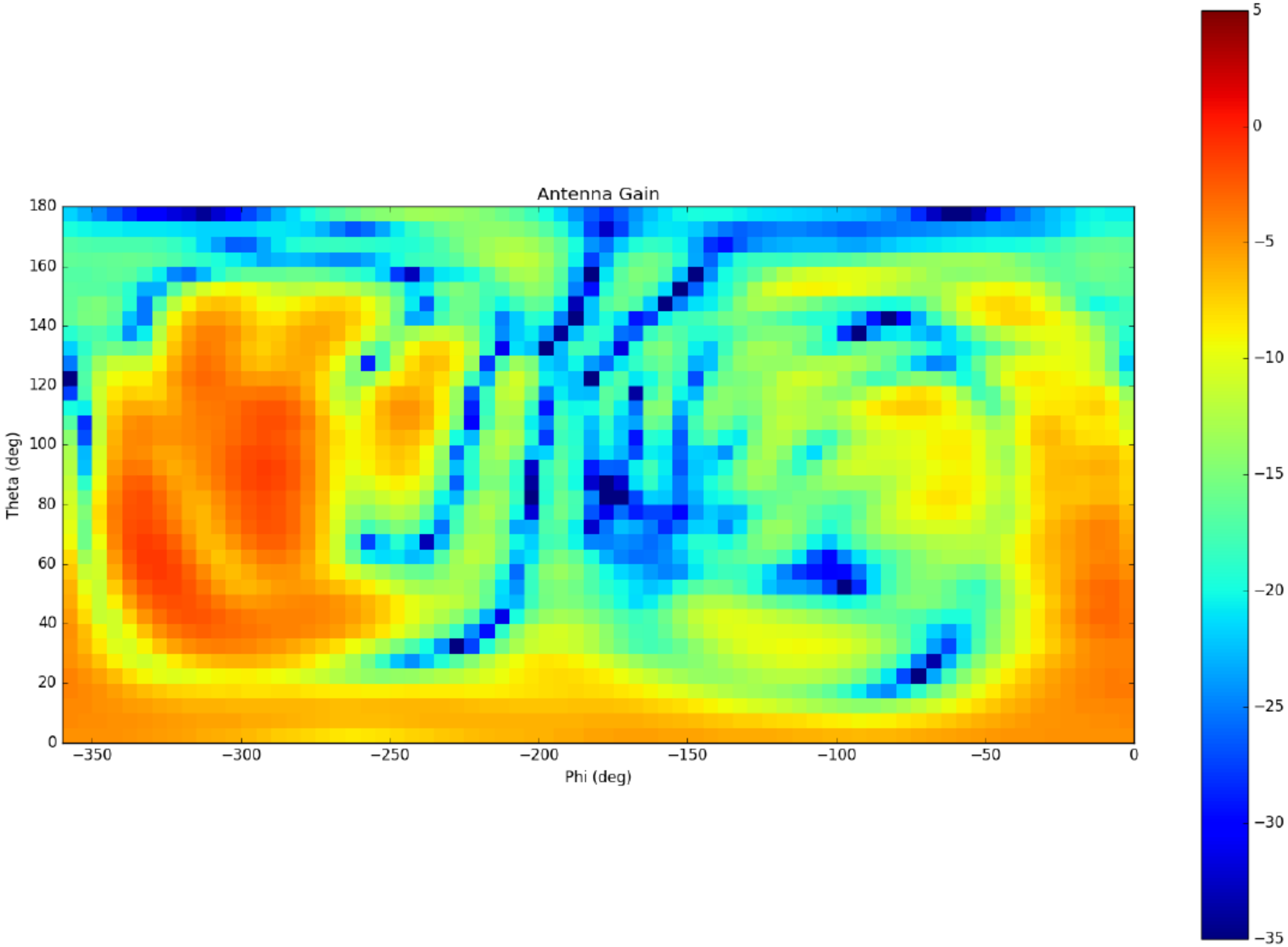

Figure 9-31: Sum Intensity Diagram, W701 @ 5502.5 MHz

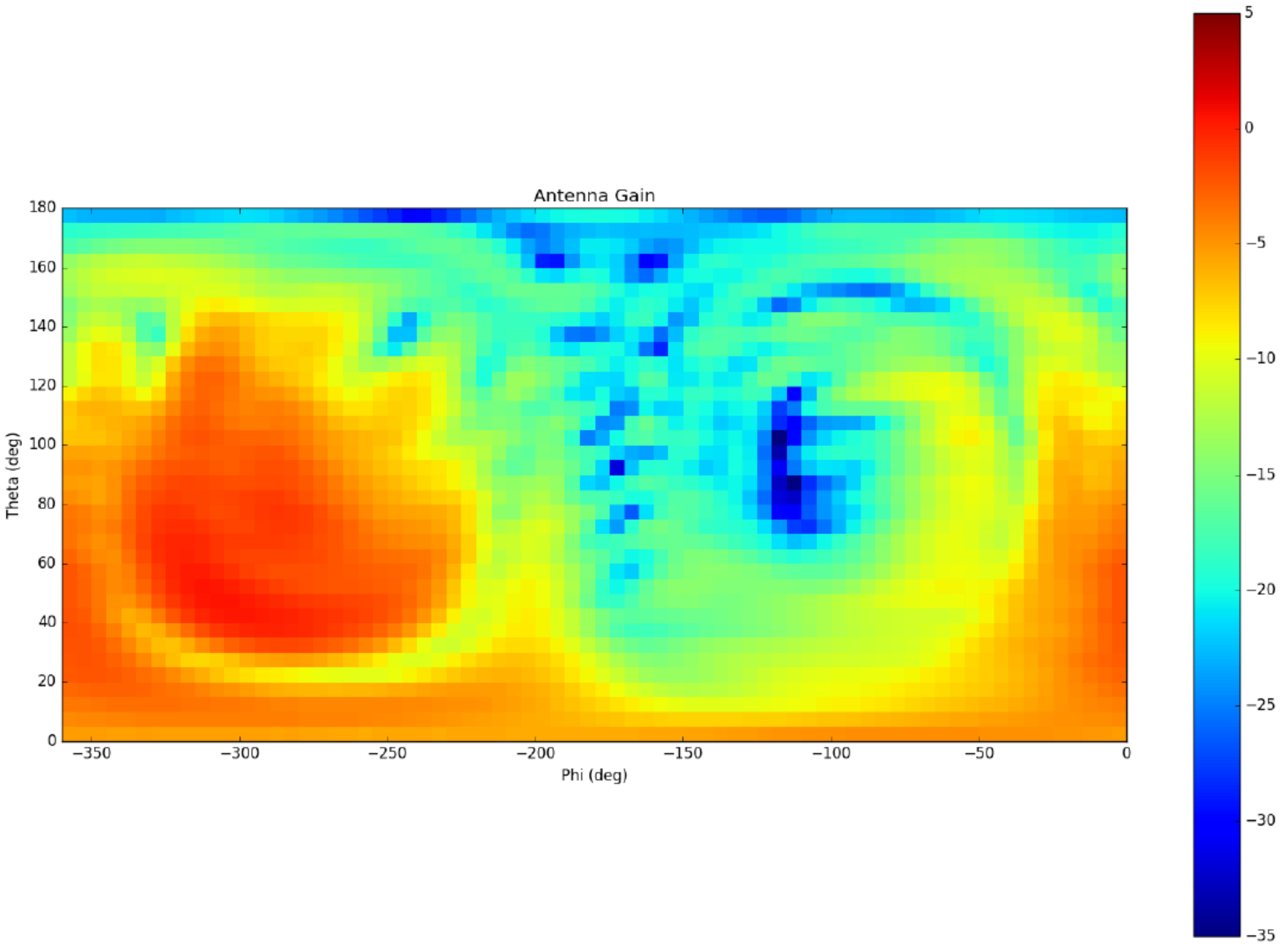

Figure 9-32: E-Theta Intensity Diagram, W701 @ 5825 MHz

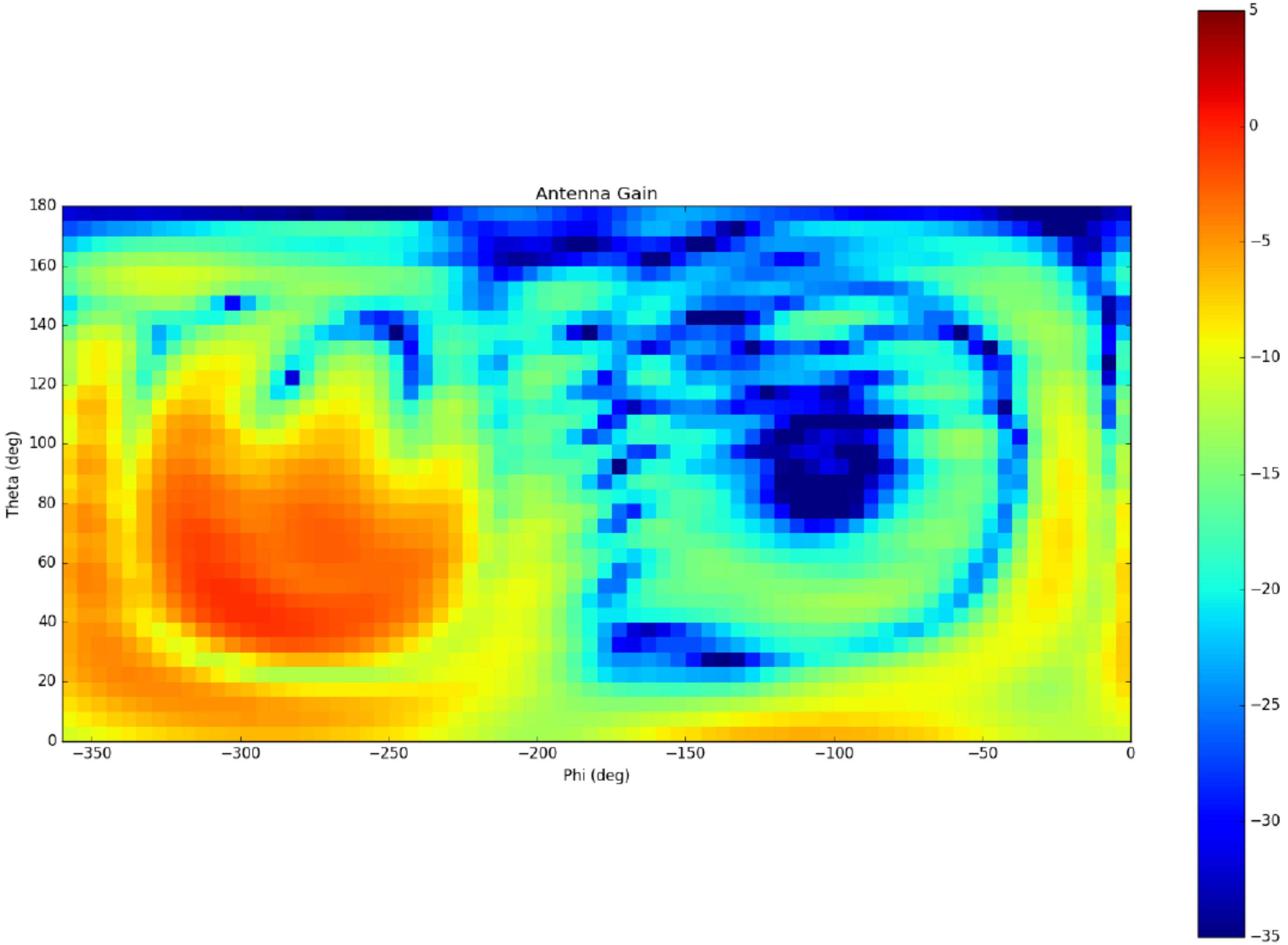

Figure 9-33: E-Phi Intensity Diagram, W701 @ 5825 MHz

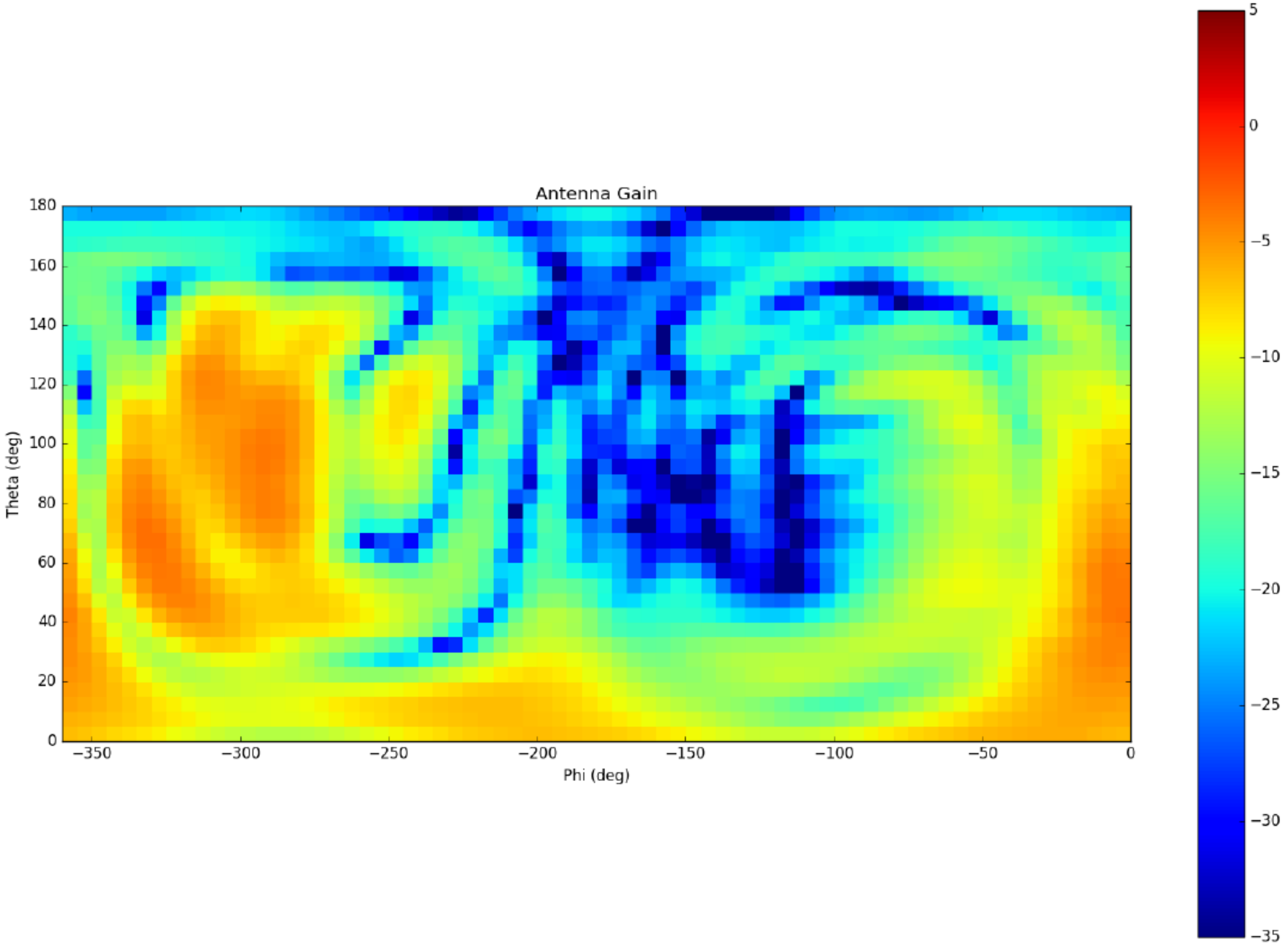

Figure 9-34: Sum Intensity Diagram, W701 @ 5825 MHz

9.7 Intensity diagrams of the W702 antenna

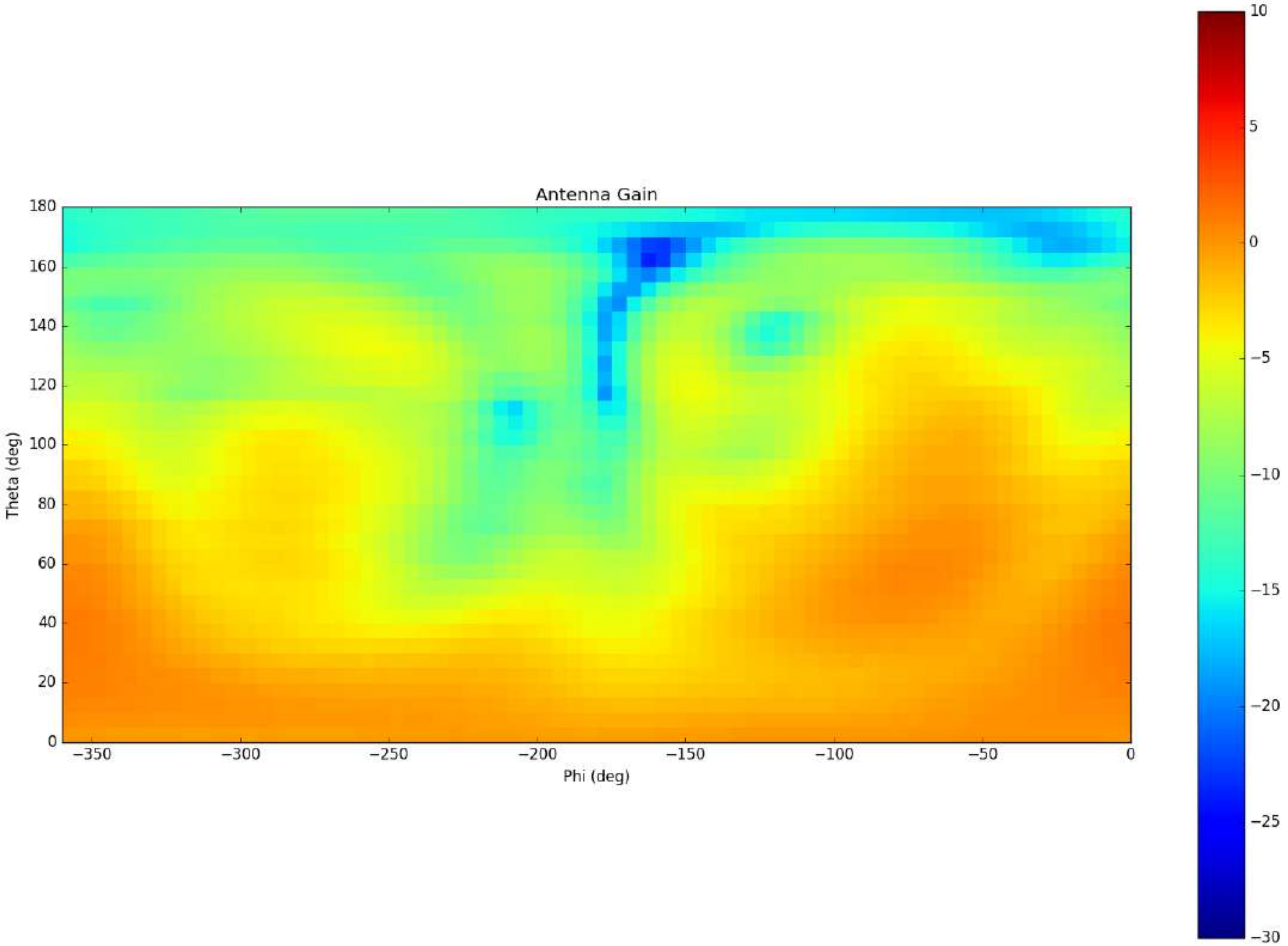

Figure 9-35: E-Theta Intensity Diagram, W702 @ 2412 MHz

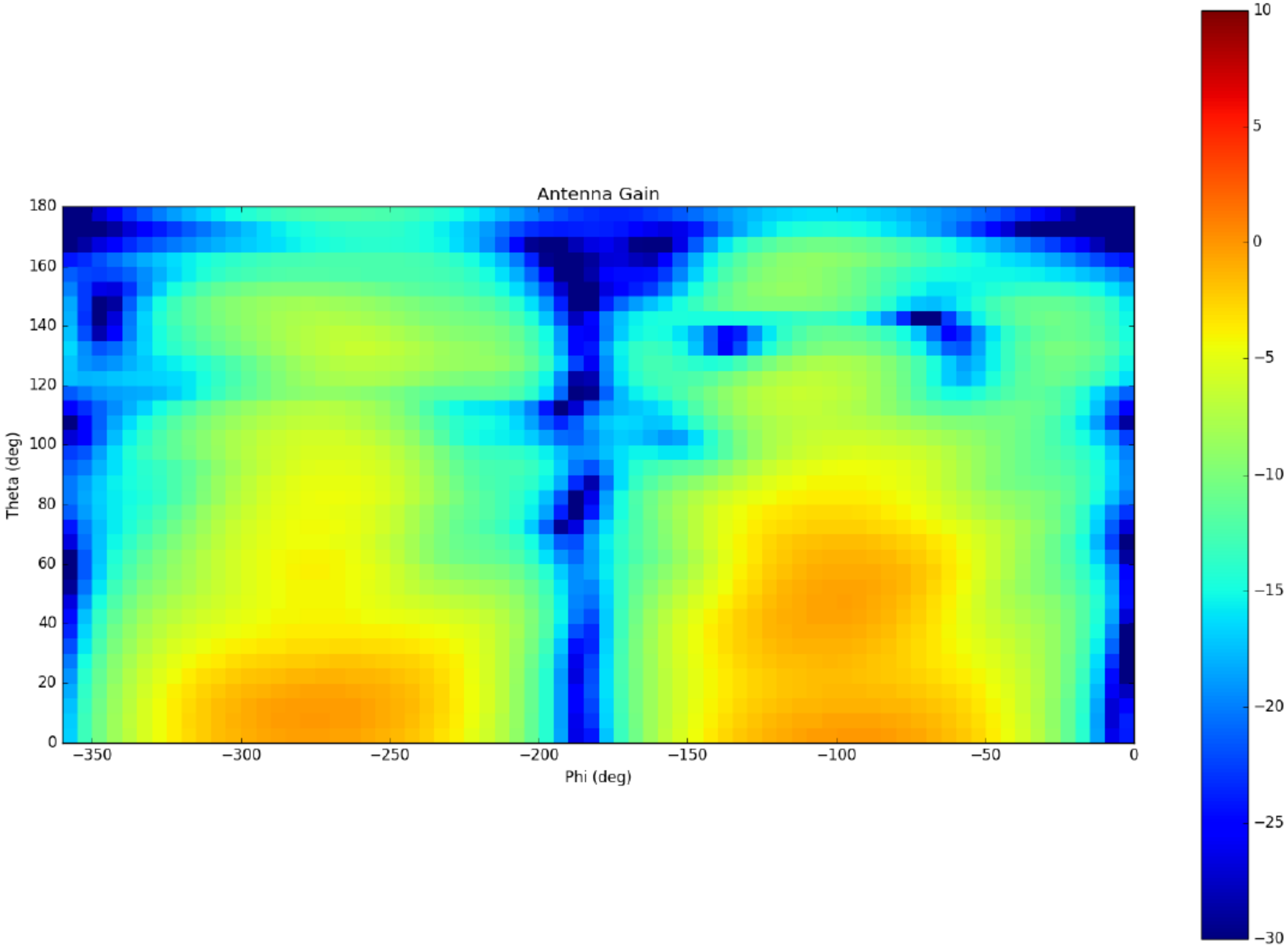

Figure 9-36: E-Phi Intensity Diagram, W702 @ 2412 MHz

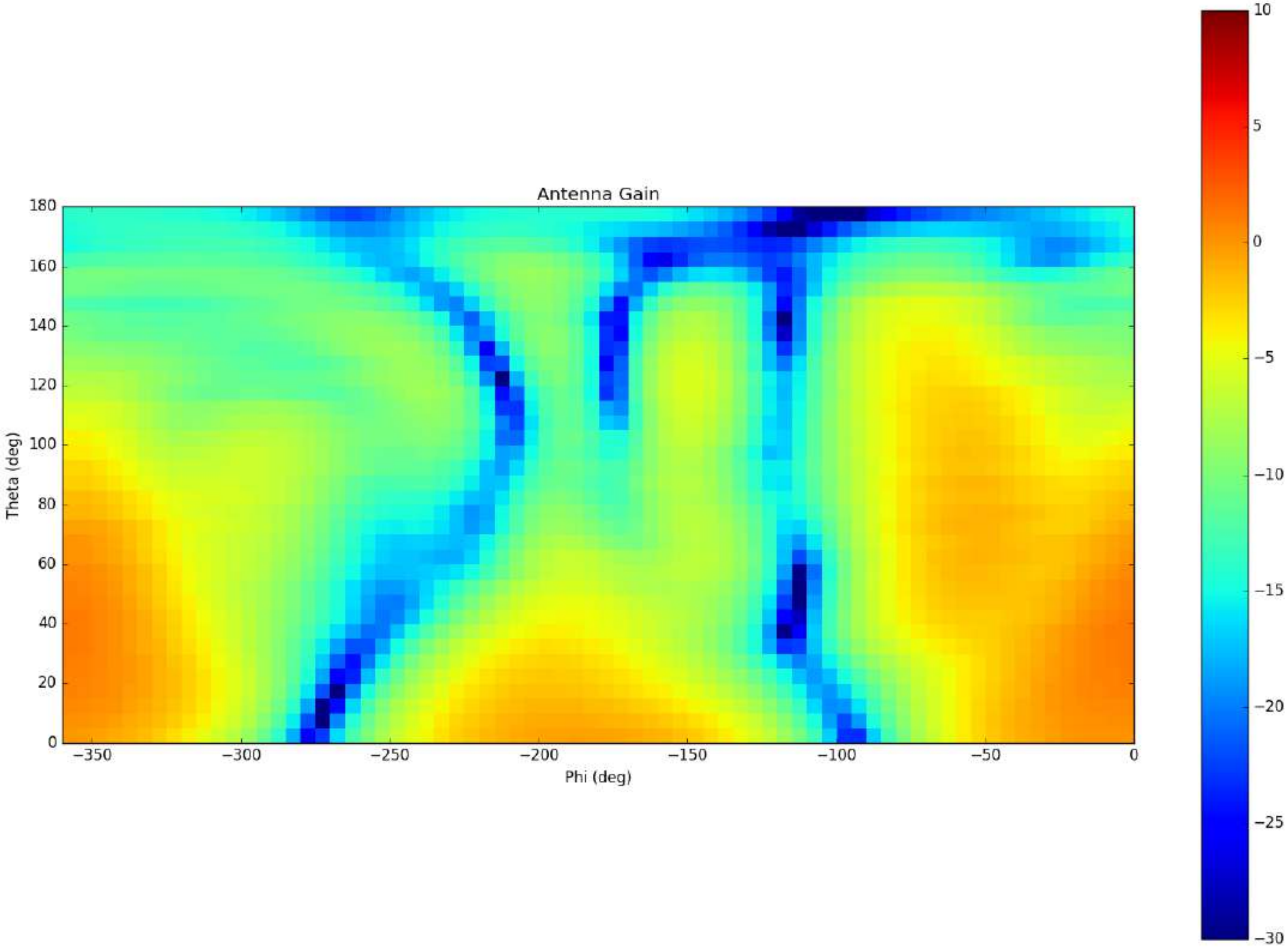

Figure 9-37: Sum Intensity Diagram, W702 @ 2412 MHz

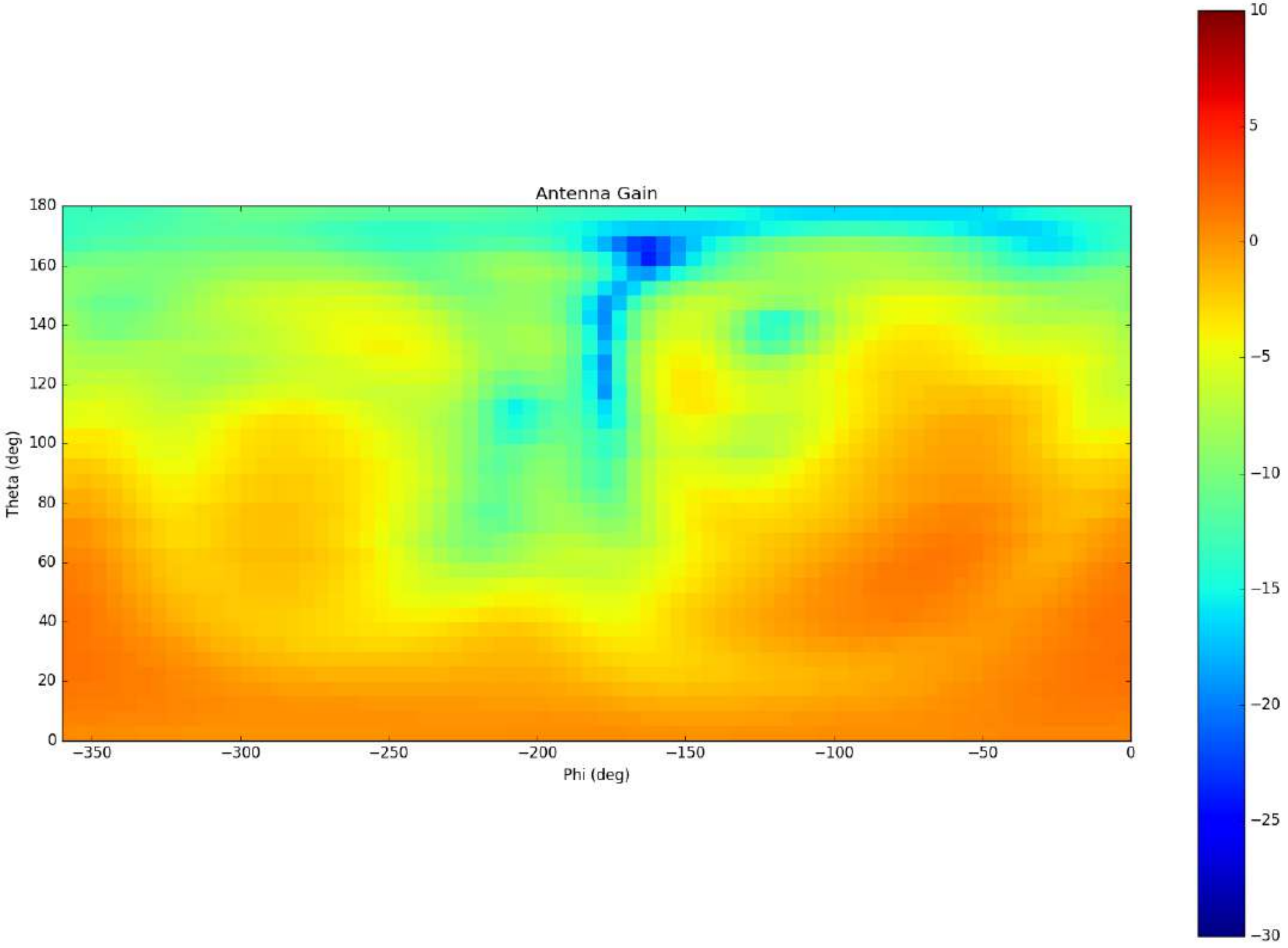

Figure 9-38: E-Theta Intensity Diagram, W702 @ 2448 MHz

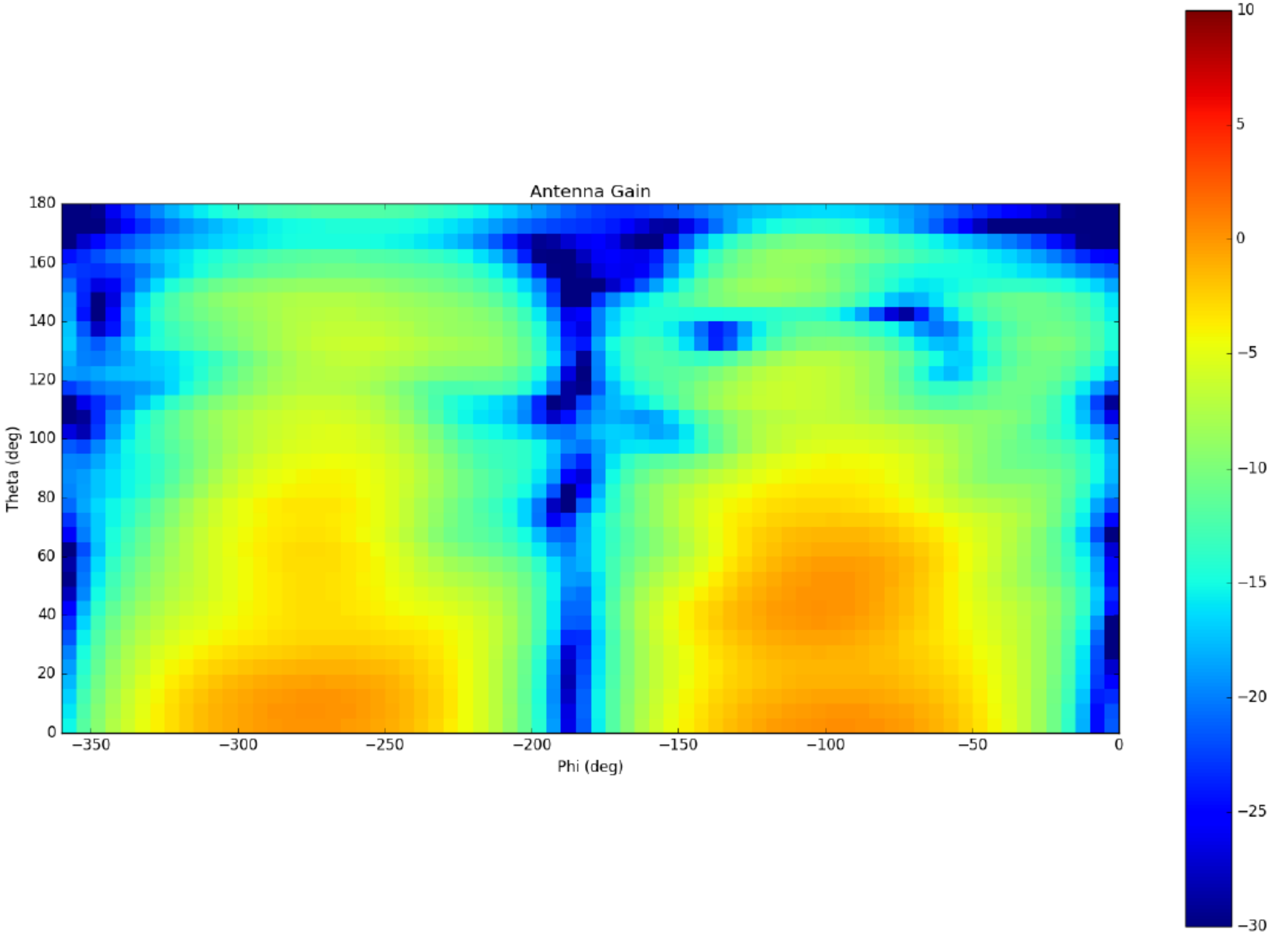

Figure 9-39: E-Phi Intensity Diagram, W702 @ 2448 MHz

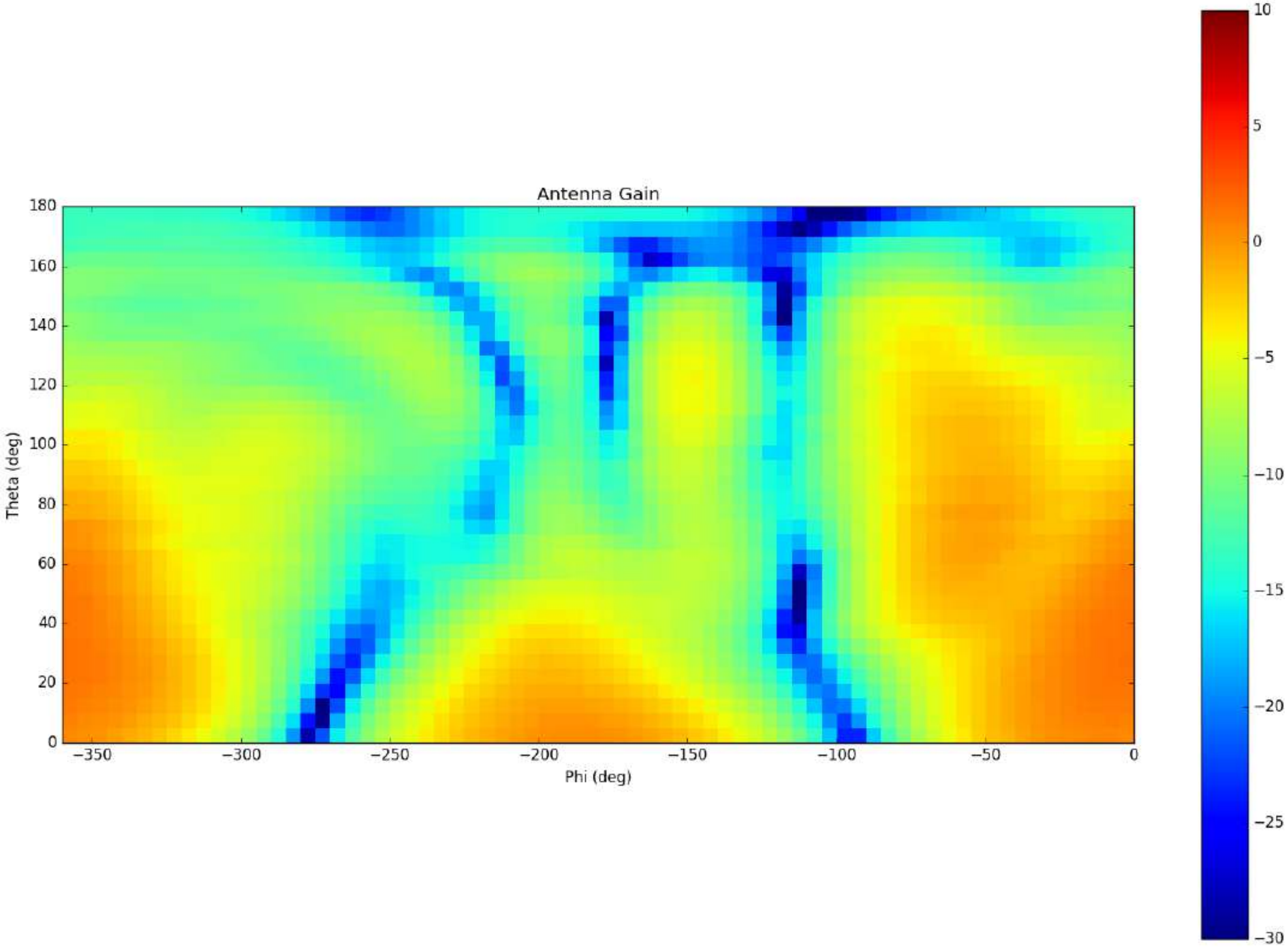

Figure 9-40: Sum Intensity Diagram, W702 @ 2448 MHz

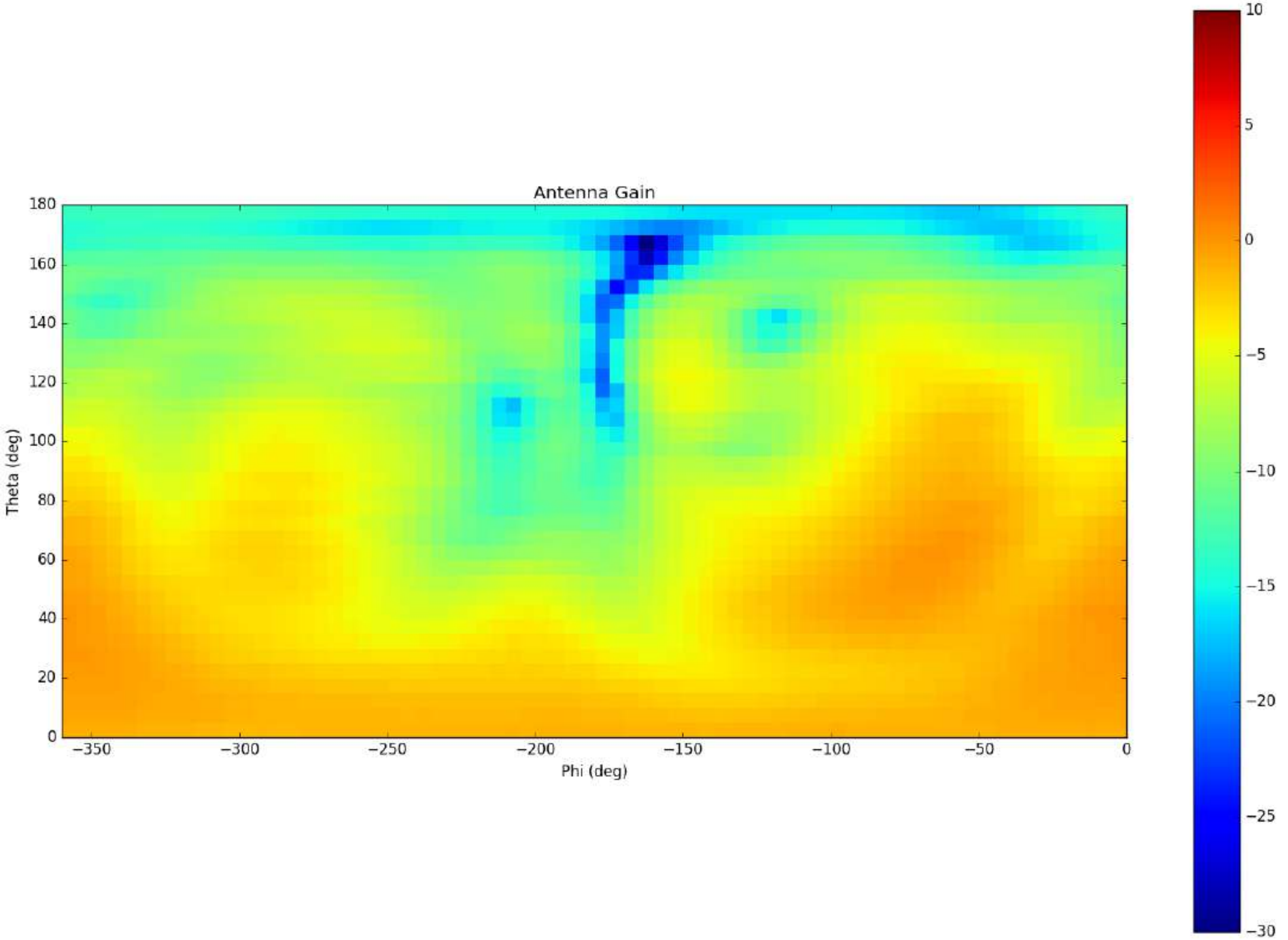

Figure 9-41: E-Theta Intensity Diagram, W702 @ 2484 MHz

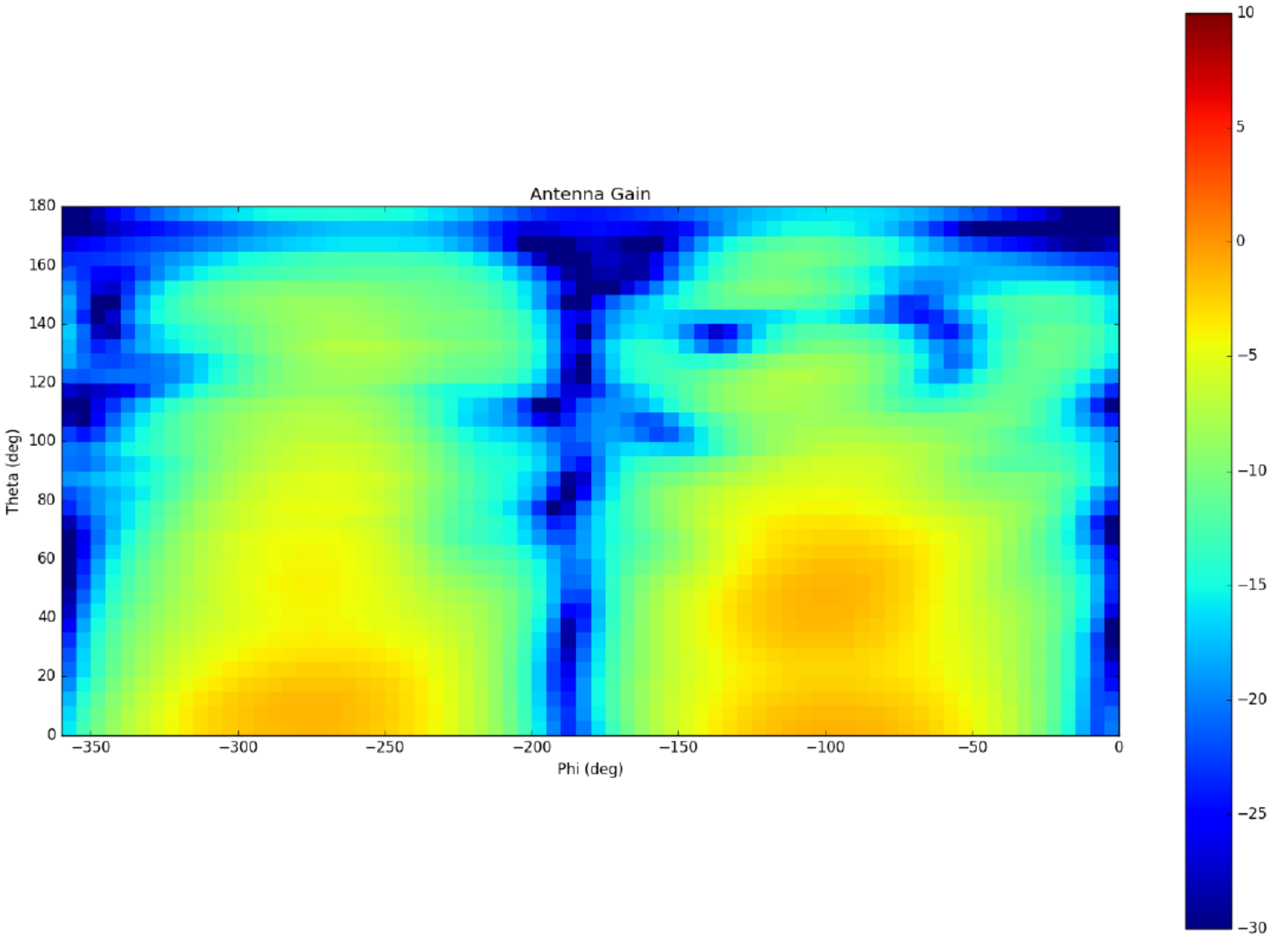

Figure 9-42: E-Phi Intensity Diagram, W702 @ 2484 MHz

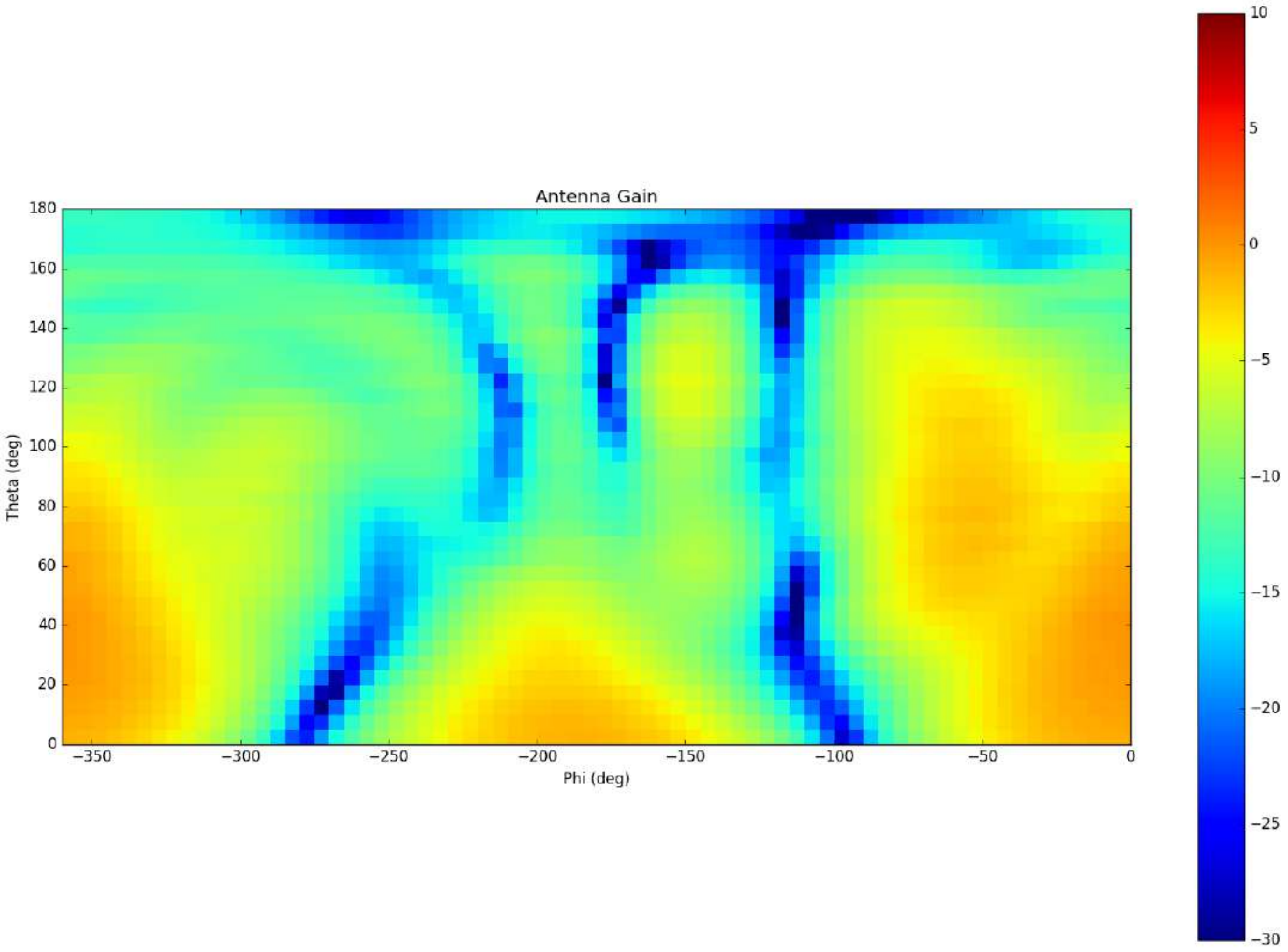

Figure 9-43: Sum Intensity Diagram, W702 @ 2484 MHz

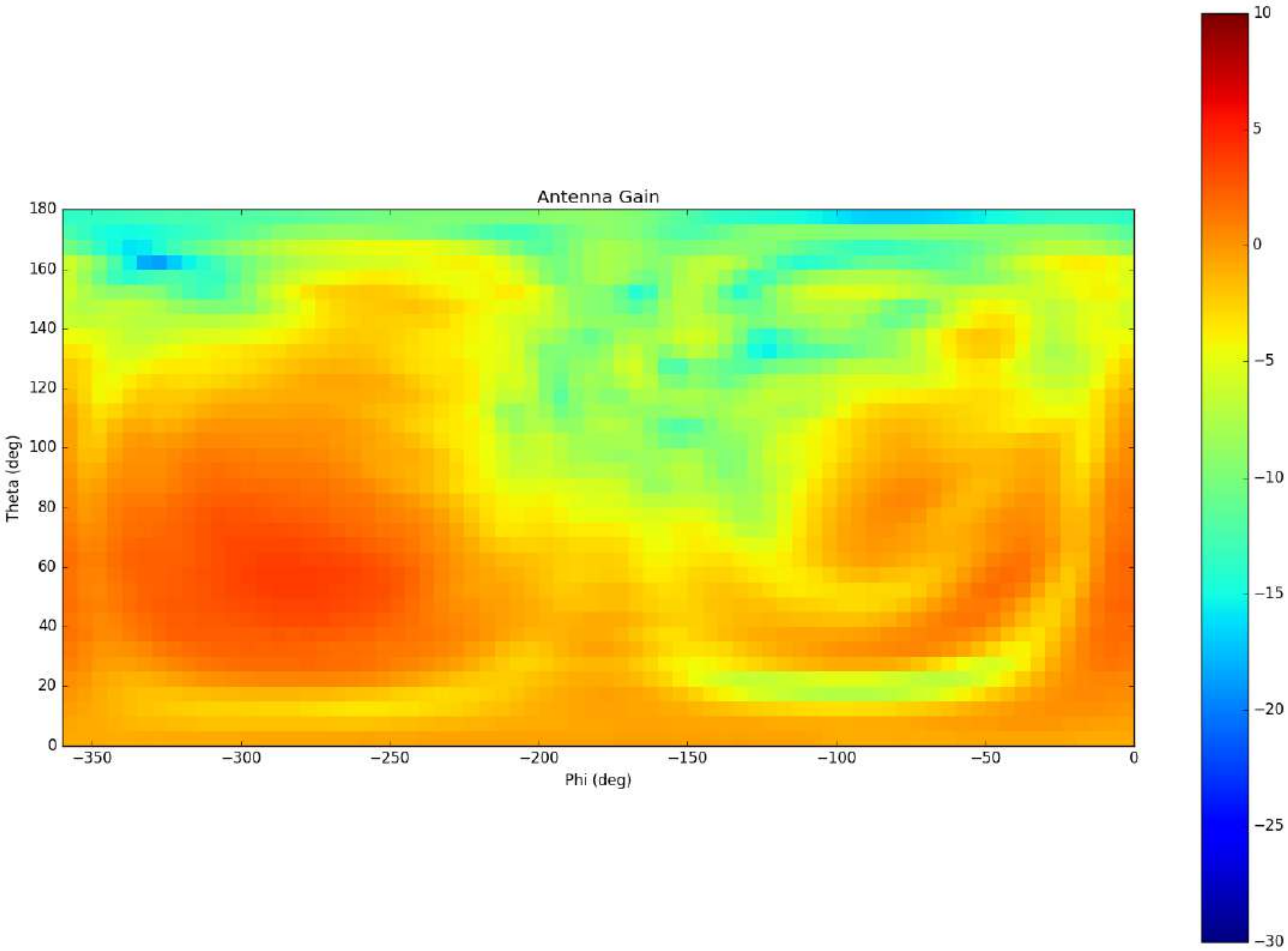

Figure 9-44: E-Theta Intensity Diagram, W702 @ 5180 MHz

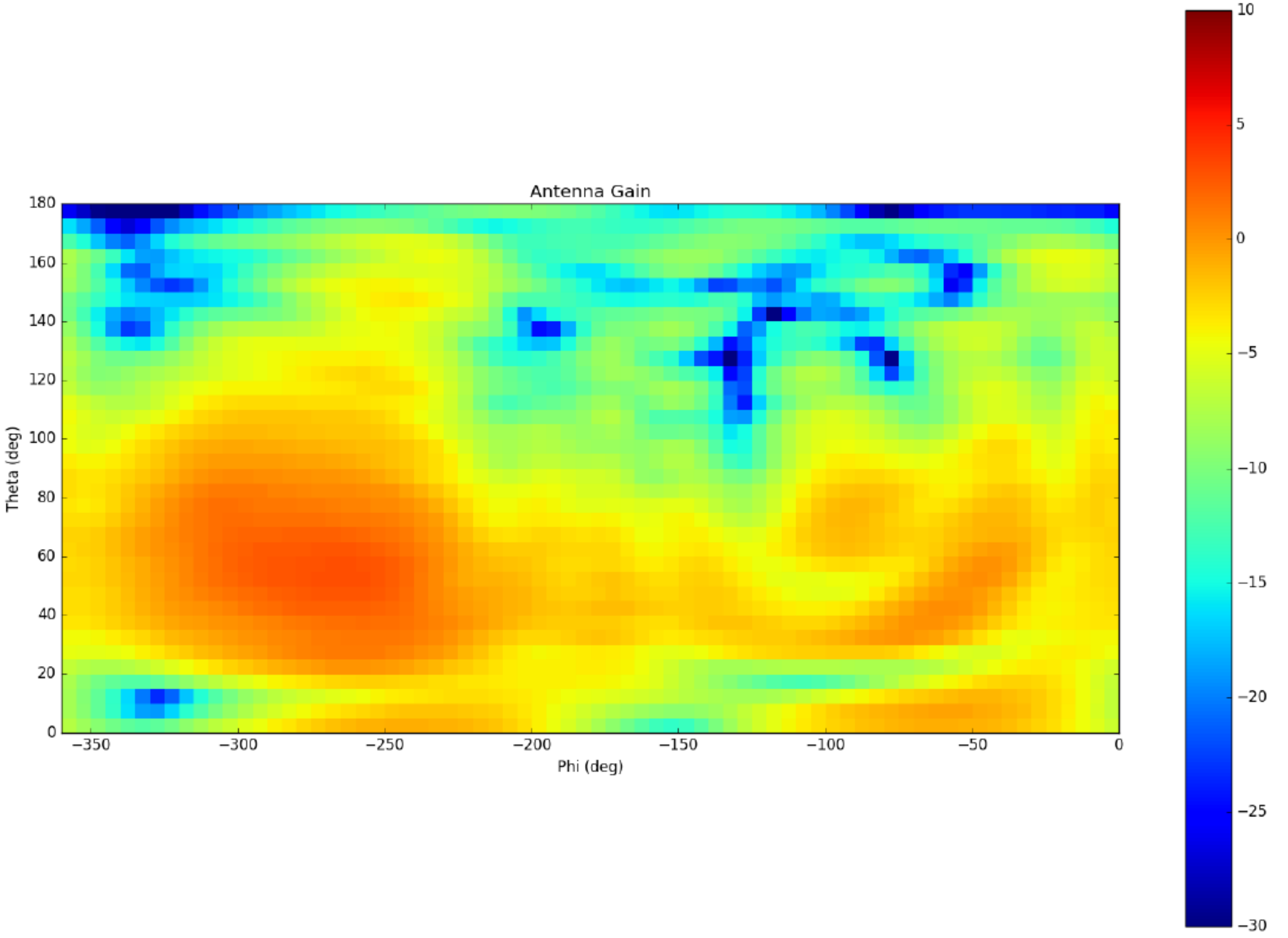

Figure 9-45: E-Phi Intensity Diagram, W702 @ 5180 MHz

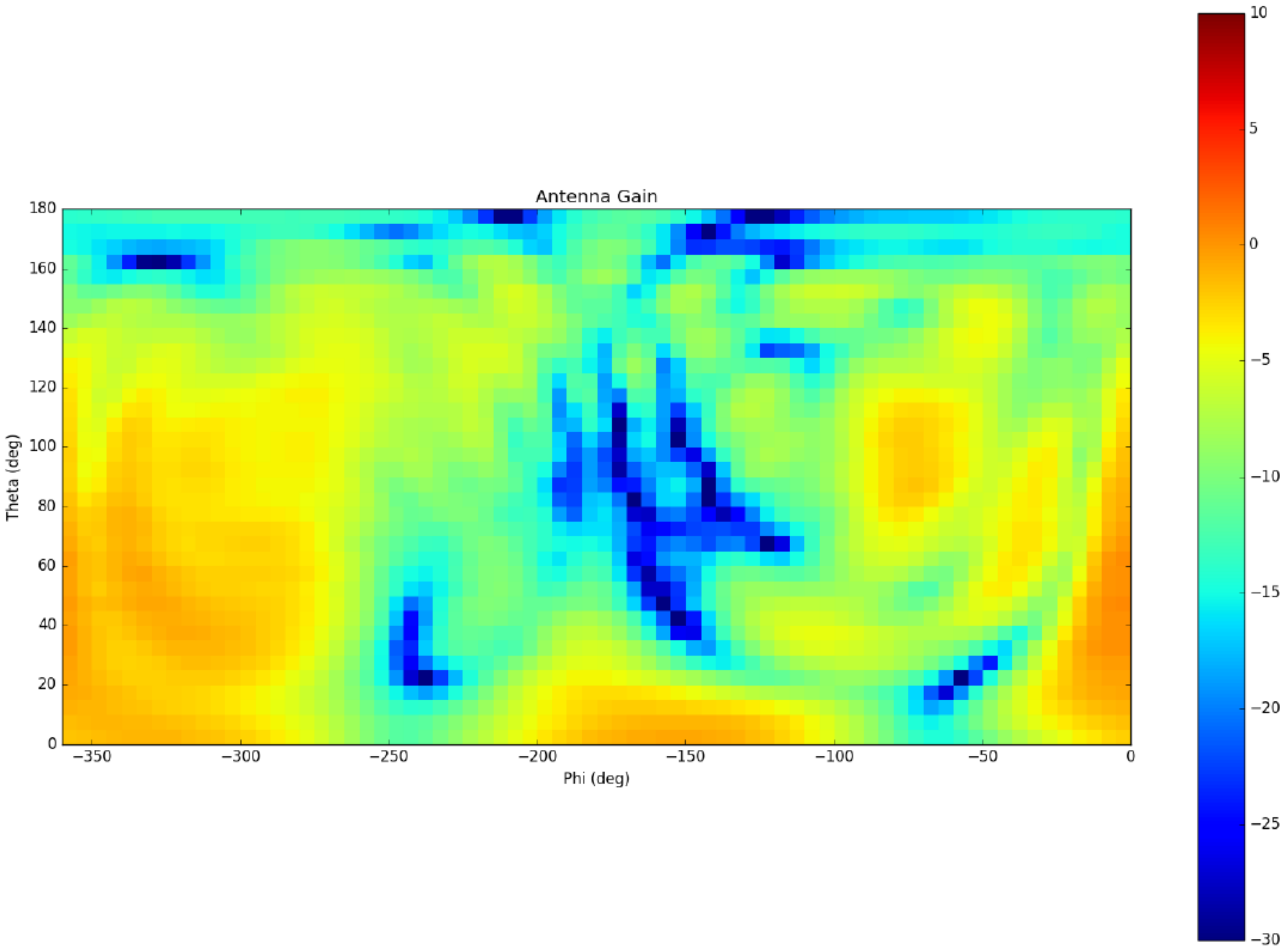

Figure 9-46: Sum Intensity Diagram, W702 @ 5180 MHz

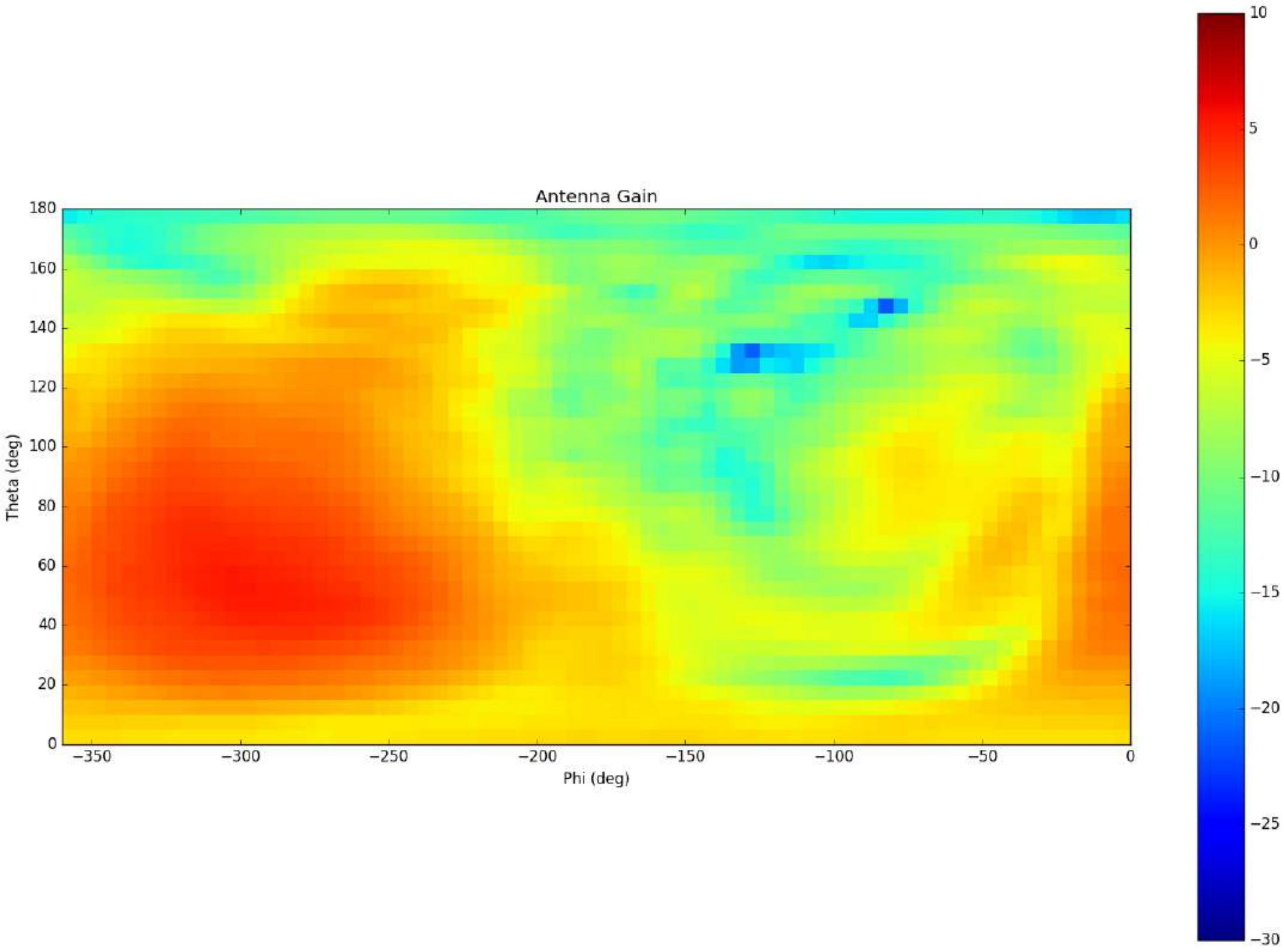

Figure 9-47: E-Theta Intensity Diagram, W702 @ 5502.5 MHz

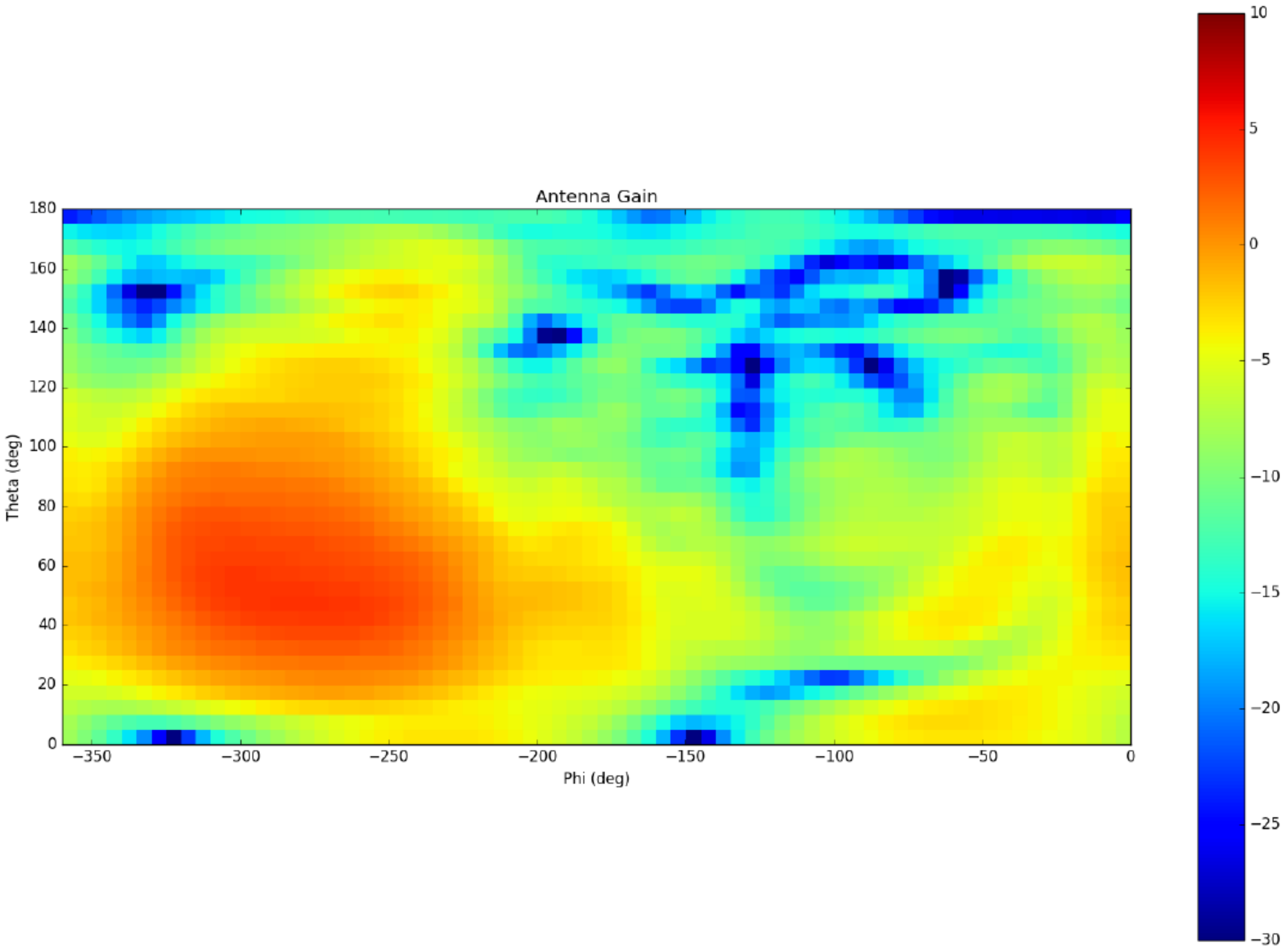

Figure 9-48: E-Phi Intensity Diagram, W702 @ 5502.5 MHz

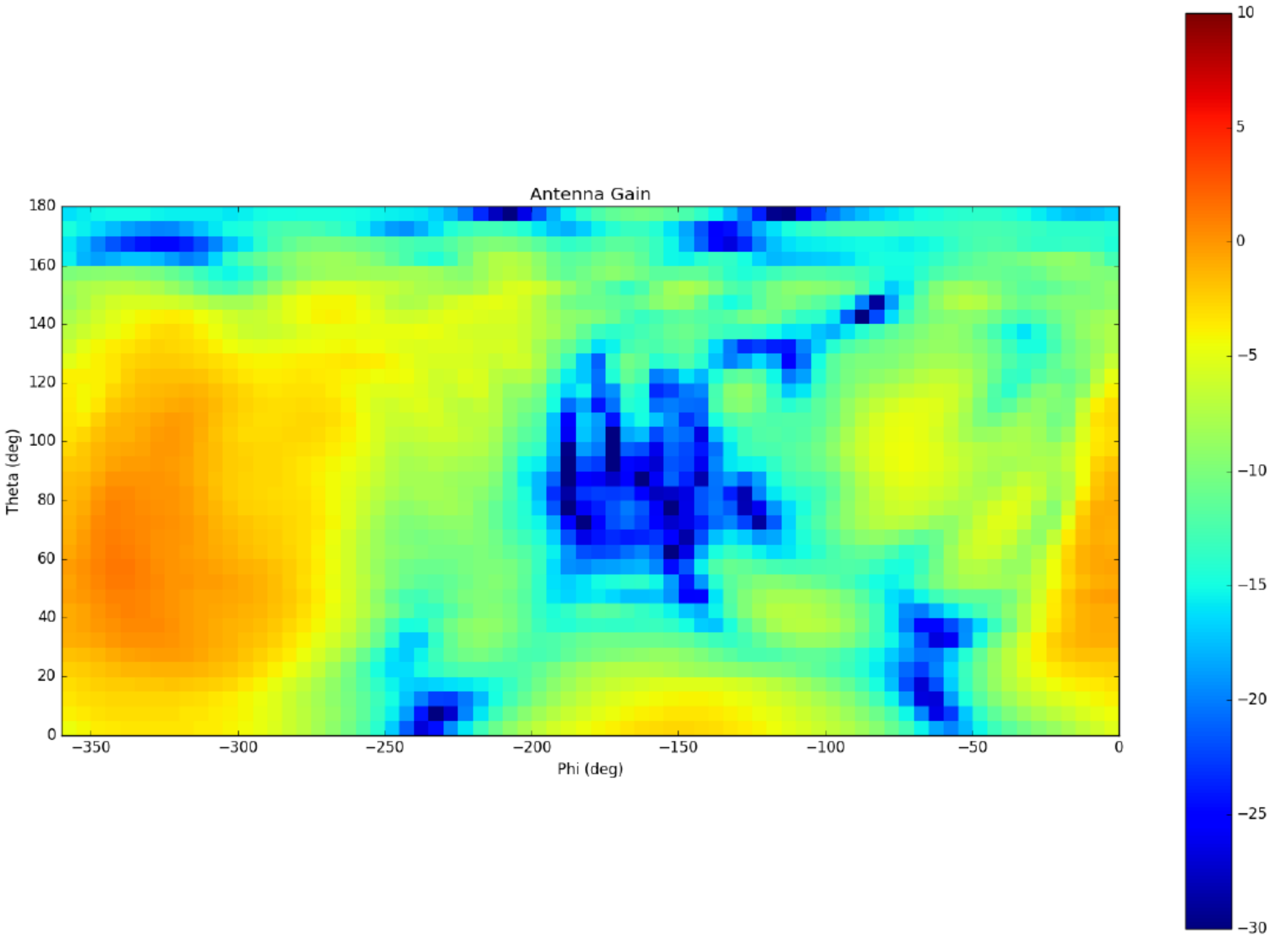

Figure 9-49: Sum Intensity Diagram, W702 @ 5502.5 MHz

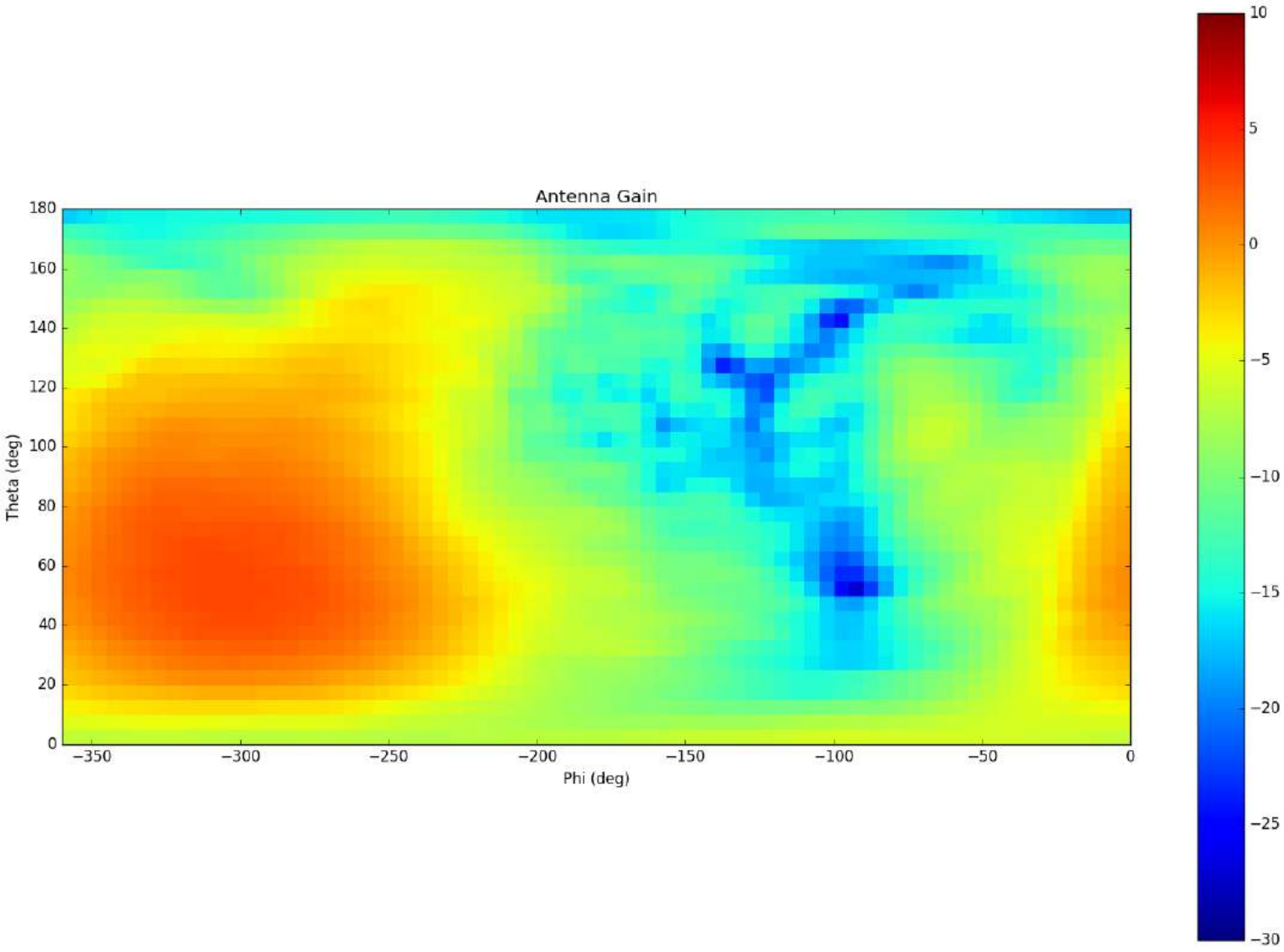

Figure 9-50: E-Theta Intensity Diagram, W702 @ 5825 MHz

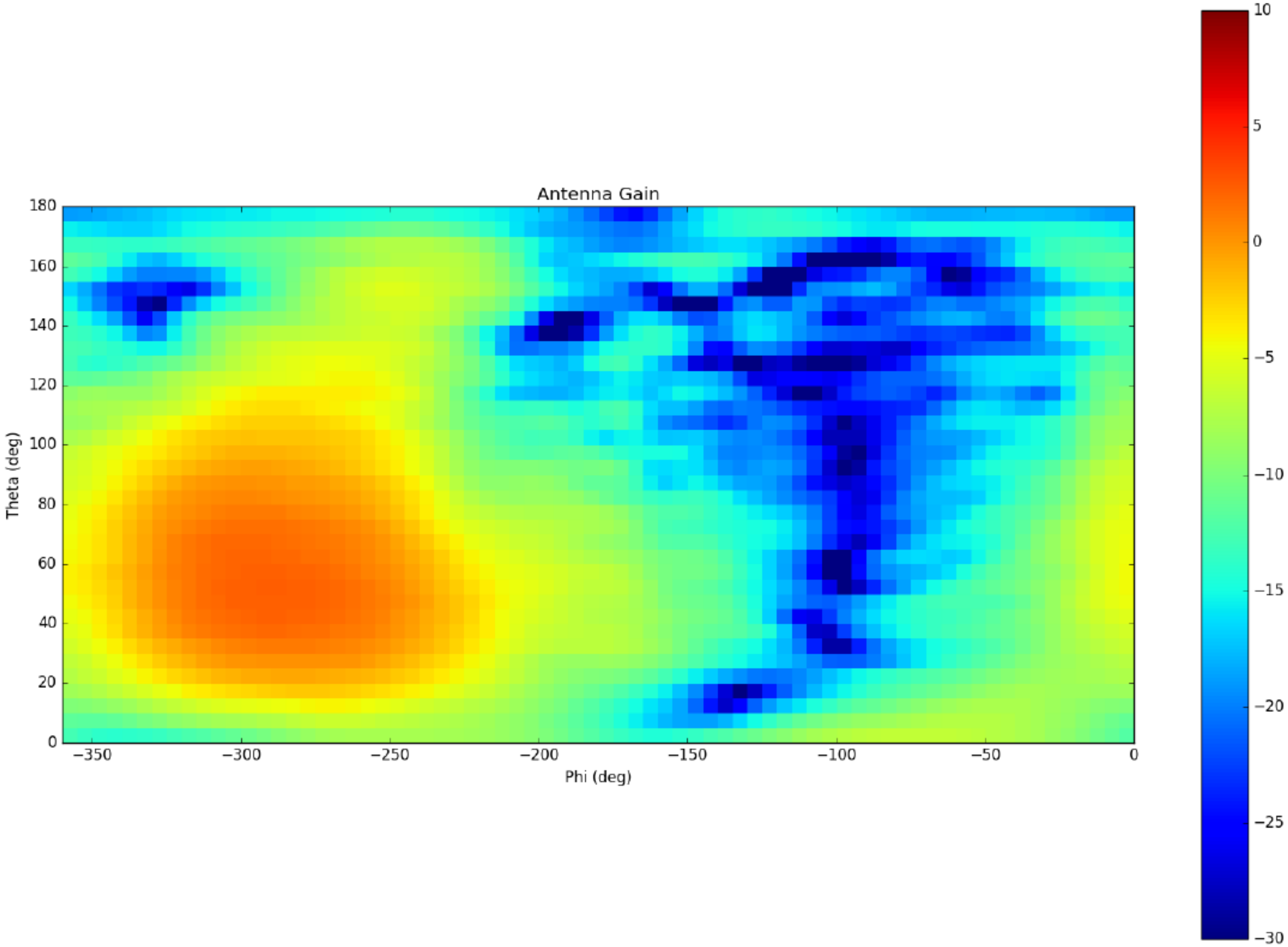

Figure 9-51: E-Phi Intensity Diagram, W702 @ 5825 MHz

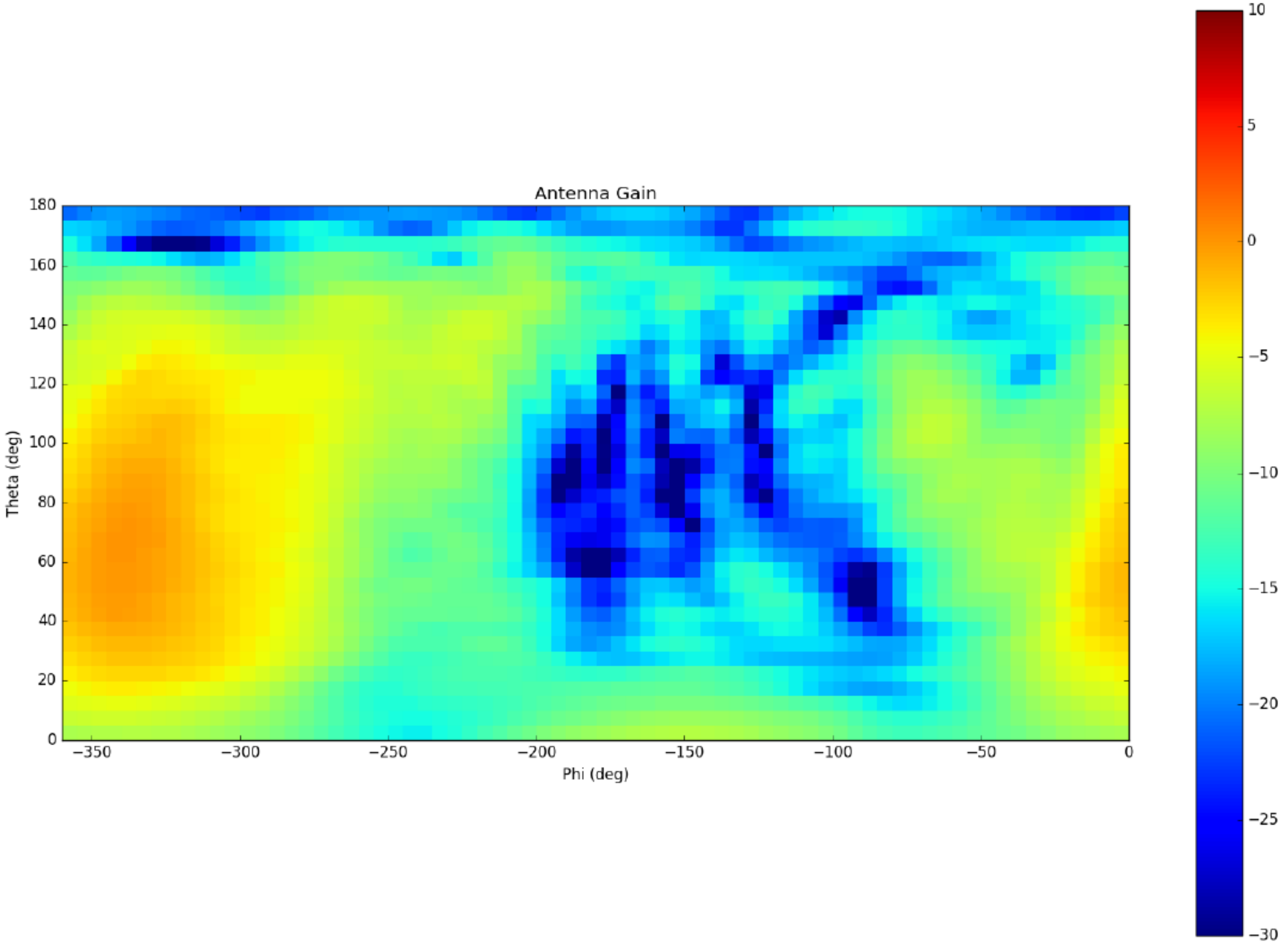

Figure 9-52: Sum Intensity Diagram, W702 @ 5825 MHz